Charles University
Faculty of Science

Study program: Biology
Branch of study: Genetics, Molecular Biology and Virology

Bc. Yana Trubitsyna

Vacuolar proteins in development of yeast colonies

Role vakuolárních proteinů při vývoji kvasinkových kolonií

Diploma thesis

Supervisor: prof. RNDr. Zdena Palková, CSc.

Prague, 2019

Declaration: I declare that all sources and literature are properly cited and that the content of this thesis or its major part was not previously used for obtaining of the same or other academic degree.

Prague, 12.08.2019

Signature

Acknowledgements:

I want to thank my supervisor prof. RNDr. Zdena Palková, CSc.for her patience, support and guidance during the work on my Diploma Thesis. Also, I would like to acknowledge my advisors, RNDr. Libuše Váchová, CSc., Mgr. Jana Maršíková and RNDr. Michaela Schierová, Ph.D. for their valuable comments and assistance. Next, I want to thank my family and my friends, namely Nandita Gupta, Milda Kvesceviciute, Lidia Short, Anastasia Kovtun and Roman Kholod for their kind support during my master study.

Furthermore, I want to express a great attitude to all members of Yeast Colony Group team for the collaboration and for creating an amazing team atmosphere.

This thesis was supported by GAUK 912218 (Study of the regulation and the function of TORC1 complex during development of yeast colonies).

Abstrakt

Laboratorní kmeny kvasinky Saccharomyces cerevisiae tvoří kolonie schopné diferencovat na dva hlavní typy buněk - U a L buňky - neboli horní a spodní buňky. Tyto buňky vykazují odlišnou morfologii, metabolismus a odolnost vůči stresu. Bylo také prokázáno, že některé metabolické dráhy probíhající v U buňkách jsou podobné buňkám rakovinným. U buňky aktivují unikátní metabolismus, který zahrnuje aktivaci TORC1 komplexu zároveň s aktivní autofagií a akumulací glykogenu, což jsou procesy charakteristické pro buňky s neaktivní TORC1 dráhou.

CORVET a HOPS komplexy spolu s vakuolárními ATPázami hrají roli v procesech, které zahrnují mimo jiné fúzi vakuol a časných a pozdních endosomů. Tyto komplexy také hrají roli v regulaci aktivity TORC1. Podjednotka HOPS komplexu - Vam6p - hraje roli v aktivaci TORC1 jako GEF pro Gtr1p GTPázu, aktivující TORC1. Cílem této práce bylo zjistit, zda se vybrané podjednotky zmíněných komplexů podílejí na regulaci aktivity TORC1 komplexu, a to hlavně v U buňkách. Dalším cílem bylo potvrdit vliv Vam6p na produkci proteinů vybraných na základě proteomické analýzy.

V rámci této práce byly připraveny kmeny s delecemi vybraných genů (VPS3, VPS8, VPS33, VPS41, VPH2, VAC7 a VAC14) a byl sledován vliv absence jejich produktů na morfologii kvasinkových kolonií. Také byla sledována aktivita TORC1 v U a L buňkách pomocí GFP-značeného Gat1p. Bylo zjištěno, že některé z vybraných proteinů přispívají k aktivaci TORC1 v U buňkách.

Vliv Vam6p na produkci vybraných proteinů v korelaci s výsledky proteomické analýzy byl potvrzen pro některé z těchto proteinů.

Tato práce obsahuje předběžné výsledky, které se musí ověřit a potvrdit dalšími pokusy.

Klíčová slova: kolonie, vývoj, TORC1, Vam6p, CORVET, HOPS, ATPáza

Abstract

The laboratory strains of yeast *Saccharomyces Cerevisiae* form colonies which can differentiate into two main cell subpopulations. U and L cells demonstrate different morphology, metabolism and stress-resistance. It was also proved that some of metabolic pathways in U cells are a similar to ones in tumor cells. The unique metabolism is activated in U cells; the TORC1 is active in these cells together with autophagy and glycogen accumulation, which are characteristic for cells with inactivated TORC1.

CORVET and HOPS complexes together with vacuolar ATPase are involved in processes related to vacuolar fusion and trafficking. Also, these complexes contribute to the regulation of TORC1 activity. Vam6p is a subunit of HOPS complex and it is also involved in regulation of TORC1 acting as GEF for Gtr1p GTPase, which activates TORC1. The aim of this study was to outline whether selected subunits of mentioned complexes affect TORC1 activity in U cells. Further aim was to confirm the effect of Vam6p on selected proteins production. These proteins were chosen based on results of proteomic analysis performed in our laboratory.

In order to investigate possible effects of proteins of interest absence on colonies' morphology, strains deleted in selected genes were prepared (*VPS3*, *VPS8*, *VPS33*, *VPS41*, *VPH2*, *VAC7* a *VAC14*). The activity of TORC1 in U and L cells was monitored using GFP-labelled Gat1p. It was demonstrated in this study that several of selected proteins contribute to TORC1 activation in U cells.

The effect of Vam6p on selected proteins production was correlated to proteomic analysis results and was confirmed for some of these proteins.

This study shows preliminary results, which must be confirmed by further experiments.

Key words: colony, development, TORC1, Vam6p, CORVET, HOPS, ATPase

Contents

List of abbreviations

Δ	gene deletion
ACO1	gene encoding aconitase
BKP	bromocresol purple
bp	base pair
BY	Saccharomyces Cerevisiae strain BY4247
CORVET	**C**lass C C**o**re **V**acuole-**E**ndosome **T**ransport
Da	Dalton
ddH2O	Double-distilled water
del F	forward primer for deletion cassette
del R	reverse primer for deletion cassette
dH2O	distilled water
DMSO	Dimethyl sulfoxide
DNA	deoxyribonucleic acid
EGOC	(**E**xit from **G**$_0$ **C**omplex)
ERG26	gene encoding C-3 sterol dehydrogenase
et al	and others
EtOH	ethanol
FAS1	gene encoding beta subunit of fatty acid synthetase
G418	geneticin
GAL	promotor of GAL1 gene
Gal F	reverse primer for GAL promoter exchange
GAT1	gene encoding Gat1p
GFP	green fluorescent protein
GM	glycerol medium
HOPS	**H**omotypic **V**acuolar Fusion and **P**rotein **S**orting
kanMX	geneticin resistance gene
L cells	cells of lower layer of yeast colony
MATa	mating type a
MATα	mating type α
MDH2	gene encoding cytoplasmic malate dehydrogenase
MRP4	gene encoding mitochondrial ribosomal protein of the small subunit
NAT	nourseothricin
Nat R	verification reverse primer for nuorseotricin resistance
nat1	nourseothricin resistance gene
over 589 R	verification reverse primer for GFP gene
over. F	verification forward primer
PCR	polymerase chain reaction
PEG	Polyethylene glycol
pGAL F	forward primer for promoter exchange cassette
pGAL R	reverse primer for promoter exchange cassette
PI(3,5)P2	phosphatidylinositol-3,5-bisphosphate
PI3P	Phosphatidylinositol 3-phosphate
PKA	protein kinase A

primer F	forward primer
primer R	reverse primer
SDS-PAGE	sodium dodecyl sulfate–polyacrylamide gel electrophoresis
ssDNA	single strand DNA
SSO1	gene encoding plasma membrane t-SNARE
TBE	Tris/Borate/EDTA buffer
TORC1	**T**arget **O**f **R**apamycin **C**omplex 1
U cells	cells of upper layer of yeast colony
v/v	volume/volume
w/v	weight/volume
wt	wild type
YEPG	glucose medium

1 Introduction

This thesis was elaborated in Yeast Colony Group at the Department of Genetics and Microbiology of the Faculty of Science, Charles University, Prague.
One of the research branches of the Yeast Colony Group is related to the differentiation of yeast colonies while growing on a solid medium. The number of metabolic and regulatory parallels were detected between differentiated yeast colonies and tumor-affected organisms [1], [2]. The study of these processes in differentiated yeast colonies can contribute to the understanding of similar processes in human tissues.

TORC1 is a conserved serine/threonine kinase which is involved in the regulation of cell growth and proliferation [3]. The lack of proper regulation of TORC1 results in cell damage and the inability to proliferate coordinately. This was also described in human cells as a trigger of cancer [4].
Yeast TORC1 is localized on the vacuolar membrane. The yeast vacuoles analogous to lysosomes of other organisms, and mTORC1, the mammalian homolog of yeast TORC1, is localized on lysosome membrane. However, this localization is temporary and depends on nutrient availability.

Yeast colonies grown on solid medium can differentiate into two subpopulations with different physiology, morphology, and metabolism. Different pathways are active in U and L cells. One of these pathways is TOR pathway which is important for nutrient sensing and coordination of cell growth and proliferation [2], [3], [5]. In U cells of differentiated colonies, TORC1 is active. Some processes, typical for cells with inactivated TORC1 are also active in U cells, for example, autophagy and accumulation of glycogen [2]. These observations allow to suggest that in U cells, TORC1 is regulated by mechanisms that have not yet been described.
TOR pathway has several known upstream regulators, for example EGO and SEA complexes. It was reported in recent years, that HOPS and CORVET complexes, and vacuolar V-ATPase can contribute to TORC1 activity regulation. The mentioned regulators are mainly involved in processes related to vacuolar fusion and trafficking [6], [7].

Vam6p/Vps39p, the subunit of HOPS complex is required for proper assembly of HOPS complex, which mediates late endosome-vacuole and vacuole-vacuole fusion. It is known that Vam6p also contributes to the regulation of TORC1 activity. Acting as the GEF for Gtr1p GTPase, a part of EGO complex, Vam6p activates TORC1 [8], [9]. It was indicated in our laboratory, that Vam6p is potentially involved in regulation of TORC1 in U cells of giant colonies (non-published data).

This study has two main aims and is divided into two parts:
The aim of first part of this study is to determine whether proteins selected on basis of the genome-wide proteomics of colonies formed by wt strain and strain deleted in *VAM6* gene are differentially produced in U and L cell of wt and *vam6* strains. A related aim was to confirm whether *VAM6* deletion influences production of these proteins. The data from Western Blot performed in this study is correlated with proteomic analysis.

The aim of the second part was to determine, if and how the absence of other selected protein-components of selected complexes influences colony development and U and L cell formation. Candidate proteins were selected based on literature search. A further aim was to analyze whether absence of these proteins influences TORC1 activity in U cells, using re-localization of Gat1p as a marker of TORC1 activity [10]. A partial aim of the second part of this study was to investigate whether absence of selected proteins affects cells viability in both U and L cells.
The results demonstrated in this study are preliminary and must be confirmed by additional experiments.

2 Literature Review

2.1 The differentiation of yeast colonies

As was discovered in recent decades, yeast cells can exist not only as a unicellular organism, but also as well-organized multicellular structures, for example, biofilms or colonies.

Saccharomyces cerevisiae is able to create colonies, which differentiate in two cell subpopulations with dissimilar properties [2], [11]. These cell subpopulations are called U cells and L cells - cells of upper (U) and lower (L) layers. Physiology, morphology, metabolism, viability, sensitivity to stress, and other properties were characterized for U and L cells.
The process of differentiation begins approximately on 7^{th} day, and from 7^{th} to 10^{th} day a boundary between U and L layers becomes higher defined. As mentioned above, U and L cells differ in many characteristics, for example, in morphology, where U cells are bigger with swollen mitochondria without cristae, large lipid droplets, and small vacuoles and L cells are smaller and contain many mitochondria, one small lipid droplet and one large vacuole (Figure 1).

U and L cells transcriptomes show significant difference when compared to each other. While U cells have upregulated genes for translation, glycolysis, pentose-phosphate shunt, fatty acid metabolism, nucleotide biosynthesis and transport, upregulating of genes in L cells is focused on genes for mitochondrial biogenesis, oxidative phosphorylation, genes for stress response and chaperons. Much less metabolic genes are expressed in L cells – for example, genes for lipid metabolism and for response to poor nutrient sources and gluconeogenetic enzymes. It was indicated, that in U cells many anabolic and catabolic genes for amino acid metabolism are active, mainly genes for biosynthesis of arginine, histidine, leucin, aromatic amino acids etc, and also genes for amino acid transporters. In L cells, only few genes for amino acid metabolism were detected, including *GLN1* gene that is coding glutamine synthetase and *GDH3* (glutamate dehydrogenase).

While amino acid content remains to be similar in U and L cells, the composition differs dramatically. U cells contain and import more glutamine, glutamate and arginine, which are considered as rich nitrogen sources. In the contrary, L cells contain more poor sources, such as alanine, lysine, and GABA, and a very low level of glutamine. Concentration of

glutamine in L cells was reported to be approximately 12-15% of the glutamine concentration detected in U cells.

U cells in general show a high level of amino acid synthesis and turnover, and as mentioned above, genes for amino acid transporters and biogenesis in U cells are upregulated. As amino acids accessibility and transport are important for ammonia signalling, which is required for colony differentiation, it was considered that ammonia signalling is also required for formation of U layer [12], [2].

U cells show characteristics of metabolically active cells, such as translation, biosynthesis and transport of nutrients, and characteristics of starving cells with activated autophagic pathways, reduced respiration and downregulation of mitochondrial genes.

As U cells behave as fermenting cells and they can grow on non-fermentable source, it was suggested that L cells could be the main nutrient provider for cells of upper layer, which slowly grow in 10-20 days-old colonies. According to transcriptome data, different degradation mechanisms are activated in L cells, that could be a source of low molecular weight nutrients for U cells, for example, sugars from cell wall degradation. Also, L cells actively produce glucose and glutamine, release amino acids, and genes for hexose transporters are upregulated in those cells. L cells, regardless of accessibility to nutrients from agar, do not grow and show signs of starving cells. Considering that and the fact that defects in above mentioned genes caused decrease of U cells viability, it was suggested that the longevity of U layer is closely related to L layer formation and metabolism. L cells also demonstrate low autophagic activity, and for U cells survival, autophagy remains to be crucial [2].

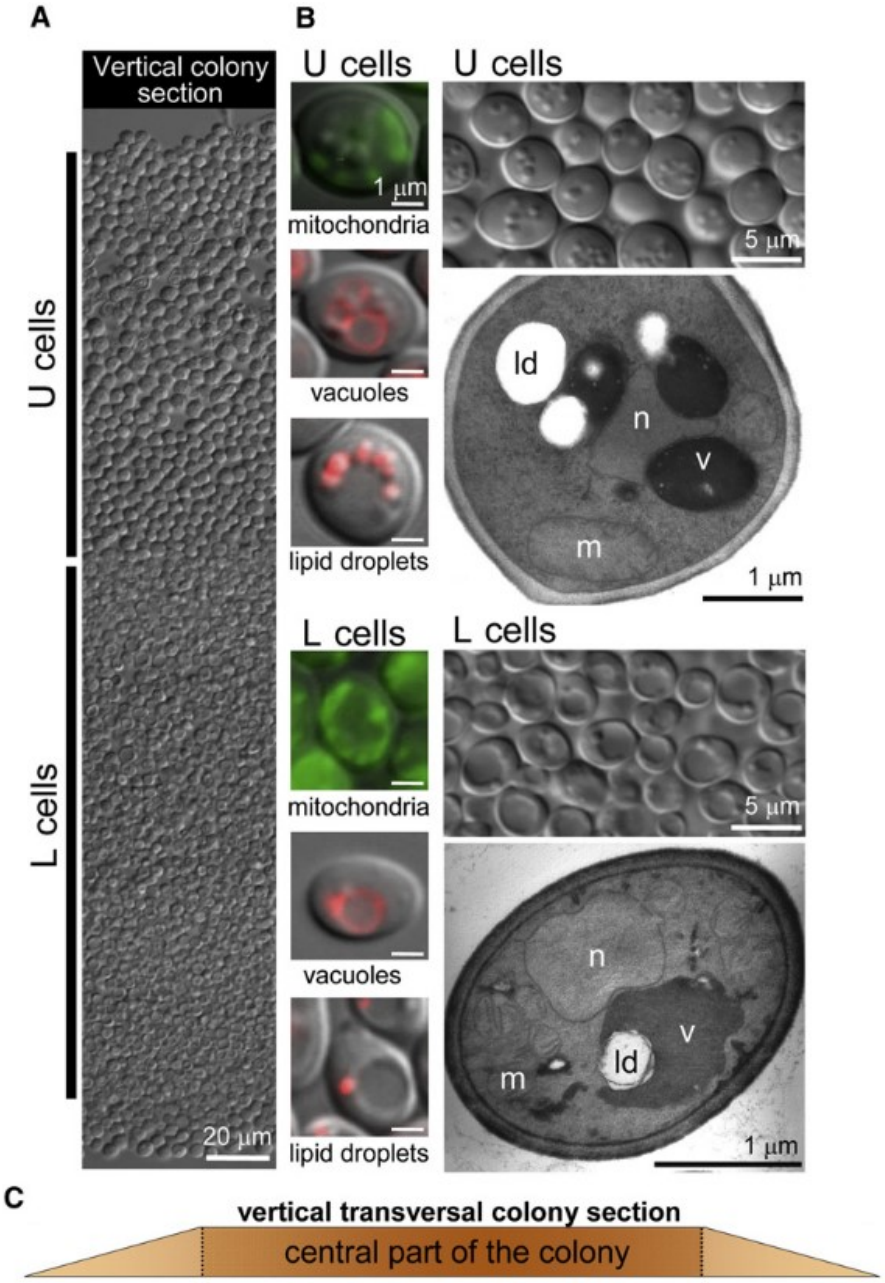

Figure 1. S. cerevisiae Colony Cells Differentiate into Two Morphologically and Physiologically Distinct Subpopulations (A) Vertical transversal cross-section of a 20-day-old BY4742 colony. (B) Details of U and L cells visualized with Nomarski contrast, fluorescence, and transmission EM. Left panels: Mitochondria were stained with DiOC6(3), vacuoles with FM4-64, and lipid droplets with Nile Red. (C) Details of U and L cells visualized with Nomarski contrast and transmission EM. n, nucleus; v, vacuole; m, mitochondria; ld, lipid droplet. (C) Vertical transversal colony section scheme. Obtained and modified from Čáp et al., 2012 [2]

It was also demonstrated that in U and L cells, different metabolic pathways are active. This statement applies mainly to nutrient-sensing pathways, such as TOR and PKA pathways.

TOR pathway is active in U cells. U cells are metabolically active cells, but also show unexpected characteristics of starving cells, such as active autophagy, which is supposed to be inhibited while TORC1 is active [13]. It was further confirmed that in U cells PKA pathway, one of autophagy inhibitors is inactive. L cells show signs of starving cells, and have inactive TOR pathway, which was confirmed by TOC1 activity tracking. For TOC1 activity tracking GFP-labelled Gat1p was used. This TOR-responsive transcription factor was reported to be present in cytosol, when TOR kinase is active, and in nucleus during TORC1 inactivation. [2], [10], [14]

Yeast colonies release ammonia as a signal molecule which is important for population development and metabolic reprogramming of colonies. The ammonia production is decreased during the following growth of colonies. These developmental phases are called first acidic, first alkali and the second acidic phases. The changes in expression of number of genes are characteristic for mentioned developmental stages [5], [11], [15].

2.1 Selected Nutrient-sensing Pathways in yeast *S. Cerevisiae*

To ensure proper regulation of cell growth, metabolism and proliferation in reaction to nutrients availability, the existence of controlling pathways is required. Several important conserved nutrient-sensing pathways were described in yeasts, such as TOR pathway, Ras/cAMP/PKA pathway, SNF pathway and others. These pathways are also connected to each other in certain points.

2.1.1 PKA Pathway

Ras/cAMP/PKA pathway responds to glucose availability and positively stimulate cell growth, ribosome biogenesis and proliferation. Active PKA kinase, serine/threonine protein kinase A also inhibits autophagy and stress-response genes expression. Two of three catalytic subunits, Tpk1p, Tpk2p or Tpk3p, and two identical Bcy1p regulatory subunits, form the PKA. PKA is stimulated by cAMP, which is produced by activated

adenylate cyclase Cdc35p. Binding cAMP to the Bcy1p results in dissociation of regulation subunits and activation of catalytic ones. Catalytic subunits then activate glycolysis and other processes required for cell growth [16]–[19].

2.1.2 TOR Pathway

In yeast cells, two TOR genes were described: *TOR1* and *TOR2*. Target of Rapamycin Complex 1 consists of Tor1p or Tor2p, Lst8p, Kog1p and Tco89p. Localized on yeast vacuolar membrane, the conserved serine-threonine kinase TORC1 has an important role in regulation of cell growth and proliferation in response to nitrogen sources [3], [8]. Active TORC1 inhibits autophagy and expression of stress-response genes and activates translation and ribosome biogenesis. [20]–[22]

2.2 Regulation of TORC1 Activity

PKA and TOR pathways regulate expression of genes required for cell growth, including genes for ribosome biogenesis and stress-responsive genes. It is known that Ras/cAMP/PKA pathway`s regulator is glucose, and TOR pathway is regulated by nitrogen sources, which is mainly amino acids. From the point of nutrient source quality, some of the sources can be considered as preferred, or rich sources. For example, in the case of nitrogen sources, the preferred ones are amino acids glutamine and arginine, and ammonia. In contrast, proline and leucin are considered as poor, or non-preferred sources of nitrogen. It means in fact, that poor sources of nitrogen are consumed, when the preferred source is not accessible. It is also known, that both preferred and non-preferred sources of nitrogen are involved in TORC1 activation, however, the quality of nitrogen source can determine TORC1 activity. It was reported that both rich and poor sources activate TORC1, but the presence of preferred nitrogen source is required for its sustained activity [23], [24].

TOR pathway has several known upstream regulators, for example EGOC, SEA complex or leucyl-tRNA-synthetase. EGOC is a well-described regulator of TORC1, which is also localized on vacuolar membrane and promotes Rag GTPase-dependent TORC1 signaling [25]–[28].

2.2.1 HOPS and CORVET Complexes

It was reported in recent few years, that HOPS and CORVET complexes, and also vacuolar V-ATPase contribute to the regulation of TORC1 activity. Those regulators are mainly involved in processes related to vacuolar fusion and trafficking (Figure 2) [7].
HOPS and CORVET complexes participate on important events related to vacuole and other membranous organelles fusion and trafficking, but also on modulation of TORC1 activity. As summarized in Figure 2 obtained from [7], the HOPS complex mediates late endosome-vacuole and vacuole-vacuole fusion, and CORVET complex takes part in mediation of early-to-late endosomal trafficking and retrograde trafficking from vacuole. Genes coding subunits of CORVET and HOPS complexes are also called vps-c class. Vps-c mutants demonstrate fragmented vacuoles and impaired interaction between EGOC and TORC1. It is known, that TORC1 is localized on vacuolar membrane and HOPS complex it required for vacuolar fusion control. Mutations of HOPS components result in fragmented vacuoles, and, therefore, in destabilization of TORC1 and limitation of interaction between TOC1 and EGOC. This destabilization, however, is not accompanied by reduction of TORC1 activity, which allows to presume that HOPS has EGOC-independent effects on TOR complex 1 [7], [29].

HOPS and CORVET complexes are homologous, both containing class C core proteins Vps11p, Vps16p, Vps18p and Vps33p and require two proteins for assembly. In case of HOPS complex it is Vps41p/Vam2p, Vps39p/Vam6p as assembly proteins and CORVET requires Vps3p and Vps8p [30].

CORVET and HOPS complexes also create transient intermediate complexes: (1) the CORVET (Vps3p-Vps8p) complex, (2) together with Vam6p and Vps8p (i-HOPS, see below), (3) in the HOPS complex, and (4) in combination with Vps3p and Vps41p (i-CORVET) [31].

Both CORVET and HOPS complexes modulate TORC1 activity upstream of EGOC and HOPS has a greater role in this modulation. It was reported that Vps-C complexes can affect TORC1 activity in different manners, such as affecting the stability of amino acid transporters and participation on vacuole integrity [32], [33]. *Vps-c* mutants fail to maintain vacuolar fusion, vacuole acidification and pH homeostasis. Further, they are also sensitive to alkaline pH.

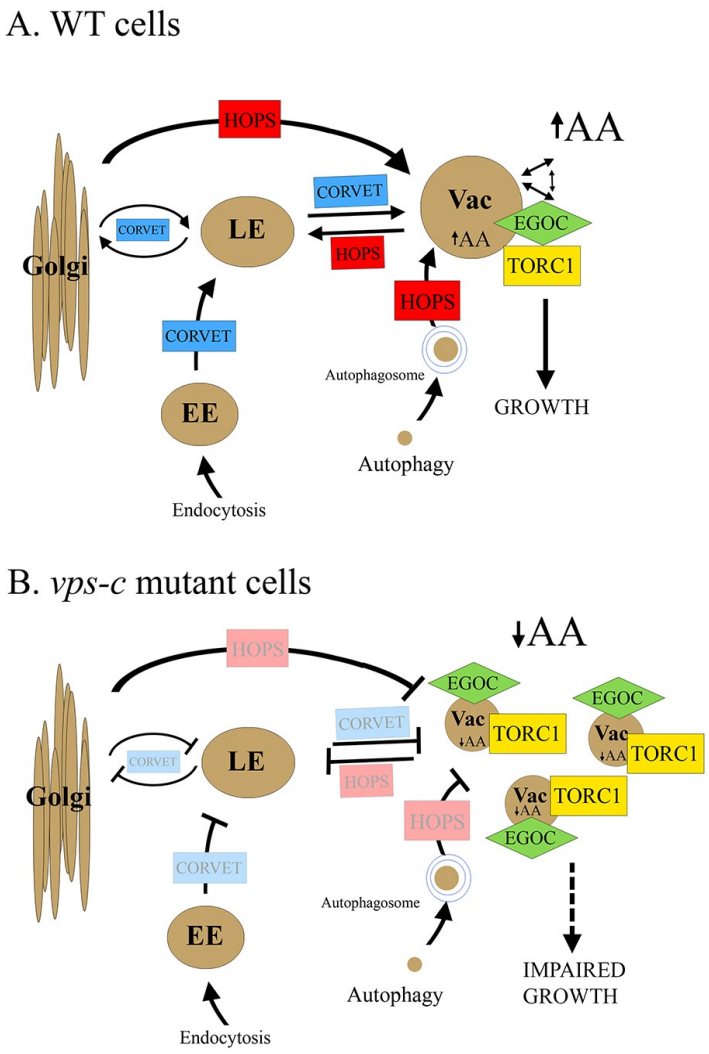

Figure 2. Proposed model for the role of Vps-C complex in promoting TORC1 signaling. **LE** – Late Endosome, **EE** – Early Endosome, **Vac** – Vacuole, **AA** – Amino Acids **A.** The Vps-C HOPS and CORVET complexes mediate multiple endomembrane fusion events and indirectly promote TORC1 activity. **B.** Disruption of Vps-C HOPS and CORVET complexes blocks endomembrane fusion events, and indirectly result in impairment of TORC1 activity and cell growth. Obtained and modified from: Kingsbury et al., 2014 [7].

2.2.1.1 Vam6p/Vps39p

VAM6 gene encodes Vam6p/Vps39p, which plays a role in two important processes in the yeast cell. First, Vam6p is required for HOPS complex assembly and interacts with Ypt7 Rab GTPase. [34]. Ypt7 Rab GTPase is involved in a process of SNARE complexes' assembly and therefore in vacuole fusion [35]. Second, Vam6p is known as a GEF factor that regulates TOC1 activity via EGOC[8], [36].

2.2.2 V-ATPase and role of phosphatidylinositol-3,5-bisphosphate in v-ATPase stabilization

Fragmented vacuoles of *Vps-c* mutants are similar to v-ATPase mutants. *Vps-c* mutants and v-ATPase mutants have several common features, such as above-mentioned defects in pH homeostasis, but also defects in vacuole acidification and V-ATPase assembly.

V-ATPase belongs to highly conserved proton pumps. Yeast V-ATPase consists of two main complexes, V_0 and V_1 and it is required for both vacuolar fusion and fragmentation [37]. For stabilization of v-ATPase and its activation phosphatidylinositol-3,5-bisphosphate (PI(3,5)P2) is required. It was reported by Deranieh et al., 2015, that even inositole depletion in cells affects V-ATPase activity, as the cell cannot syntetize enough of PI(3,5)P2 for its stabilization. PI(3,5)P2 is also the major phospholipid of the vacuolar membrane and its level in cell is increased during the hyperosmotic stress [38], [39], [40].

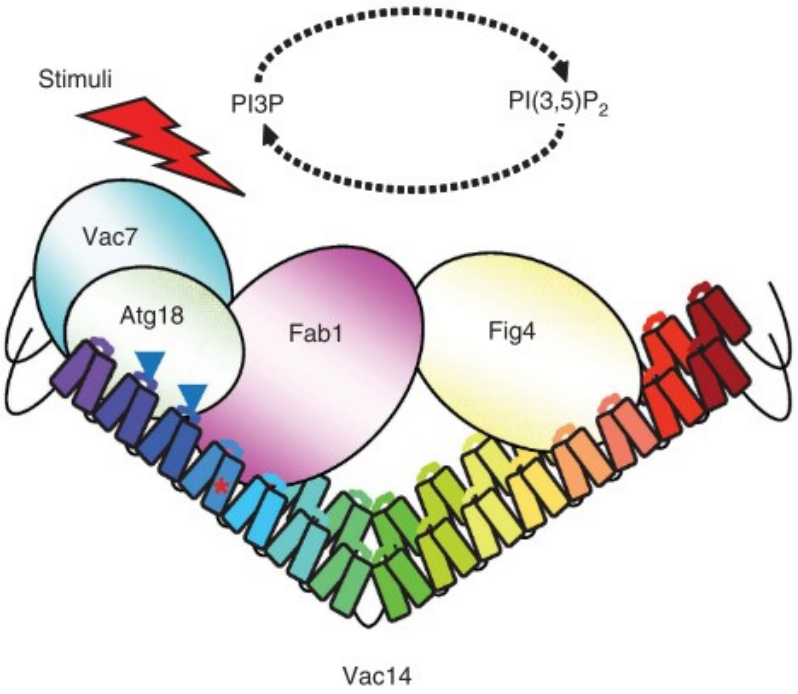

Figure 3. The proposed model of Vac14 complex. Vac14 protein binds both Fab1p and Fig4p and brings them into contact, undergoing the conformation change in response to stimuli. Obtained and modified from Jin et al., 2008 [41].

Vac14p was described as a nucleation factor for the complex regulating PI3P and PI(3,5)P2 interconversion. This complex consists of Fab1p, Vac7p and Atg8p, where Vac7p is an activator of Fab1p and Atg18p is a negative regulator and binding sites between those three proteins overlap. Lipid kinase Fab1p is activated or inhibited by mentioned regulators during the hyperosmotic stress in yeast. Vac14p facilitates Vac7p- and Atg8-dependent regulation of Fab1p. In Vac14 complex Fab1p can also be in contact with 3,5-bisphosphate phosphatase, Fig4p. As Fig4p lacks transmembrane domain, it is recruited to vacuolar membrane by Vac14p. Fig4p and Fab1p do not interact directly, but bind to opposite ends of Vac14p and the conformation change of Vac14p enables their interaction (Figures 3 and 4) [39], [41], [42].

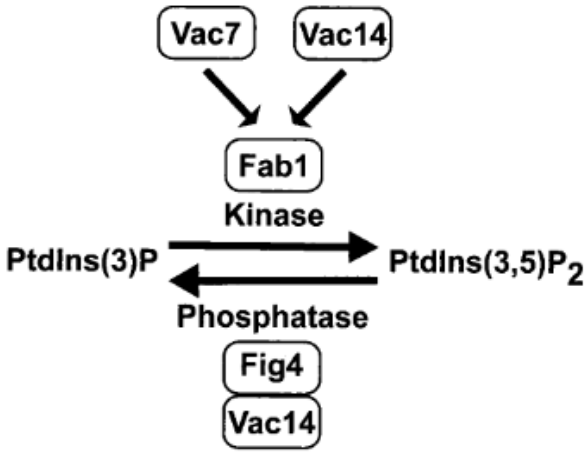

Figure 4. Proposed model of Vac14p role in regulation of Fab1p kinase and Fig4p phosphatase. Obtained from Rudge et al., 2004 [39].

Another protein, Vph2p, which is localized on ER, plays an important role in v-ATPase assembly and stabilization. Not being an actual v-ATPase subunit, this protein is required for V_0 complex stability, and in cells lacking *VPH2* gene the rapid degradation of V_0 complex occurs. The mutants lacking Vph2p also lack both v-ATPase hydrolytic activity and proton-pumping activity [43], [44]. Vph2p was also reported to influence on both vacuolar fission and TORC1 activity regulation [45].

It was demonstrated that vps-c mutants also have v-ATPase assembly defects, which can be partially rescued by *VPH2* overexpression [7]. It was reported in *Candida albicans,* that the deletion of *VPH2* gene caused defects in endocytosis and homeostasis of vacuolar pH [46].

TORC1 is localized on vacuolar membrane, and v-ATPase is important for both pH maintenance of vacuole and for its fusion and fission. This makes v-ATPase stability crucial for regulation of metabolism and other important processes.

In our laboratory it was indicated that TORC1 activation in U cell is affected by Vam6p. Also, it was proved that absence of Vam6p results in different production of further proteins in U and L cells. The experiments performed in this thesis were proposed based on mentioned findings.

3 Aims of the Thesis

This thesis has two main aims:

1. To determine, whether proteins selected based on the genome-wide proteomics of colonies formed by wt strain and strain deleted in *VAM6* gene are differentially produced in U and L cell of wt and BY-*vam6* strains.
   1a. To confirm whether *VAM6* deletion influences production of these proteins.

2. To determine effects of absence of selected protein-components of HOPS and CORVET complexes and proteins related to regulation of V-ATPase stability on the development of the colonies, U and L cell formation, and viability. To analyze whether and how is TORC1 activity affected by absence of these proteins.

4 Materials and Methods

4.1 Materials

4.1.1 Microorganism

BY4742 strain of *Saccharomyces cerevisiae* was used in this thesis. This strain was obtained from Euroscarf collection.

4.1.2 Saccharomyces cerevisiae strains used in this thesis

Following Saccharomyces cerevisiae strains were used in this thesis:
BY4742 (BY) – MATα, *his3Δ, ura3Δ, leu2Δ, lys2Δ*, haploid laboratory strain which creates smooth colonies. This strain was obtained from Euroscarf collection.
BY-*vam6* – MATα, *his3Δ, ura3Δ, leu2Δ, lys2Δ*, *vam6Δ*, haploid strain that creates smooth colonies, derived from BY4742. This strain was created by Ing. Ladislava Hatáková. RNDr.
BY-Gat1p-GFP – MATα, *his3Δ, ura3Δ, leu2Δ, lys2Δ*, GAT1-GFP, KanMX, derived from BY strain.

Other strains that are presented in Table 13 (5.1.1.) and Table 14 (5.2.1) were created by the author of this study.

4.1.3 Plasmids used

Maps of plasmids used in this study is demonstrated in Figure 5.

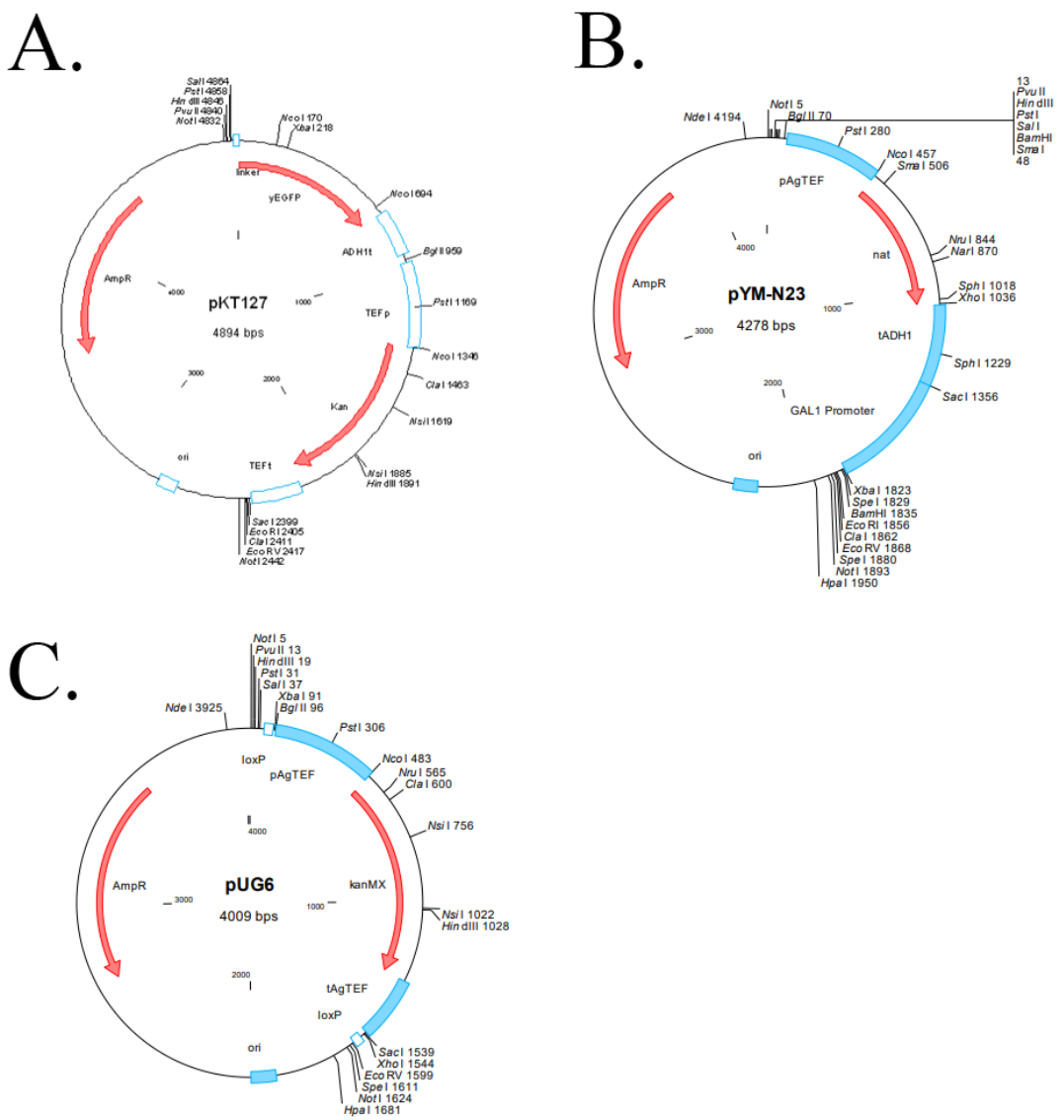

Figure 5. Maps of plasmids used in this thesis. A. Map of pKT127 plasmid. pKT127 (g418) plasmid was used for cassettes preparation for GFP tagging in BY and BY-*Vam6* strains. B. Map of pYM-N23 plasmid. pYM-N23 (NAT) plasmid was used for promotor exchange in BY-Gat1p-GFP strain. C. Map of pUG6 Plasmid. pUG6-25 (NAT) plasmid was used for gene deletion in BY-Gat1p-GFP strain. pUG6-25 was derived from pUG6 plasmid by Ing. Otakar Hlaváček, Ph.D. KanMX (Kanamycin resistance) in pUG6 was replaced by NatMX (Nourseothricin resistance) Plasmid maps were obtained from http://www.euroscarf.de (European Saccharomyces cerevisiae archive for functional analysis).

4.1.4 Primers used

To design the primers software SnapGene downloaded from https://www.snapgene.com was used.Gene sequences were obtained from SGD (Saccharomyces Genome Database): https://www.yeastgenome.org

Lists of genes for GFP tagging, deletion and promoter exchange are represented in the tables below.

Gene name	Coding sequence length including adjacent regions (1000bp each)
ACO1	4337
ERG26	3050
FAS1	8156
MDH2	3134
MRP4	3185
SSO1	2873

Table 1. List of genes for GFP tagging. These genes were chosen for future experiments on basis of the proteomic analysis performed in our laboratory.

Gene name	Coding sequence length including adjacent regions (1000bp each)
VPS3	5036
VPS8	5825
VPS33	4076
VPS41	4979
VPH2	2648
VAC7	5498
VAC14	4643

Table 2. List of genes for knock-outs and promoter change. These genes were chosen on basis of literature search as the candidate genes, products of which are potentially involved in TORC1 regulation.

4.1.4.a Transformation primers designed in this study

Primer name	Sequence
ACO1 GFP F	GGTTCAAATATGGTTCTGCCTTAAATAAAATTAAGGCCGATGAGAAGAAAggtgacggtgctggttta
ACO1 GFP R	CAGAAGACAAAATAAATAATAACCTTTAAAAGATTATAACAATGTTTTCAtcgatgaattcgagctcg
MRP4 GFP F	GAGCTGGCCAAAGAGGCTTGCAAAATCGCTTGGCCAGAAATAACGAAAAAggtgacggtgctggttta
MRP4 GFP R	TGGGCATATGTACAAGTTTAGGTTAACAAGCCAAAAGAAAATAAAAGTGTtcgatgaattcgagctcg
SSO1 GFP F	TTGTAGTCGTTGTTGTTGTCGTTGTTGTCCCAGCCGTTGTCAAAACGCGTggtgacggtgctggttta
SSO1 GFP R	TATACAAAAGGGGAGTTCGGATAGAATAGAAATATAGAAAATAGTTGGAAtcgatgaattcgagctcg
MDH2 GFP F	AAAATATCGATAAGGGCTTGGAATTCGTTGCATCGAGATCTGCATCATCTggtgacggtgctggttta
MDH2 GFP R	ACGGGAATATTATCAATTTGCTGCATTCTTATGCTTCGGTCCGATGCTCAtcgatgaattcgagctcg
FAS1 GFP F	CCGAACCTATCAAGGAAATCATCGACAACTGGGAAAAGTATGAACAATCCggtgacggtgctggttta
FAS1 GFP R	AGGAGTTTCAAAGTTAAATATTTCTTACGGTTATATAATCACTTAAGAAAtcgatgaattcgagctcg
ERG26 GFP F	GTATTGAAGAAGGAATTAACAAAACGTTGGCCTGGATGGACGAAGGTTTGggtgacggtgctggttta
ERG26 GFP R	CAACATACTATCTTTCGATAATCGGATCAAAAAGCTCCTAACGATTGCCAtcgatgaattcgagctcg

Table 3. Primers used for GFP-fusion in strains BY and BY-*vam6*.

Primer name	Sequence
VPH2 del F	AAAAGGTAAGATAGGATAATTGACGATTGGCATCACATAAAAGAACTCTAcagctgaagcttcgtacgc
VPH2 del R	AAGAATTATATGCTCTCGGATCTCGGAGTTCTTATTTATAAAATGATCAGgcataggccactagtggatctg
VPS41 del F	CAAAATAAAAAAGCATTTTAACGAAGAGTATATACCTACTATTAGACATTAcagctgaagcttcgtacgc
VPS41 del R	GTACATTCCTGAAGTGTACACTTGCCTTGTGTATTAAATGATGATTCGATAgcataggccactagtggatctg
VPS33 del F	GAAGAAAAAGCTGATATTGCCCATCTCCAACTTTATCAAATCATTTCACGcagctgaagcttcgtacgc
VPS33 del R	AAAAAGCACATTTGCATATACAAAAAATTAACAAATCTATCATATAATAAgcataggccactagtggatctg
VPS8 del F	AATAAGTGTAAAATATATATCTGCCGAGACCATTACTCATTACACCTAGAcagctgaagcttcgtacgc
VPS8 del R	TATAAATTTTACTTTTATGTAACCAAAGTTGTATTAAATATTTAGAAATGgcataggccactagtggatctg
VAC7 del F*	ATCGTTTCATCTCAGGCAAGTTAAAGCATTTGGGAAACGTGCTAGcagctgaagcttcgtacgc
VAC7 del R*	AAAGAAAAATACCCAGCTTTGACGAAAAAGCTACATTCTTAACACgcataggccactagtggatctg
VAC14 del F*	GATGCTGCTGTGCTTATCTGCTCAGGCTACAACAGGAACTGGAACcagctgaagcttcgtacgc
VAC14 del R*	GGTCCATTTCTTAACCAAAGATGCTTTCAATCAGGTAATGGGTAGgcataggccactagtggatctg
VPS3 del F*	AAGGAGACTACCTTTTTTTGGTTGCAACCATAATATTATAGAACCcagctgaagcttcgtacgc
VPS3 del R*	ATTTGAATTGTATGCCTGAACAGAAAAAGAATAGGTGGGCTCTTCgcataggccactagtggatctg

Table 4. Primers used for knock-out in strain BY-Gat1p-GFP. Primers marked with * were designed by Ing. Ladislava Hatáková. RNDr.

Primer name	Sequence
VPS41 pGAL F	AAAGCATTTTAACGAAGAGTATATACCTACTATTAGACATTAATGcgtacgctgcaggtcgac
VPS41 pGAL R	TGATTGTTGATCCAAAACAGAATCATTCTGATGATTATCTGTAGTcatcgatgaattctctgtcg
VPS33 pGAL F	AGCTGATATTGCCCATCTCCAACTTTATCAAATCATTTCACGATGcgtacgctgcaggtcgac
VPS33 pGAL R	ATCGGCATTTGTTAATGAAAATTTCTTAGTATTCCAAAATCTATTcatcgatgaattctctgtcg
VPS8 pGAL F	TAAAATATATATCTGCCGAGACCATTACTCATTACACCTAGAATGcgtacgctgcaggtcgac
VPS8 pGAL R	CGTATCGATGCTAGATCTGCTGTCGTGGTCAAGGCCATTTTGCTCcatcgatgaattctctgtcg
VPS3 pGAL F	GAGACTACCTTTTTTTGGTTGCAACCATAATATTATAGAACCATGcgtacgctgcaggtcgac
VPS3 pGAL R	TTCCTTTACTTCTTTTCCTTTGTCATTATTCGTTTTCTTTTTTACcatcgatgaattctctgtcg

Table 5. Primers used for promotor exchange in BY-Gat1p-GFP strain

4.1.4.b Primers for verification of clones and estimated product sizes for different primer combinations

ACO1-GFP				
primer F	ACO1 over. F	primer R	GFP over 589 R	product size (bp)
	GAGACCAAGGTATCAAGTGG		GATGGTCCAGTCTTGTTA	1001
MRP4-GFP				
primer F	MRP4 over. F	primer R	GFP over 589 R	product size (bp)
	CTCTAATGACAATCCCACCG		GATGGTCCAGTCTTGTTA	904
SSO1-GFP				
primer F	SSO1 over. F	primer R	GFP over 589 R	product size (bp)
	CAGCAGATCTTCTCACAAGC		GATGGTCCAGTCTTGTTA	972
MDH2-GFP				
primer F	MDH2 over.	primer R	GFP over 589 R	product size (bp)
	CATGGAACCTACTATGTGCC		GATGGTCCAGTCTTGTTA	876
FAS1-GFP				
primer F	FAS1 over. F	primer R	GFP over 589 R	product size (bp)
	GTTGCAGCTGGTGATCTAAG		GATGGTCCAGTCTTGTTA	1068
ERG26-GFP				
primer F	ERG26 over. F	primer R	GFP over 589 R	product size (bp)
	GCAAGATGTGCACAATGCAG		GATGGTCCAGTCTTGTTA	1264

Table 6. Primers for verification of clones with GPF fusion in BY and BY-*vam6* strains.

Verification of *VPS3* gene deletion					
primer F		primer R		product size (bp)	result
Vps3 del over F	GGATTTGAGAGGAGTTCAGA	Nat R	AGTACGAGACGACCACGAA	1134	+
Vps3 del over F	GGATTTGAGAGGAGTTCAGA	Vps3 over R	GACATTATCTTCTGCGCTGC	664	-
Vps3 over F	GGTTGCGGTGATGAAACAAT	Vps3 del over R	CATAGGCAAGTAACAGGAGA	607	-
Verification of *VPS8* gene deletion					
primer F		primer R		product size (bp)	result
vps8 over F ext	CTGGTTACGATGATATACCTG	Nat R	AGTACGAGACGACCACGAA	881	+
vps8 over F ext	CTGGTTACGATGATATACCTG	vps8 over R	CCCGTGATATTAGTGGAGAC	895	-
vps8 over F int	CACGACAGCAGATCTAGCAT	vps8 over R	CCCGTGATATTAGTGGAGAC	763	-
Verification of *VPS33* gene deletion					
primer F		primer R		produktbp	vysledek
vps33 over F ext	GCTGATATTGCCCATCTCCA	Nat R	AGTACGAGACGACCACGAA	811	+
vps33 over F ext	GCTGATATTGCCCATCTCCA	vps33 over R	GTCCACAGTTGGTTCGTTCA	855	-
vps33 over F int	CGATGGACTATGTGCTACCT	vps33 over R	GTCCACAGTTGGTTCGTTCA	770	-
Verification of *VP41* gene deletion					
primer F		primer R		product size (bp)	result
vps41 over F ext	GGATCACATTGAACCAGTGC	Nat R	AGTACGAGACGACCACGAA	1007	+
vps41 over F ext	GGATCACATTGAACCAGTGC	vps41 over R	GGCCCTTCATATCAGAGGAT	1006	-
vps41 over F int	GGATCAACAATCAGGCGAAC	vps41 over R	GGCCCTTCATATCAGAGGAT	734	-
Verification of *VPH2* gene deletion					
primer F		primer R		product size (bp)	result
vph2 over F ext	CGTGATAGGGTAATGAATGGC	Nat R	AGTACGAGACGACCACGAA	1137	+
vph2 over F ext	CGTGATAGGGTAATGAATGGC	vph2 over R	CCACATCTGCTACTAAGACCA	917	-
vph2 over F int	GCGAAAGTTCAAGAATAGCGC	vph2 over R	CCACATCTGCTACTAAGACCA	509	-
Verification of *VAC7* gene deletion					
primer F		primer R		product size (bp)	result
vac7 del over F	GACCTTGTAAGTCTTCCTGG	Nat R	AGTACGAGACGACCACGAA	1049	+
vac7 del over F	GACCTTGTAAGTCTTCCTGG	vac7 over R	CGTGGCATCGGAATCCATTA	531	-
vac7 over F	CGTGAAGCCAAGCACGAAAA	vac7 del over R	GAGTTGCATAACCCTCACTC	531	-
Verification of *VAC14* gene deletion					
primer F		primer R		product size (bp)	result
vac14 del over F	CGATGAGCTAGAGTTTGTTG	Nat R	AGTACGAGACGACCACGAA	1089	+
vac14 del over F	CGATGAGCTAGAGTTTGTTG	vac14 over R	CGGCCAACATCGTTTATTCC	556	-
vac14 over F	CATCCGTTTCTGCATAAGTG	vac14 del over R	TCAGTGGTGTTACCGAGAAG	741	-

Table 7. Primers for verification of clones with selected genes deletion in BY-Gat1p-GFP strain. Symbol "+" represents a positive result, where band is detectible and it corresponds to the calculated product size
Symbol "-" represents a negative result, where a band is not detectible due to the part of gene being deleted. If the band of calculated size is detectible, then the part of gene was not deleted, therefore the clone cannot be concluded as successfully transformed.

GAT1-GFP-pGAL VPS3					
primer F		primer R		product size (bp)	result
VPS3 over F	GCAGCGCAGAAGATAATGTC	VPS3 over R	CTTCGTGCGCACAAGCTTTA	576	+
Gal F	TTCCTGAAACGCAGATGTGC	VPS3 over R	CTTCGTGCGCACAAGCTTTA	1276	+
GAT1-GFP-pGAL VPS8					
primer F		primer R		product size (bp)	result
vps8 over F ext	CTGGTTACGATGATATACCTG	Nat R	AGTACGAGACGACCACGAA	846	+
Gal F	TTCCTGAAACGCAGATGTGC	vps8 over R	CCCGTGATATTAGTGGAGAC	1204	+
GAT1-GFP-pGAL VPS33					
primer F		primer R		product size (bp)	result
VPS33 over F ext	GCTGATATTGCCCATCTCCA	Nat R	AGTACGAGACGACCACGAA	776	+
Gal F	TTCCTGAAACGCAGATGTGC	vps33 over R	GTCCACAGTTGGTTCGTTCA	1234	+
GAT1-GFP-pGAL VPS41					
primer F		primer R		product size (bp)	result
VPS41 F ext	GGATCACATTGAACCAGTGC	Nat R	AGTACGAGACGACCACGAA	972	+
VPS41 F int	GGATCAACAATCAGGCGAAC	VPS41 over R	GGCCCTTCATATCAGAGGAT	734	+
Gal F	TTCCTGAAACGCAGATGTGC	Vps41 over R	GGCCCTTCATATCAGAGGAT	1189	+
GAT1-GFP-pGAL VPH2					
primer F		primer R		product size (bp)	result
VPH2 over F ext	CGTGATAGGGTAATGAATGGC	Nat R	AGTACGAGACGACCACGAA	1102	+
Gal F	TTCCTGAAACGCAGATGTGC	Vph2 over R	CCACATCTGCTACTAAGACCA	970	+

Table 8. Primers for verification of clones with promotor exchange in BY-Gat1p-GFP strain. Symbol "+" represents a positive result, where band is detectible, therefore it corresponds to the calculated product size.

4.1.5 Medium used

Liquid medium:

Liquid YEPG medium:

Component	Concentration
Yeast Extract	1% (w/v)
Peptone	1% (w/v)
Glucose	2% (w/v)

Liquid YEPG medium contains antibiotics, this was used for yeast cultivation before transformation. Antibiotic Edicine was added to avoid bacterial contamination of medium.

Solid media:

Solid YEPG medium:

Component	Concentration
Yeast Extract	1% (w/v)
Peptone	1% (w/v)
Agar	2% (w/v)
Glucose	2% (w/v)

Solid YEPG medium with addition of relevant antibiotic was used for selection of positive clones after the transformation. Antibiotics were also used to avoid any bacterial contamination of medium. Antibiotics used are shown in section 4.1.7.

GM (Glycerol medium):

Component	Concentration
Glycerol	3% (w/v)
Agar	2% (w/v)
Yeast lysate	1% (w/v)

After sterilization of medium following chemicals were added: 10 ml of 1M $CaCl_2$, 10 ml of 5% glucose, 10 ml of Uracil (2mg/ml) and 10ml of 96% Ethanol.
For preparation of GM BKP medium, BKP with 10ml of ethanol was added.

GM medium with addition of BKP was used for visualization of development phases of colonies. Colonies grown on GM + BKP, were later used for isolation of U and L cells for Western Blot analysis.

GM medium without BKP was used for observation of morphology changes. Colonies which grown on GM medium were later used for preparation of colony sections.

Storing medium:

Component	Concentration
Glycerol	60% (v/v)
Glucose	10% (w/v)
Peptone	2% (w/v)
Yeast lysate	1% (w/v)

Storing medium was used for long-term storing of transformed strains.

4.1.6 Other chemicals used in experiments in this thesis

1 M LiAc	10,2 g CH3COOLi dissolved in 100 ml H2O
50 % PEG	50 g PEG fill with H2O to 100 ml
BKP in EtOH	100 mg BKP dissolved in 10 ml 96 % EtOH
5x TBE	24,2 g of 0,2M TRIS, 27,9 g of 0,45M Boric Acid, 3,72g of 10mM EDTA (pH 8) dissolved in 1 l H2O
0,5 TBE	100 ml TBE + 900 ml H2O
2mg/ml Uracil	0,2g of uracil dissolved in 100 ml H2O
5% Glucose	5g of Glc + 100 ml H2O
1M CaCl2	14,7g in 100 ml H2O
1M NaOH	1g NaOH + 25ml H2O
20mM NaOH for DNA isolation	20 µl 1M NaOH + 980 µl H2O

4.1.7 Antibiotics used

Antibioitic	Concentration	Purpose of use
Edicine	0,002% (w/v)	Used for prevention of bacterial contamination.
G418	0,02% (w/v)	Used for selection of positive clones after transformation.
Nourseothricin	0,01% (w/v)	Used for selection of positive clones after transformation.

4.1.8 Software

Software for primer design:

SnapGene

Software photo editing and scheme creation:

NIS-Elements AR 3.1

ImageJ 1.50i

Adobe Photoshop CS6

Databases:

Saccharomyces Genome Database (SGD): www.yeastgenome.org
National Center for Biotechnology Information (NCBI): www.ncbi.nlm.nih.gov
Euroscarf: European Saccharomyces Cerevisiae Archive For Functional Analysis: http://www.euroscarf.de

4.2 Methods

4.2.1 Sterilization

Distilled and demineralized water, solutions, mediums, micropipettes tips, micro tubes and toothpicks were sterilized in autoclave under 120 kPa pressure for 20 minutes. Laboratory glassware was sterilized under 180 °C for 3 hours. Plastic tubes for centrifugation were sterilized with peroxyacetic acid vapor in closed polyethylene bag for at least 24 hours. Glass sticks for microbiology sowing were sterilized with ethanol and flame.

4.2.2 DNA isolation and DNA amplification

4.2.2.1 DNA isolation for PCR

1-day old biomass of *Saccharomyces Cerevisiae* was resuspended in 40 µl of NaOH. NaOH concentration was 20mM. The mixture of NaOH and biomass were than vortexed and denatured in 95°C for 15 minutes. After centrifugation supernatant containing DNA was used in PCR reaction for verification of clones after transformation.

4.2.2.2 DNA amplification

DNA amplification was used for transformation cassettes preparation and for verification of mutants after transformation. Reaction mixture components and thermal cycle conditions are shown in Tables 9 and 11.

4.2.3 Construction of new strains

New strains were prepared by transformation LiAc/SS-Carrier DNA/PEG method [47]. Transformation cassette, containing antibiotic resistance gene, was inserted into competent cells. Besides antibiotic resistance gene, transformation cassette contained GFP gene sequence or GAL promoter sequence. Both ends of cassette were homologous to the target sequence in genome. After transformation and cultivation on medium with antibiotics, clones were chosen for future experiments. Those clones had transformation cassette integrated into genome. Cassette integration in correct place of genome was verified by PCR. In case of knock-out it was also verified, if the target fragment was removed. In Figures 10 (5.1.1) and 47 (5.2.1) is shown the principle of new strains construction.

4.2.4 Transformation cassettes preparation

All transformation cassettes were prepared by PCR reaction in thin walled PCR tubes. Reaction mixture volume was 50 µl. LA DNA polymerase was used for GFP tagging and promoter change cassettes. PPP PCR Master Mix was used in case of gene knock-out. DNA amplification was performed in PCR cycler (BIOER GenePRO, BIOER XP). Reaction mixture composition and thermocycling conditions are shown in table 10. After PCR cassettes were verified by DNA electrophoresis by using agarose gel.

PCR mixture composition and thermocycling conditions for transformation cassettes.					
PCR mixture composition					
PCR - knock-out/promotor exchange cassettes			PCR - GFP tagging cassettes		
Component		Volume in µl	Component		Volume in µl
PPP Mastermix		25	ddH2O		32
ddH2O		19	DMSO		2
100x diluted plasmid (pUG6-25)		1	100x diluted plasmid (pKT127)		2,5
Primer F		2	Primer F		3
Primer R		2	Primer R		3
			LA buffer		5
			LA polymerase		1
			dNTP mix		2,5
Thermocycling conditions					
PCR program - knock-out/promotor exchange cassettes			PCR program - GFP tagging cassettes		
	Temperature	Time		Temperature	Time
dsDNA denaturation	94°C	2:00	dsDNA denaturation	94°C	3:00
ds DNA denaturation	94°C	0:15	ds DNA denaturation	94°C	0:30
Primer annealing	59°C	0:15	Primer annealing	60°C	0:30
Elongation	72°C	2:00	Elongation	68°C	2:30
Final elongation	72°C	7:00	Final elongation	68°C	10:00
Final hold	4°C	--:--	Final hold	4°C	--:--

Table 9. PCR mixture composition and thermocycling conditions for transformation cassettes.

4.2.5 Transformation

The transformation was performed as per LiAc/SS-Carrier DNA/PEG method [47]. 1-day old biomass of parental yeast strain was inoculated in 10ml of liquid YEPG. Then incubated on a shaker (Kühner, Lab-Therm; Multitron Standard, INFORS HT) overnight in 28°C. Next day 1ml of the culture was added to 25 ml of YEPG medium and incubated for approximately 4 hours to allow at least two cell divisions. Then cell number was calculated on a basis of spectrometry data (Novaspec Plus, Amersham Biosciences). The culture was centrifuged (3 000 g, 5 min, 22°C; Hettich Universal 320 R, Hettich Zentrifugen). Supernatant was removed and pellet was washed with 25 ml of distilled water and centrifuged again under same conditions. Supernatant was removed again, and pellet was resuspended in 1ml of distilled water and centrifuged. Appeared pellet was diluted for final cell concentration $2x10^7$ cells/ml. 100 µl of this suspension was centrifuged and the transformation mix was added to the pellet as per Table 10.

Component	**Volume [µl]**
1 M LiAc	36
50% (w/v) PEG	240
distilled water	40
ssDNA (10 mg/ml)	10

Table 10. Composition of the transformation mixture.

Transformation cassette in volume 34 µl was also added to cell pellet and transformation mix. After 20 minutes of heat-shock in 42°C transformation mixture was incubated in 28°C for next 20 minutes (Thermoblock Torrey Pines Scientific, Kühner, Lab-Therm; Multitron Standard, INFORS HT). Then the mixture was centrifuged, the pellet was resuspended in 1 ml of liquid YEPG and incubated in 28 °C for 3 hours on a shaker. After this incubation the mixture was centrifuged again, pellet was resuspended in 250 µl H_2O and then placed on Petri dishes with solid YEPG with relevant antibiotic for selection as shown in Figure 6 and cultivated in 28 °C for 3-5 days in thermostat.

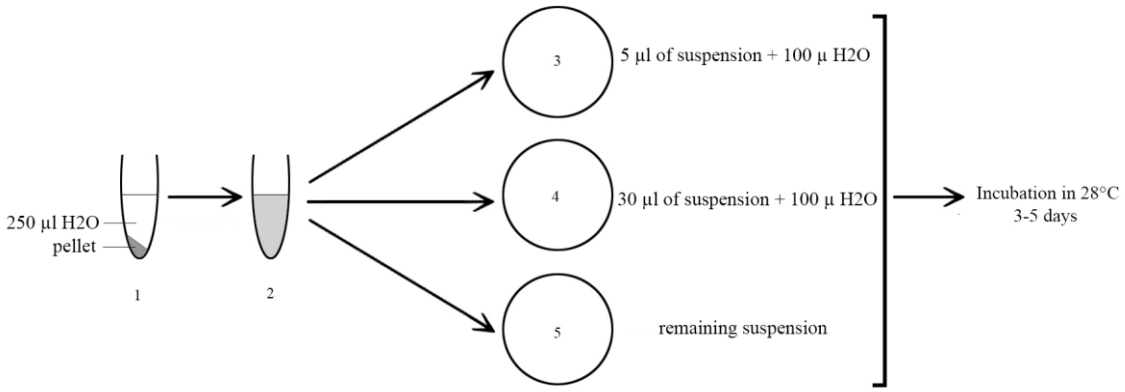

Figure 6. Scheme of plating suspension of cells after transformation. **1**. – Microtube with cell pellet after transformation and 250 µl H2O added. **2.** – Microtube with cell pellet after transformation resuspended in 250 µl H2O. **3., 4., 5.** – Petri dishes with YEPG solid medium and antibiotic for selection.

4.2.6. Clone verification

After transformation cell colonies grown on solid YEPG with relevant antibiotic for selection for 3-4 days were placed on a new YEPG with antibiotic and cultivated overnight in 28°C. DNA was then isolated from those colonies and verified with PCR and electrophoresis. Primers used for verification and calculated product sizes are shown in the tables 7, 8 and 9. In this phase only a presence of relevant antibiotic resistance verified. Positive clones were placed on a YEPG medium with edicine, incubated 1 more day and then transferred into a storage medium and stored in -80 °C in deepfreeze.

PCR mixture composition and thermocycling conditions for clone verification after transformation					
PCR - knock-out/promotor exchange verification			PCR - GFP tagging verification		
Component		Volume in µl	Component		Volume in µl
PPP mastermix (polymerase, dNTPs, Mg2+)		5	PPP mastermix (polymerase, dNTPs, Mg2+)		5
ddH2O		3	ddH2O		3
Primer F		1	Primer F		1
Primer R		1	Primer R		1
DNA		1	DNA		1
PCR program - knock-out/promotor exchange verification			PCR program - GFP tagging verification		
dsDNA denaturation	94°C	2:00	dsDNA denaturation	94°C	2:00
ds DNA denaturation	94°C	0:15	ds DNA denaturation	94°C	0:30
Primer anealing	59°C	0:15	Primer anealing	54°C	0:15
Elongation	72°C	1 minute for 1000bp	Elongation	72°C	1 minute for 1000bp
Final elongation	72°C	7:00	Final elongation	72°C	7:00
Final hold	4°C	--:--	Final hold	4°C	--:--

Table 11. PCR mixture composition and thermocycling conditions for clone verification after the transformation.

4.2.7. Clone purification – knock-out and promoter change in BY-Gat1p-GFP strain

Positive clones were placed on a YEPG medium with edicine, incubated 1 more day and then transferred into a storage medium and stored in -80 °C in deepfreeze. Monocolonies were also placed on a solid GM and cultivated in 28°C for another 4-5 days. Solid GM was used to restrict growth of mutants with respiration defects. DNA was then isolated from those colonies and verified with PCR and electrophoresis. Primers used for verification and calculated product sizes are shown in Tables 7 and 8. The principle of primer design is also illustrated in Figure 11 (5.1.2.1) and Figure 48 (5.2.2).

4.2.8. DNA visualization

After PCR DNA was visualized by electrophoresis on 1% agarose gel. Agarose was dissolved in TBE buffer, the final concentration was 1%. For DNA visualization was used EtBr, added in 1/2000 of volume of agarose/TBE mixture.

4.2.9. Clone storing

Yeast strains were stored in micro tubes with storing medium in -80 °C. For using a strain in experiment, small volume of biomass was placed on a YEPG + edicine and incubated in

thermostat overnight in 28 °C. Then this biomass was either placed on s relevant solid medium and cultivated in thermostat in 28 °C or placed into a liquid YEPG and incubated in 28 °C on a shaker (Kühner, Lab-Therm; Multitron Standard, INFORS HT).

4.2.10. Characterization of clones

4.2.10.1. Microscopy of cells

Fluorescent microscope Leica DMR was used for cell observation and JENOPTIK Progres® Mfcool camera was used for taking pictures of cells and colony sections. Images were taken in Nomarski contrast. For capturing GFP fluorescent signal filter 513852 and excitation filter 470/40 was used. Capturing of GFP signal was performed without Nomarski contrast.

4.2.10.2. Monitoring of colony development using magnifier loupe

Colony morphology was observed on a giant colonies of different age and in different conditions with binocular magnifier loupe Leica MZ 16 F, Nikon Digital Sight DS-U1 camera and lightening system Leica CLS 150X.

4.2.10.3. Monitoring of colony development visualized by changes in pH of surrounding medium

Ability of colonies to alkalize surrounding medium was observed in giant colonies. Giant colonies were placed on agar by especial manner that was developed in Yeast Colony Group Laboratory. A scheme of placing is shown in Figure 7. 6 giant colonies were placed on a Petri dish with glycerol medium with addition of BKP. Each giant colony grew from 10 µl of cell suspension in concentration 12 mg/ml.

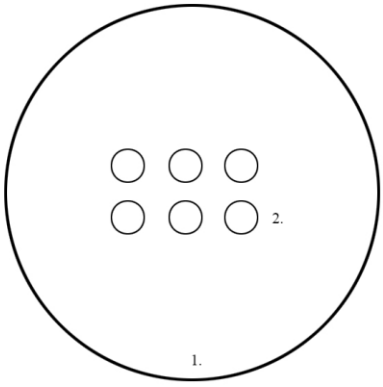

Figure 7. Scheme of giant colonies placing on Petri dish with glycerol medium for alkalization test. 1. – Petri dish with glycerol medium or glycerol medium with BKP. 2. – giant colonies – six per dish. Colonies were placed 1,5 cm from each other.

4.2.10.4. Microtome sections preparation

The method of colony section was developed in Yeast Colony Group Laboratory. This method is used for observation of colony differentiation. On 14th day, one colony was cut out and poured over with 3% agarose. After agarose harden, the sample was cut on microtome, sections were placed on microscope slide, covered with cover slip and analyzed.

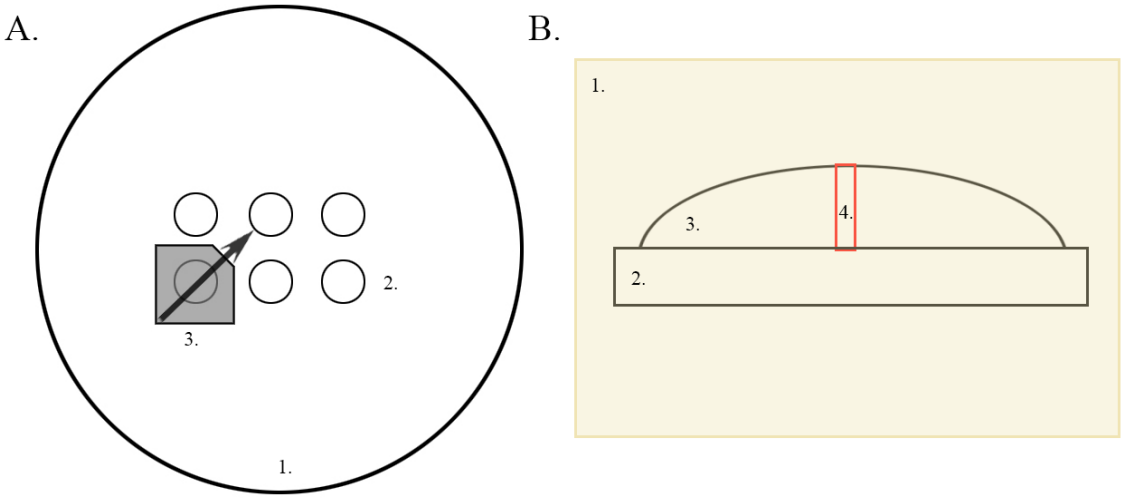

Figure 8. A. Scheme of excision of giant colony from GM or GM+BKP for section preparation. 1. – Petri dish with medium, 2. – giant colony, 3. – Shape of excision. Arrow shows the direction of future section. B. Scheme of giant colony section. 1. – Agarose, 2. – Medium, 3. – Giant colony, 4. – Part of colony section to analyze with microscopy.

4.2.10.5. U and L cells isolation for microscopy

U and L cells were separated with a razor blade. Cells of upper layer (U cells) were separated and placed into a 1 ml tube and resuspended with water. Cells of middle layer were removed and were not analyzed in this study. Cells of lower layer (L cells) were collected with a toothpick, placed into a 1 ml tube and resuspended with water. U and L cells were then analyzed by microscopy.

4.2.11. Protein quantification

4.2.11.1. U and L cells isolation for Western Blot analysis

U and L cells were separated with a razor blade. Cells of upper layer (U cells) were separated and placed into a 1 ml tube and weigh. Cells of middle layer were removed and were not analyzed in this study. Cells of lower layer (L cells) were collected with a toothpick and placed into a 1 ml tube and weigh. The cells were frozen in liquid nitrogen and stored in -80°C.

4.2.11.2. Extraction of proteins from cells

The biomass was resuspended in MES buffer with addition of protease inhibitors. The glass beads were added into the mentioned suspension, which was then homogenized using electric homogenizer FASTPREP. The homogenization was repeated five times (20s each) with at least two minutes breaks for cooling the samples. The homogenized suspension was then placed into new tubes and centrifuged. From the supernatant, 50µl was used for protein concentration quantification.

4.2.11.3. Protein concentration measurement – Bradford protein assay

The protein concentration was measured using spectrophotometer. 200 µl of Bradford reagent was added to 800 µl of diluted sample. After 10 minutes, the absorbance was measured. 800 µl of demineralized water with addition of 200 µl of Bradford reagent was used as a blank sample. 800 µl of BSA (µg/ml) with addition of 200 µl of Bradford reagent was used as a standard sample.

4.2.11.5. SDS-PAGE

Glass plates were assembled according to the vertical electrophoresis tank instructions. The separation gel was injected into a gap of two glass sheets and covered with isopropanol.

After that the polymerization of the separation gel the isopropanol was removed and washed out with water. The stacking gel was injected, and the comb was placed in order to ensure the formation of sample holes. After the stacking gel polymerized, the comb was removed.

Solutions and buffers:

Separation buffer:

Tris	1,5 M
SDS	0,4% (w/v)
pH	8,8

Stacking buffer:

Tris/HCl	0,5 M
SDS	0,4% (w/v)
pH	6,8

Separation gel – 9%:

Deionized H2O	4,5 ml
Acrylamide	3 ml
Separation buffer	2,5 ml
TEMED	10 ml
Ammonium persulfate	30 ml

Separation gel – 12%:

Deionized H2O	3,5 ml
Acrylamide	4 ml
Separation buffer	2,5 ml
TEMED	10 ml
Ammonium persulfate	30 ml

Ammonium persulfate (10%) was used for initiation of acrylamide polymerization.

Stacking gel – 4%:

Deionized H2O	3,05 ml
Acrylamide	0,65 ml
Stacking buffer	1,25 ml
TEMED	10 ml
Ammonium persulfate	30 ml

The samples were diluted with MES to concentration 0,5 µg/µ. 50 µl of diluted sample was mixed with 12,5 µl of denaturation buffer, and 12,5 µl of the mixture was placed in a sample hole of a gel. After the SDS electrophoresis the gel was removed from the cassette

and the stacking gel was trimmed away. The transfer stack was assembled as demonstrated in Figure 9.

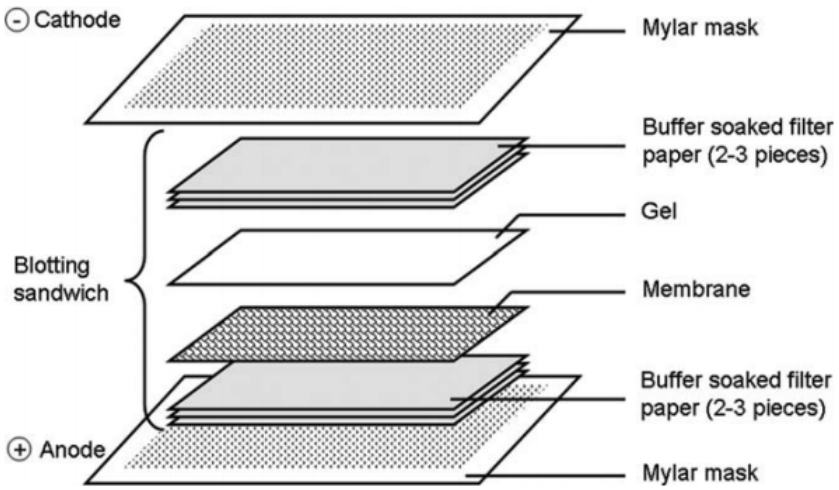

Figure 9. Transfer stack assembly. Obtained from Stewart&Veenstra, 2008 [48].

After blotting proteins to the membrane, the membrane standard was cut away. The membrane was colored in Coomassie Blue solution. The dry membrane was then scanned. The membrane was activated by wetting in 100% methanol, washed with water and then blocked with 1% casein + PBS and Tween for 1 hour. Membrane was then washed with PBS and Tween.

The membrane was incubated with GFP antibody (1000x diluted) for 1 hour. After the incubation the membrane was washed with PBS buffer and incubated with detection substrate. The sensitive sheet of photographic film is placed against the membrane in order to visualize the bands from the gel. Different exposure times were used, depending on a signal intensity. Photographic films were also scanned for further evaluation.

5 Results

5.1. Comparison of BY and vam6 strains: Colony morphology and level of expression of selected proteins

Previous proteomic analysis, performed in our laboratory, compared level of proteins in U and L cells separated from differentiated colonies of BY strain and the strain BY-*vam6* deleted in *VAM6* gene in genome-wide scale (non-published data). Based on this analysis, several proteins differentially present in U and L cells of BY and BY-*vam6* were selected for further analysis in this study. The major aim of this analysis was to confirm the differential expression of selected proteins in BY and BY-*vam6* colonies and to further characterize the profile of their expression in colonies. The list of proteins, their function, and data from the proteomic study (provided by prof. RNDr. Zdena Palková, CSc.) is summarized in the Table 12.

Considering the fact that in differentiated giant colonies different processes occur in U and L cells, such as activating of different metabolic pathway and gene reprogramming, it was assumed that the effects of Vam6p absence can affect either one or both of U and L cells. Further, these effects can also differ from each other. For example, proteomic data indicated that the deletion of *VAM6* gene affects the level of protein expression in U and L cells. Hence, according to proteomic data, the level of most of the proteins selected for this study seem to be affected more in U than in L cells by *VAM6* deletion.

To investigate, what effects will occur in cells lacking Vam6p, new strains with GFP-fused proteins of interest were created. Each protein of interest was fused with GFP in BY and BY-*vam6* strains. After transformation, successfully verified clones were selected for experiments that aimed to show the effects of *VAM6* deletion on protein-GFP expression. Those experiments are described below and include characterization of developmental phases of colonies formed by prepared strains, fluorescent microscopy of single cells, light microscopy of vertical cross-section of the colonies, and protein quantification by Western Blots.

Protein name	Protein function			
Aco1p	Aconitase involved in the tricarboxylic acid (TCA) cycle and required for mitochondrial genome maintenance[49]			
Erg26p	C-3 sterol dehydrogenase, catalyzation of the second of three steps required to remove two C-4 methyl groups from an intermediate in ergosterol biosynthesis[50]			
Fas1p	Beta subunit of fatty acid synthetase, which catalyzes the synthesis of long-chain saturated fatty acids[51]			
Mdh2p	Cytoplasmic malate dehydrogenase, catalyzes interconversion of malate and oxaloacetate [52]			
Mrp4p	Mitochondrial ribosomal protein of the small subunit [53]			
Sso1p	Plasma membrane t-SNARE, fusion of secretory vesicles at the plasma membrane and in vesicle fusion during sporulation[54]			
Protein name	Comparison of protein levels			
	vam6-U/BY-U	vam6-L/BY-L	vam6-U/vam6-L	BY-U/BY-L
Aco1p	7,81	1,02	5,51	0,72
Erg26p	3,05	1,02	1,47	0,49
Fas1p	2,63	1,12	1,43	0,61
Mdh2p	2,70	1,15	0,82	0,35
Mrp4p	3,82	0,79	1,49	0,31
Sso1p	3,58	1,80	1,10	0,55

Table 12. List of proteins selected for this study to analyse the impact of *VAM6* knockout. Upper part of table contains a brief description of protein function, and lower part contains data from proteomic analysis provided by prof. RNDr. Zdena Palková, CSc.

5.1.1. Construction of new strains

Aim: To prepare strains with proteins of interest fused with GFP at the C-terminus for following comparison of protein localization and level of protein expression in BY and vam6 strains.

New strains with GFP-tagged proteins were derived from BY and BY-*vam6* strains. Construction of new strains is described in Section 4.2.3. and also shown in Figure 10.

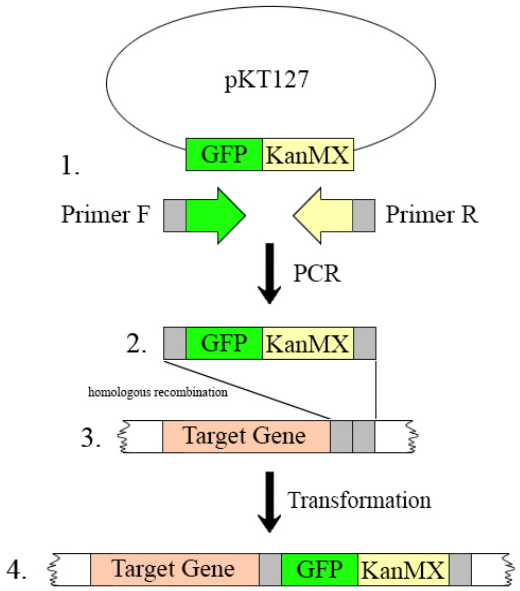

Figure 10. Scheme of target gene GFP-tagging in BY and BY-*vam6* strains. Fragment of plasmid pKT127 **(1.)** with GFP and KanMX gene (geneticin, G418 resistance) amplified by PCR. **2.** – transformation cassette. **3.** – target gene. **4.** – target gene is fused with GFP and KanMX gene. Final gene contains target gene fused with GFP gene and G418 resistance, which will be used for the following positive selection of clones

For preparation of strains with GFP-tagged proteins of interest, plasmid pKT127 was used (4.1.3, Figure 5). pKT127 plasmid contains gene coding GFP and the gene for geneticin resistance, which was used as a positive selection marker. Primers used for amplification of transformation cassettes are listed in Table 3 (4.1.4.a); the primers were designed using SnapGene software. Each forward primer consisted of 50 nucleotides of gene to be tagged excluding stop codon, fused to 18 nucleotides of GFP-KanMX locus of plasmid. Reverse primers consisted of 50 nucleotides of reverse complement of tagged gene fused to 18 nucleotides of reverse complement strand of GFP-KanMX locus on a plasmid. Transformation cassettes were prepared as described in 4.2.4, and transformation was performed as described in 4.2.5.

Strains prepared in this study are listed in Table 13.

Parental strain	Prepared Strain	Phenotype
BY	BY-Aco1p-GPF	MATα, *his3Δ, ura3Δ, leu2Δ, lys2Δ*, KanMX, *ACO1*-GPF
	BY-Erg26p-GFP	MATα, *his3Δ, ura3Δ, leu2Δ, lys2Δ*, KanMX, *ERG26*-GFP
	BY-Fas1p-GFP	MATα, *his3Δ, ura3Δ, leu2Δ, lys2Δ*,, KanMX, *FAS1*-GFP
	BY-Mdh2p-GFP	MATα, *his3Δ, ura3Δ, leu2Δ, lys2Δ*, KanMX, *MDH2*-GFP
	BY-Mrp4p-GFP	MATα, *his3Δ, ura3Δ, leu2Δ, lys2Δ*, KanMX, *MRP4*-GFP
	BY-Sso1p-GFP	MATα, *his3Δ, ura3Δ, leu2Δ, lys2Δ*, KanMX, *SSO1*-GFP
BY-*vam6*	BY-*vam6*-Aco1p-GPF	MATα, *his3Δ, ura3Δ, leu2Δ, lys2Δ*, *vam6Δ*, KanMX, *ACO1*-GPF
	BY-*vam6*-Erg26p-GFP	MATα, *his3Δ, ura3Δ, leu2Δ, lys2Δ*, *vam6Δ,* KanMX, *ERG26*-GFP
	BY-*vam6*-Fas1p-GFP	MATα, *his3Δ, ura3Δ, leu2Δ, lys2Δ*, *vam6Δ,* KanMX, *FAS1*-GFP
	BY-*vam6*-Mdh2p-GFP	MATα, *his3Δ, ura3Δ, leu2Δ, lys2Δ*, *vam6Δ*, KanMX, *MDH2*-GFP
	BY-*vam6*-Mrp4p-GFP	MATα, *his3Δ, ura3Δ, leu2Δ, lys2Δ*, *vam6Δ*, KanMX, *MRP4*-GFP
	BY-*vam6*-Sso1p-GFP	MATα, *his3Δ, ura3Δ, leu2Δ, lys2Δ*, *vam6Δ*, KanMX, *SSO1*-GFP

Table 13. List of strains prepared in this study. C-terminal GFP fusion aimed to enable observations, compare protein localization, and evaluate signal intensity in both BY and BY-*vam6* strains.

5.1.2. Strain verification

Newly prepared strains were verified by PCR and fluorescent microscopy. This verification aimed to confirm the successful GFP-fusion of proteins of interest.

5.1.2.1. Verification by PCR

Aim: To verify correct genomic cassette integration.

Afterwards, transformation clones were grown on YEPG medium with antibiotic geneticin. Geneticin (G418) is aminoglycoside antibiotic which blocks polypeptide synthesis by inhibiting the elongation step. As transformation cassette contained gene KanMX encoding product providing resistance to geneticin, only successfully transformed cells were supposed to grow on medium with geneticin. Clones lacking integrated cassettes were not supposed to have a proper photosynthesis and therefore, they were not meant to survive. This selection, however, can show false positive results, caused by mutations and other possible effects, even clones lacking KanMX gene can sometimes grow on geneticin and for this reason, clones growing on YEPG + G418 medium were verified by PCR.

Principle of PCR reaction, including PCR mixture composition and thermocycling condition, is described in Section 4.2.2. All used primers, calculated product sizes, and expected PCR reaction results are shown in Table 6, Section 4.1.4.a. Figure 11 highlights a principle of primers design for verification of transformation cassette presence in genome.

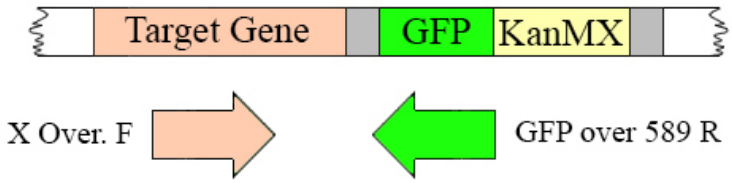

Figure 11. Primers design for verification after transformation. Arrows represent forward primers (orange arrow) and reverse (green arrow) primers. X is a target gene name.

Clones grown on YEPG + G418 medium were chosen for verification; they were transferred to a new Petri dish with new YEPG + G418 medium and were grown overnight in 28°C. The next day, DNA was isolated from the clones and added into a PCR mixture with corresponding primers. For negative control reaction, DNA isolated from parental strain was used. After PCR, DNA was visualized by electrophoresis on 1% agarose gel and bands detected on gel were compared to the calculated product size. Successfully verified clones with positive reaction and product size corresponding to calculated size, were then analyzed by fluorescent microscopy. In Figure 12 an example of verification by PCR reaction is shown.

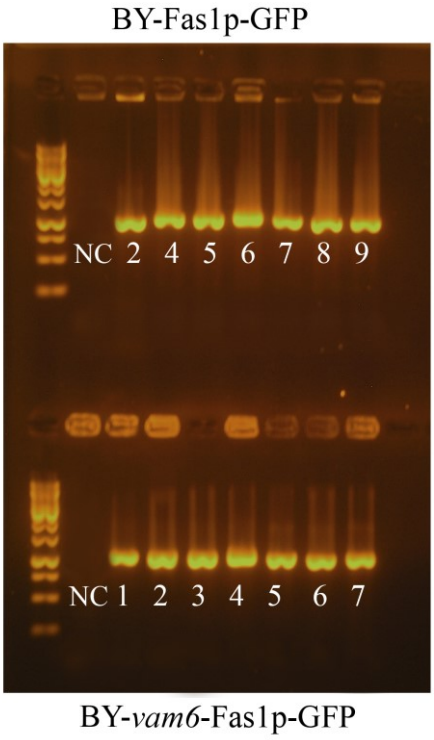

Figure 12. Image of electrophoresis gel – example of verification after transformation for strains BY-Fas1p-GFP and BY-*vam6*-Fas1p-GFP. Abbreviation NC represents negative control sample, where DNA isolated from parental strain was used. The size of amplified fragment is 1068 bp.

5.1.2.2. Verification by fluorescent microscopy

Aim: To confirm the presence of the fluorescent signal and to compare localization and intensity of a signal in BY and vam6 strains.

After the transformation and verification by PCR, selected clones were verified by fluorescent microscopy, as described in Section 4.2.10.1. Verification by fluorescent microscopy aimed to confirm the presence of fluorescent signal of GFP-tagged proteins.

Cellular localization of GFP-tagged proteins of interest was compared to the reference data from Saccharomyces Genome Database (SGD, www.yeastgenome.org/). As it was suggested that the protein localization and the level of protein expression might be affected by *VAM6* gene knockout, the localization and the intensity of fluorescent signal was also compared between strains derived from BY and BY-*vam6.* For each strain at least five clones were verified by fluorescent microscopy to ensure that the observed localization and intensity of the fluorescent signal is the same. A small amount of biomass was grown overnight on YEPG medium with addition of G418 was resuspended in water and analyzed by fluorescent microscopy. Data obtained in this experiment was then compared to reference data, as shown in Figure 13. All photos were captured in exposition 1,5s, with exception of BY-*vam6*-Mdh2p-GFP and BY-*vam6*-Sso1p-GFP where 3s exposition was used. All selected clones exhibited a fluorescent signal comparable between BY and BY-*vam6* strains.

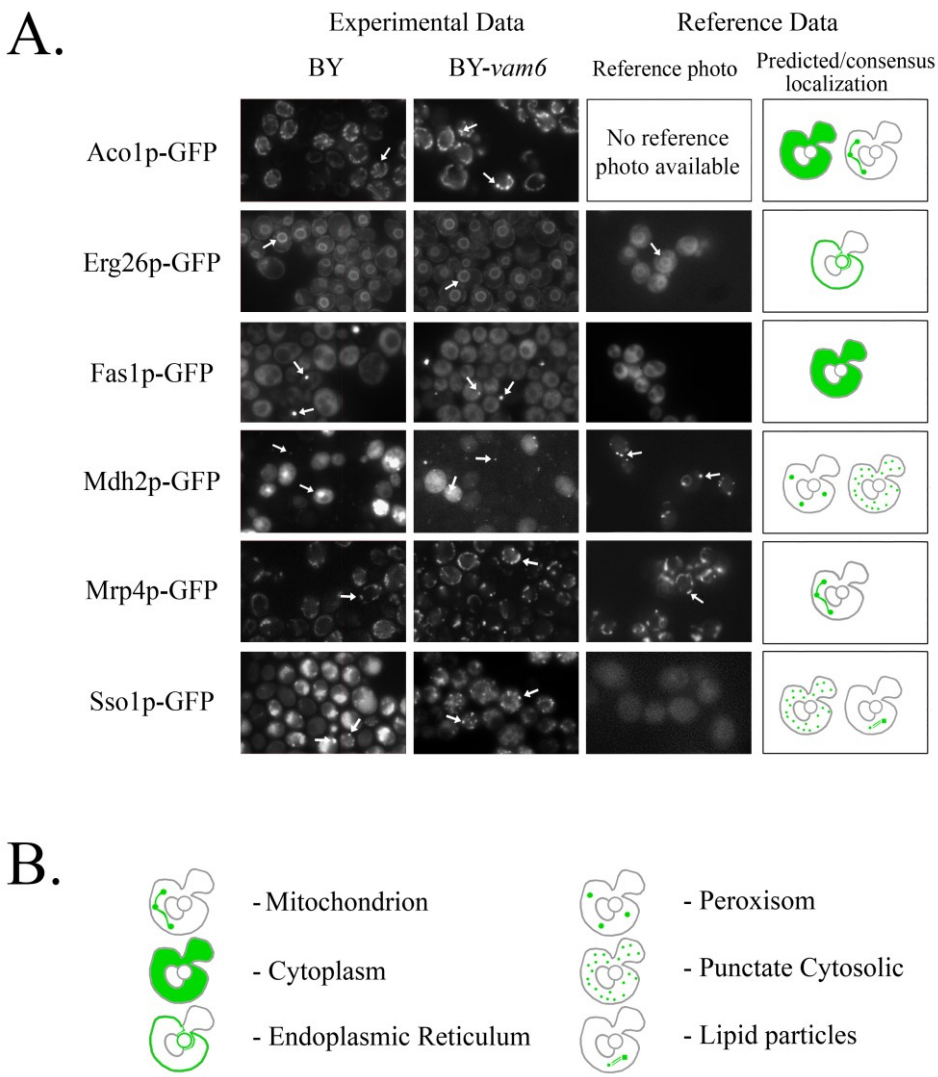

Figure 13. A. Comparison of fluorescent signal in strains with C-terminal GFP-fusion derived from BY and BY-*vam6* with reference data. All photos were taken in exposition 1,5s, except for BY-*vam6*-Mdh2p-GFP and BY-*vam6*-Sso1p-GFP, where 3s exposition was used. Arrows show target protein localization. Reference data were obtained from Saccharomyces Genome Database (www.yeastgenome.org/). **B.** Interpretation of symbolic images of predicted protein localization, obtained from Saccharomyces Genome Database (www.yeastgenome.org/). Green color represents localization of proteins tagged by GFP.

5.1.3. Monitoring of colony development

Aim: To compare the development of giant colonies formed by BY and BY-vam6 derived strains by monitoring of developmental phases visualized by changes in pH of surrounding medium. To characterize possible effects of C-terminal GFP-fusion on morphology of colonies.

S. cerevisiae strain BY and its derivatives including BY-*vam6* create smooth colonies, while growing on a semi-solid medium. Using glycerol medium with addition of BKP (GM+BKP, Section 4.1.5.), it is possible to track changes in pH of surrounding medium. pH dye indicator bromcresol purple changes color at pH ~ 6. 8 from yellow (acidic phase) to violet (alkali phase). [55]. pH changes of medium surrounding giant colonies are caused by production and release of ammonia, which is an important signal molecule in the process of colony development. Firstly, giant colonies pass through an acidic phase, followed by the alkali phase, and then again the acidic phase. In this experiment, only two phases were observed: first acidic and then alkali. Several clones from each transformation were verified by PCR and fluorescent microscopy and three of them were then chosen for further examination. Ability of colonies formed by transformed strains to alkalize surrounding medium was always compared to the parental strain colonies (BY and BY-*vam6*). In Figures 14-26, the lines represent different clones' development and alkalization period (days 5 to 20), and the rows represent the age of colonies in days.

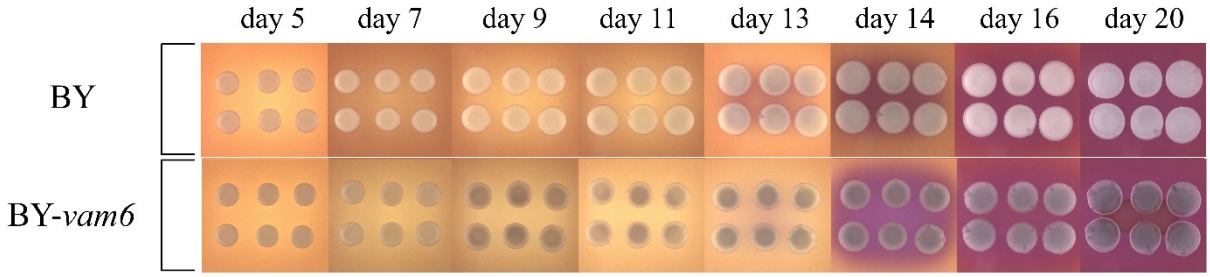

Figure 14. Monitoring of colony development. Comparison of BY and BY-*vam6* giant colonies alkalization.

As shown in Figure 14, the transition to alkali phase for both BY and BY-*vam6* strain started on 13th day. On 14th day BY-*vam6* alkalization is more intensive, than in BY strain. Starting from 11th day, giant colonies of BY-*vam6* strain grow slower in contrast with BY.

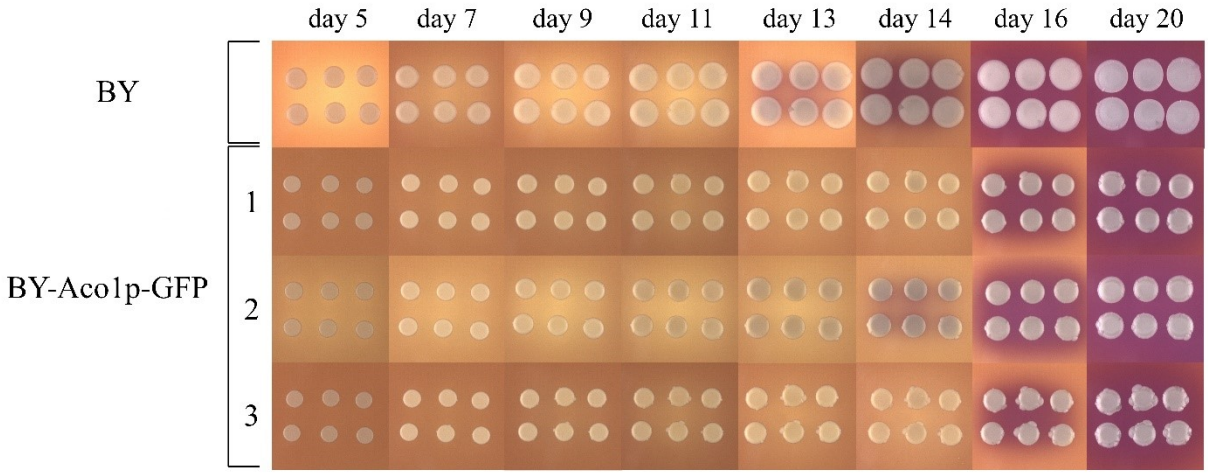

Figure 15. Monitoring of colony development of colonies formed by BY-Aco1p-GFP strain in comparison with wt strain BY. Clone 2 was chosen for further experiments.

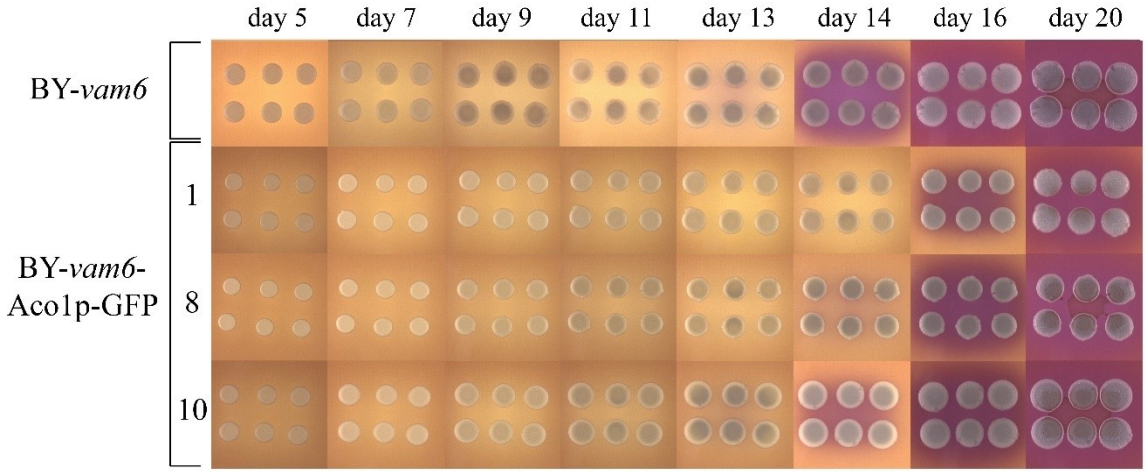

Figure 16. Monitoring of colony development of colonies formed by BY-*vam6*-Aco1p-GFP strain and comparison with parental strain BY-*vam6*. Clone 10 was chosen for further experiments.

BY-Aco1p-GFP and BY-*vam6*-Aco1p-GFP strains formed smaller colonies and their ability to alkalize surrounding medium was less efficient in comparison to parental strains (BY and BY-*vam6*, respectively). Those colonies were also more sectored than colonies formed by parental strains, as shown in Figures 15 and 16. For preparation of colony sections and microscopy, clone 2 (BY-Aco1p-GFP strain) and clone 10 (BY-*vam6*-Aco1p-GFP) were chosen.

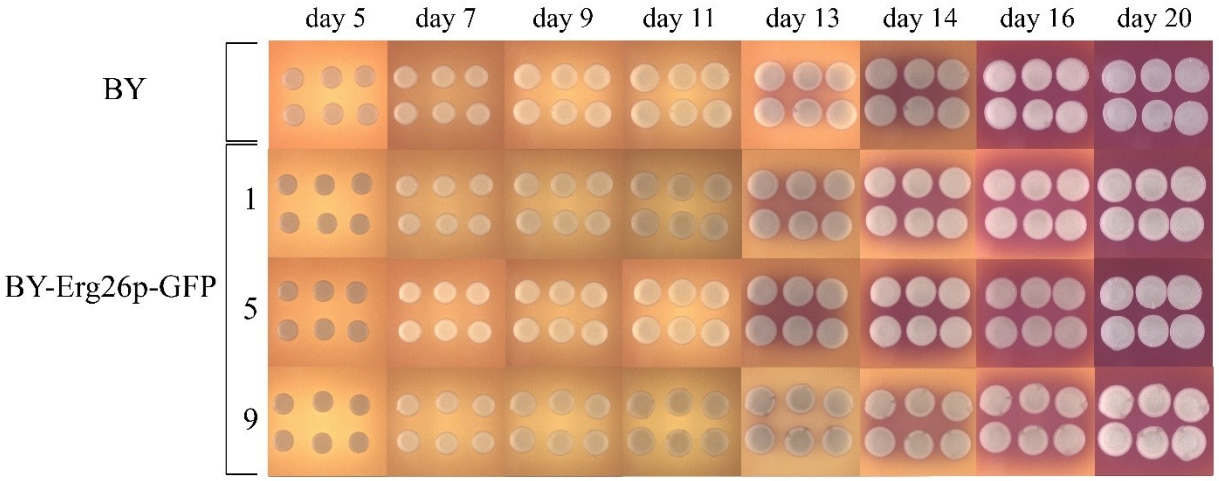

Figure 17. Monitoring of colony development of colonies formed by BY-Erg26p-GFP strain comparison with parental strain BY. Clone 1 was chosen for further experiments.

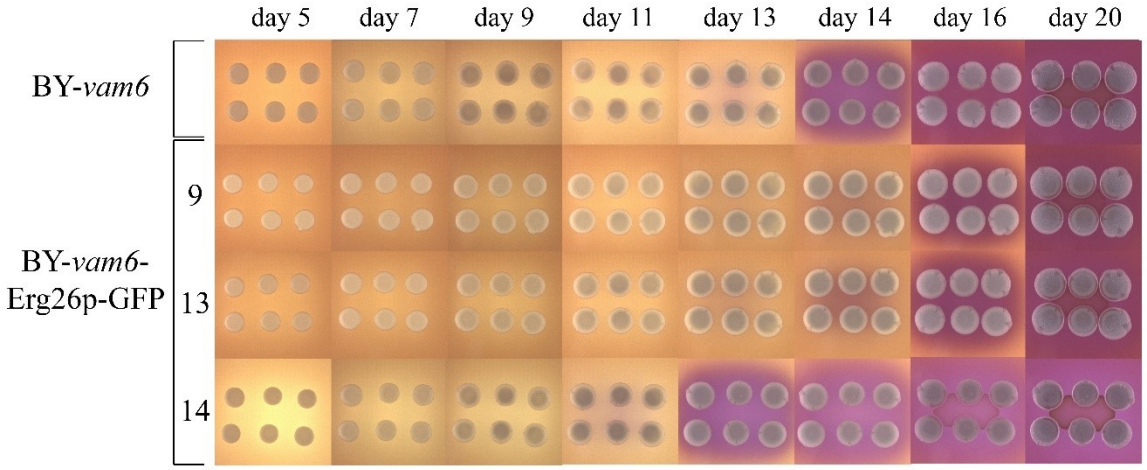

Figure 18. Monitoring of colony development of colonies formed by BY-*vam6*-Erg26p-GFP strain and comparison with parental strain BY-*vam6*. Clone 13 was chosen for further experiments.

BY-Erg26p-GFP and BY-*vam6*-Erg26p-GFP colony morphology resembled morphology of colonies of parental strains (Figures 17 and 18). However, the alkalization seemed to be comparable to parental strain only in case of BY-Erg26p-GFP strain. Two clones of BY-*vam6*-Erg26p-GFP strain delayed beginning of their colony alkalization. On the contrary, colonies of the third clone started to alkalize two days before the parental strains; furthermore, the alkalization was more intense. Clone 1 (BY-Erg26p-GFP) strain and clone 13 (BY-*vam6*-Erg26p-GFP) strain were chosen for further experiments.

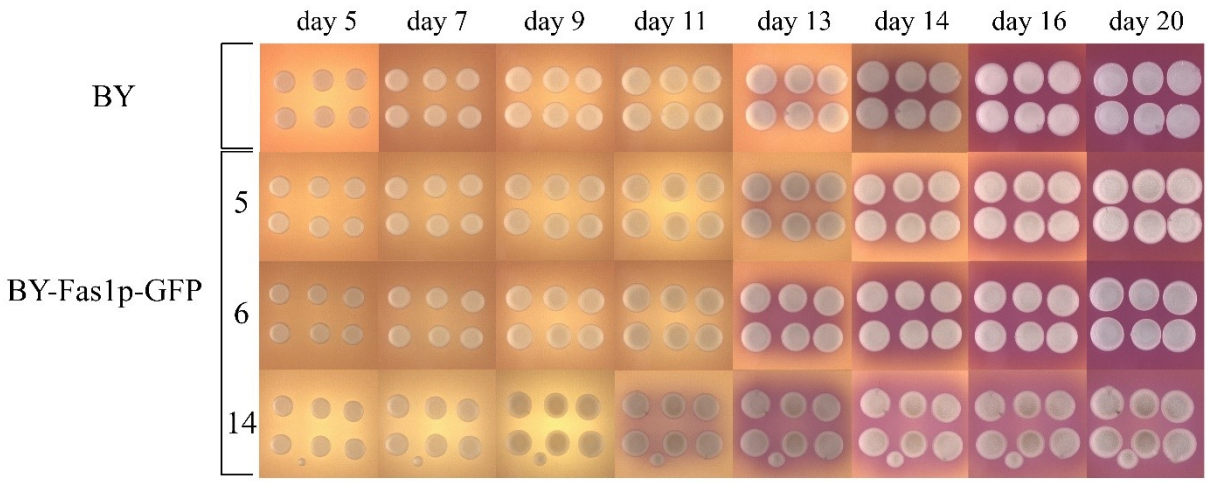

Figure 19. Monitoring of colony development of colonies formed by BY-Fas1p-GFP strain and comparison with parental strain BY. Clone 5 was chosen for further experiments.

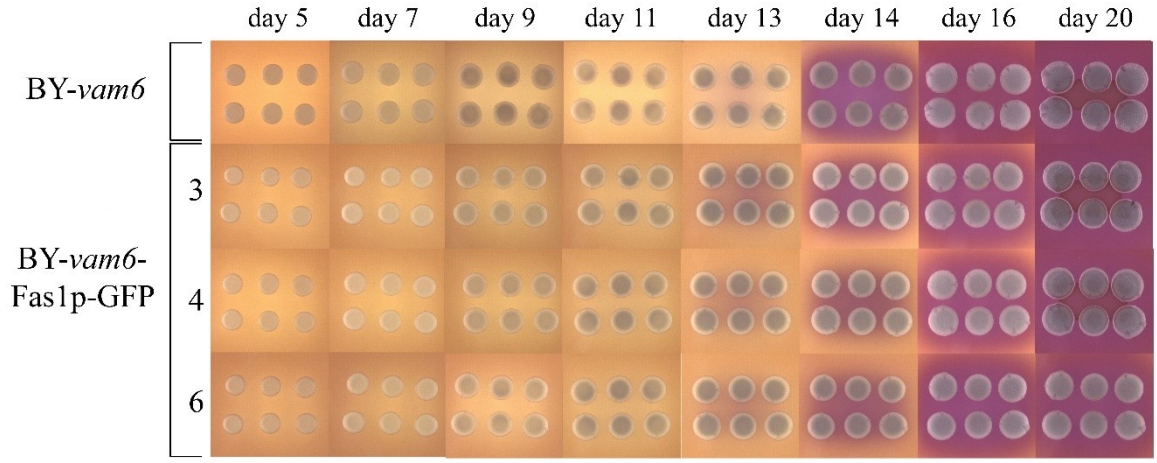

Figure 20. Monitoring of colony development of colonies formed by BY-*vam6*-Fas1p-GFP strain and comparison with parental strain BY-*vam6*. Clone 3 was chosen for further experiments.

Figures 19 and 20 show colony development of strains BY-Fas1p-GFP and BY-*vam6*-Fas1p-GFP. In BY-*vam6*-Fas1p-GFP strain alkalization of all clones was similar to the parental strain. Clone 3 from BY-*vam6*-Fas1p-GFP strain was chosen for additional experiments. Clone 5 from BY-Fas1p-GFP strain was chosen as the most comparable to wt.

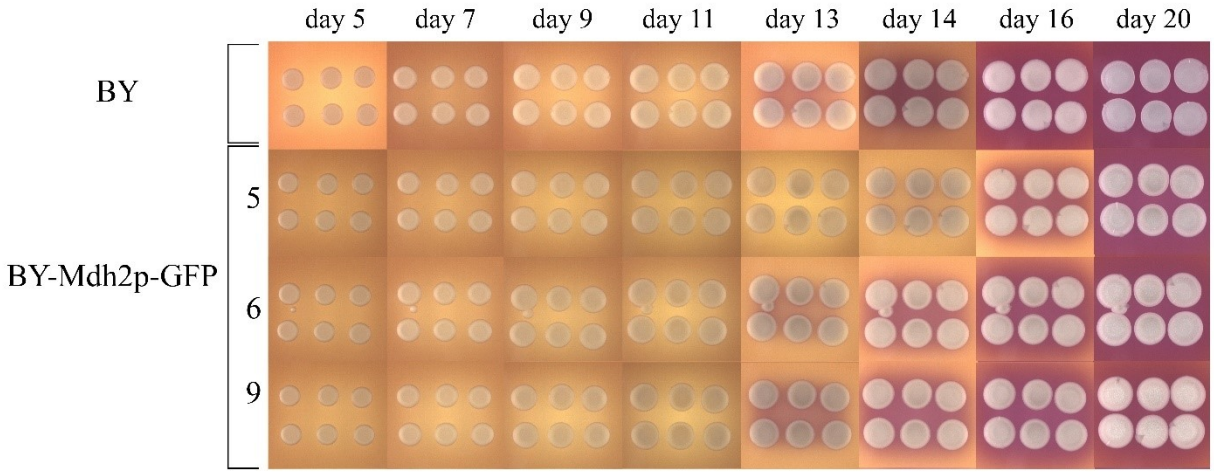

Figure 21. Monitoring of colony development of colonies formed by BY-Mdh2p-GFP strain and comparison with parental strain BY. Clone 9 was chosen for further experiments.

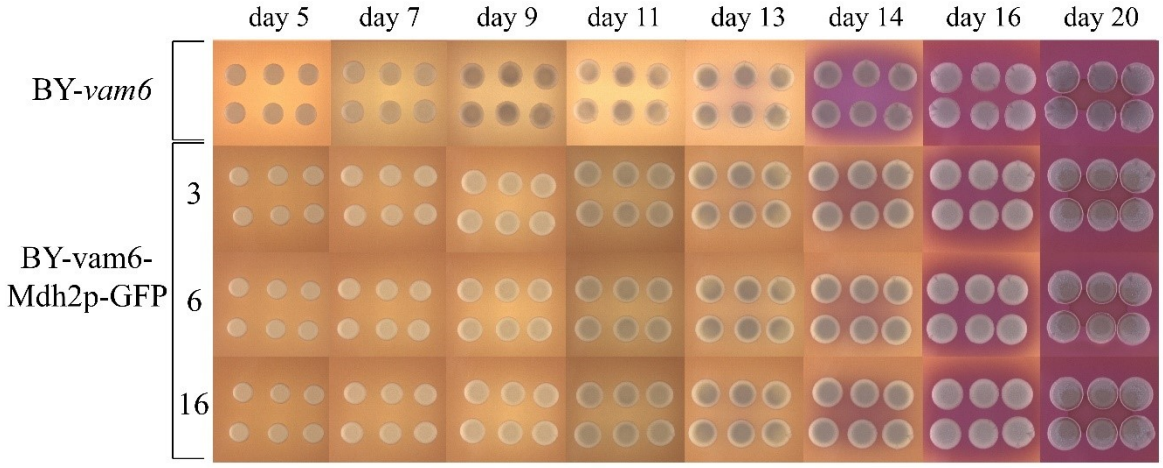

Figure 22. Monitoring of colony development of colonies formed by BY-*vam6*-Mdh2p-GFP strain and comparison with parental strain BY-*vam6*. Clone 16 was chosen for further experiments.

BY-Mdh2p-GFP strain alkalization test (Figure 21) shows that the alkalization ability of clones 6 and 9 is very similar to parental strain, and clone 5 alkalization is postponed, which was caused in this case by a thicker layer of GM in a Patri dish. For following experiment, clone 9 was chosen. In BY-*vam6*-Mdh2p-GFP strain testing none of examined clones were showing differences in morphology, however, alkalization started one day after parental strain and was less intensive (Figure 22).

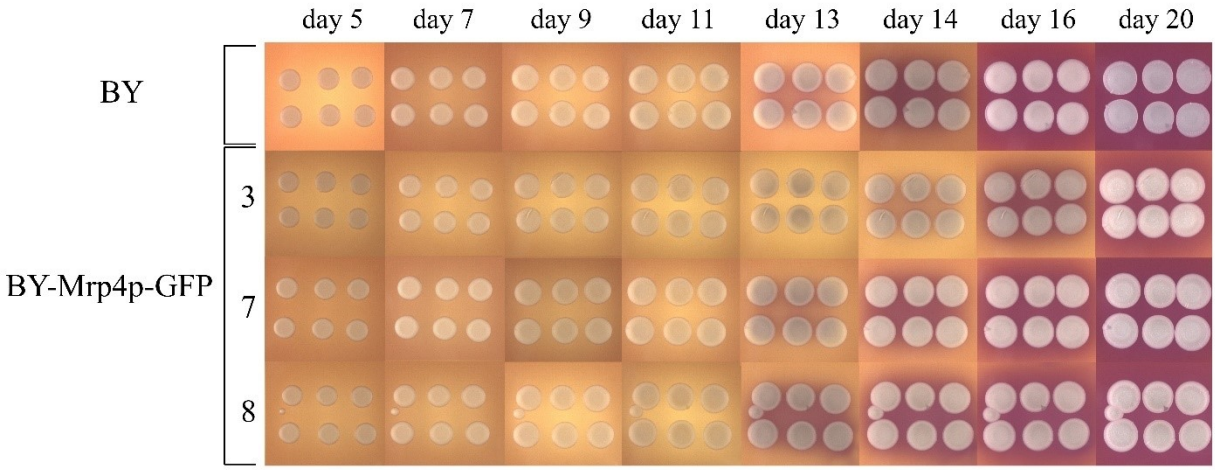

Figure 23. Monitoring of colony development of colonies formed by BY-Mrp4p-GFP strain and comparison with parental strain BY. Clone 7 was chosen for further experiments.

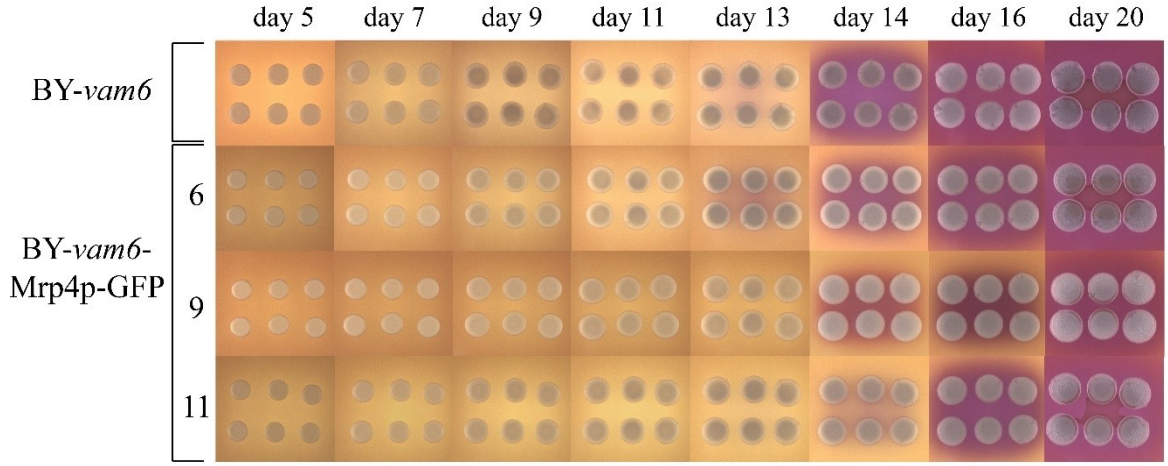

Figure 24. Monitoring of colony development of colonies formed by BY-*vam6*-Mrp4p-GFP strain and comparison with parental strain BY-*vam6*. Clone 6 was chosen for further experiments.

In both BY-Mrp4p-GFP and BY-*vam6*-Mrp4p-GFP strains (Figures 23, 24) alkalization differed between different clones. Clone 7 from BY-Mrp4p-GFP strain and clone 6 from BY-*vam6*-Mrp4p-GFP strain were chosen as mostly corresponding to parental strain.

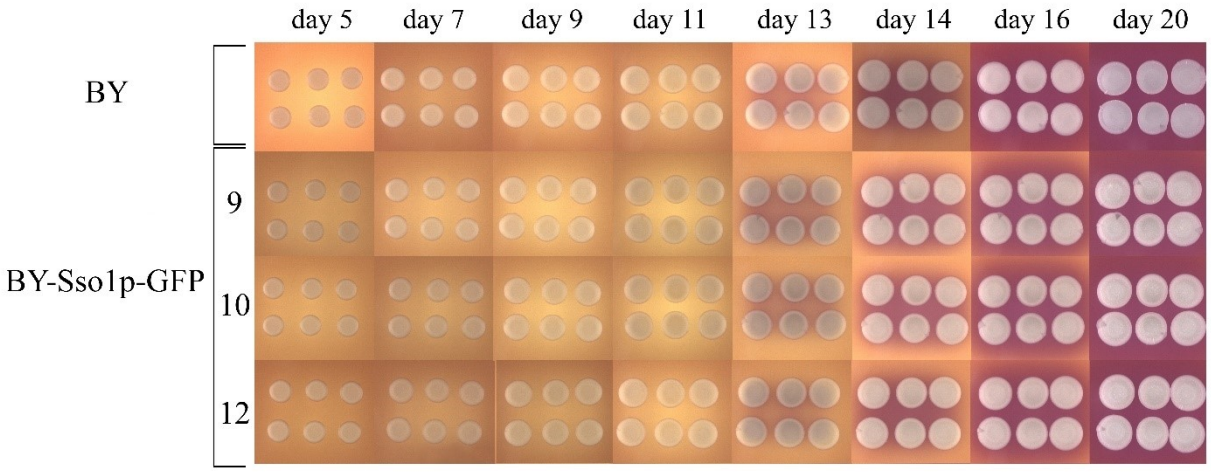

Figure 25. Monitoring of colony development of colonies formed by BY-Sso1p-GFP strain and comparison with parental strain BY. Clone 9 was chosen for further experiments.

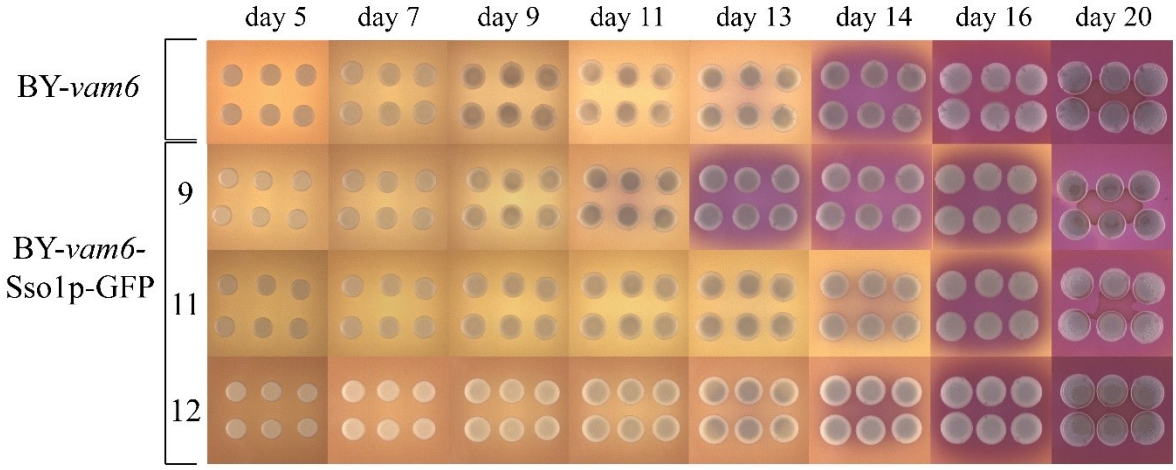

Figure 26. Monitoring of colony development of colonies formed by BY-*vam6*-Sso1p-GFP strain and comparison with parental strain BY-*vam6*. Clone 12 was chosen for further experiments.

BY-Sso1p-GFP strain shows almost identical alkalization in the case of all three analyzed clones (Figure 25). Clone 9 from BY-Sso1p-GFP strain was chosen for next experiments, and from BY-*vam6*-Sso1p-GFP (Figure 26) strain clone 12 was chosen, as mostly corresponding to parental strain.

5.1.4. Vertical sections within colonies

Aims:

1. To characterize differentiation to U and L cells of colonies formed by BY- and BY-vam6 derived strains. To inspect whether C-terminal GFP-fusion affects differentiation of colonies. 2. To compare GPF-signal intensity and a level of expression of GFP-tagged proteins of interest in U and L cells of BY- and BY-vam6 derived colonies

To investigate, if C-terminal GFP fusion has any effects on development of giant colonies, vertical sections were prepared (4.2.10.4) and observed with microscopy. For this experiment, 14-days-old giant colonies were used. Colonies for this experiment were selected on the basis of monitoring of colony development using pH-sensitive indicator BKP (Section 5.1.3). As it was assumed that localization and quantity of these proteins can differ between U and L cells of BY and BY-vam6 strains, and also between U and L cells within the particular colonies (Table 12), the U and L cells of 14-days-old were separated and examined by fluorescent microscopy.

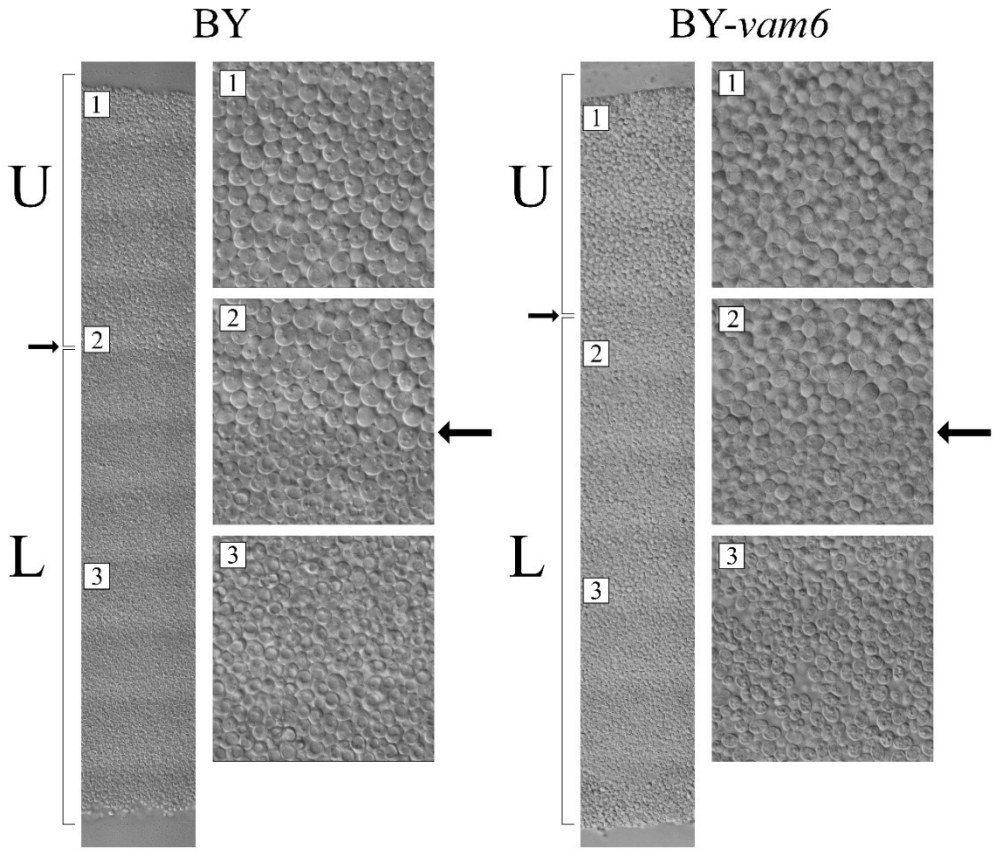

Figure 27. Vertical sections within giant colonies of BY and BY-*vam6* strains. Arrows show the boundary between U and L cells. Numbers on enlargement squares correspond with numbers on section, where the enlarged segment was taken from. Letters U and L represent upper and lower cells, respectively.

As shown in Figure 27, colonies created by both BY and BY-*vam6* strains differentiate two major subpopulations of cells with dissimilar morphology and well-defined boundary between upper and lower layer. As demonstrated in Figures 28-45, the differentiation ability of colonies created by the below mentioned strains, seemed to be partially affected by C-terminal GFP fusion. On these figures is also demonstrated the localization of selected proteins tagged by GFP. The localization is compared between U and L cells of colonies created by both BY and BY-*vam6* strains.

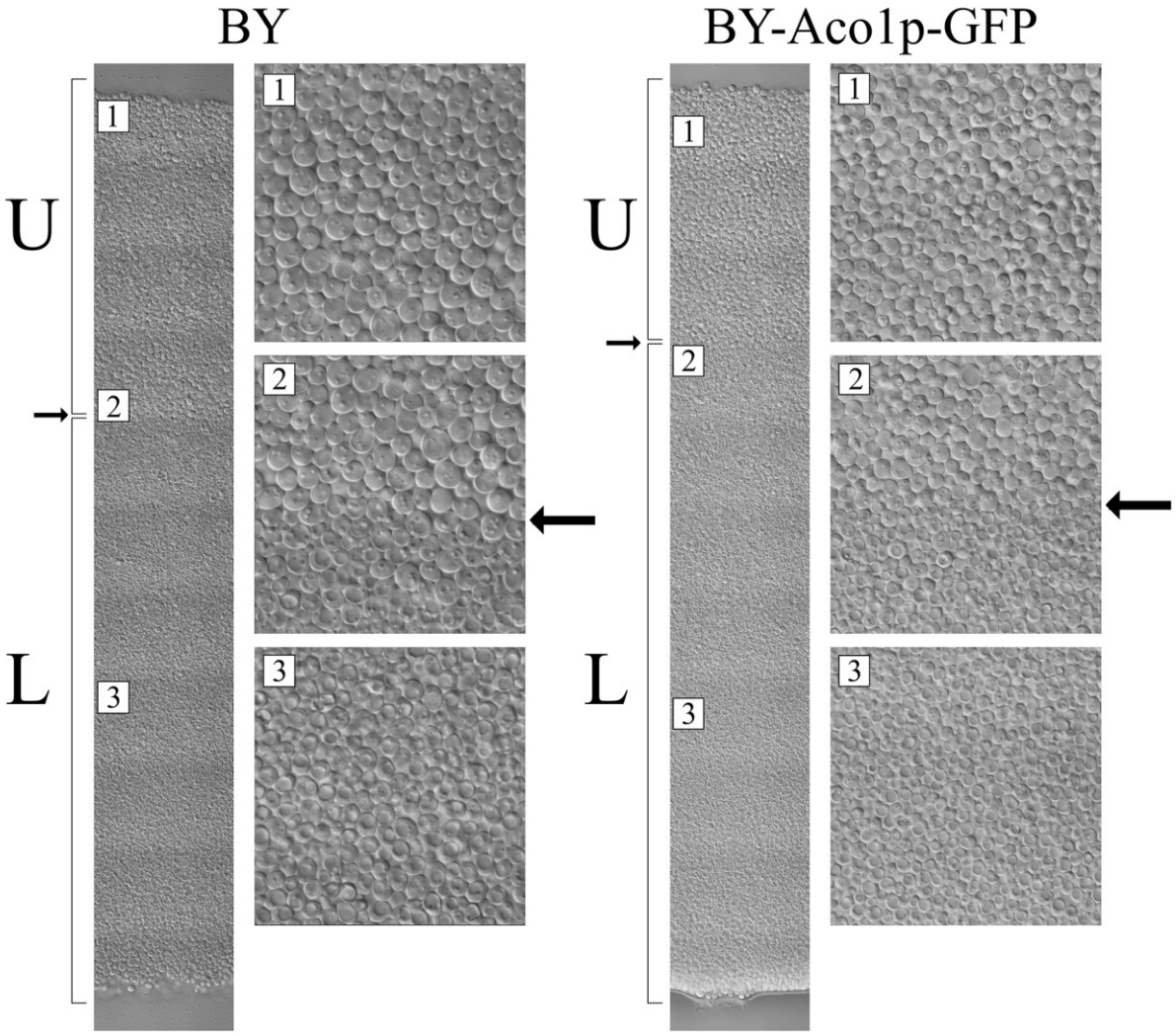

Figure 28. Vertical sections within giant colonies of BY and BY-Aco1p-GFP strains. Arrows show the boundary between U and L cells. Numbers on enlargement squares correspond with numbers on section, where the enlarged segment was taken from. Letters U and L represent Upper and Lower cells, respectively.

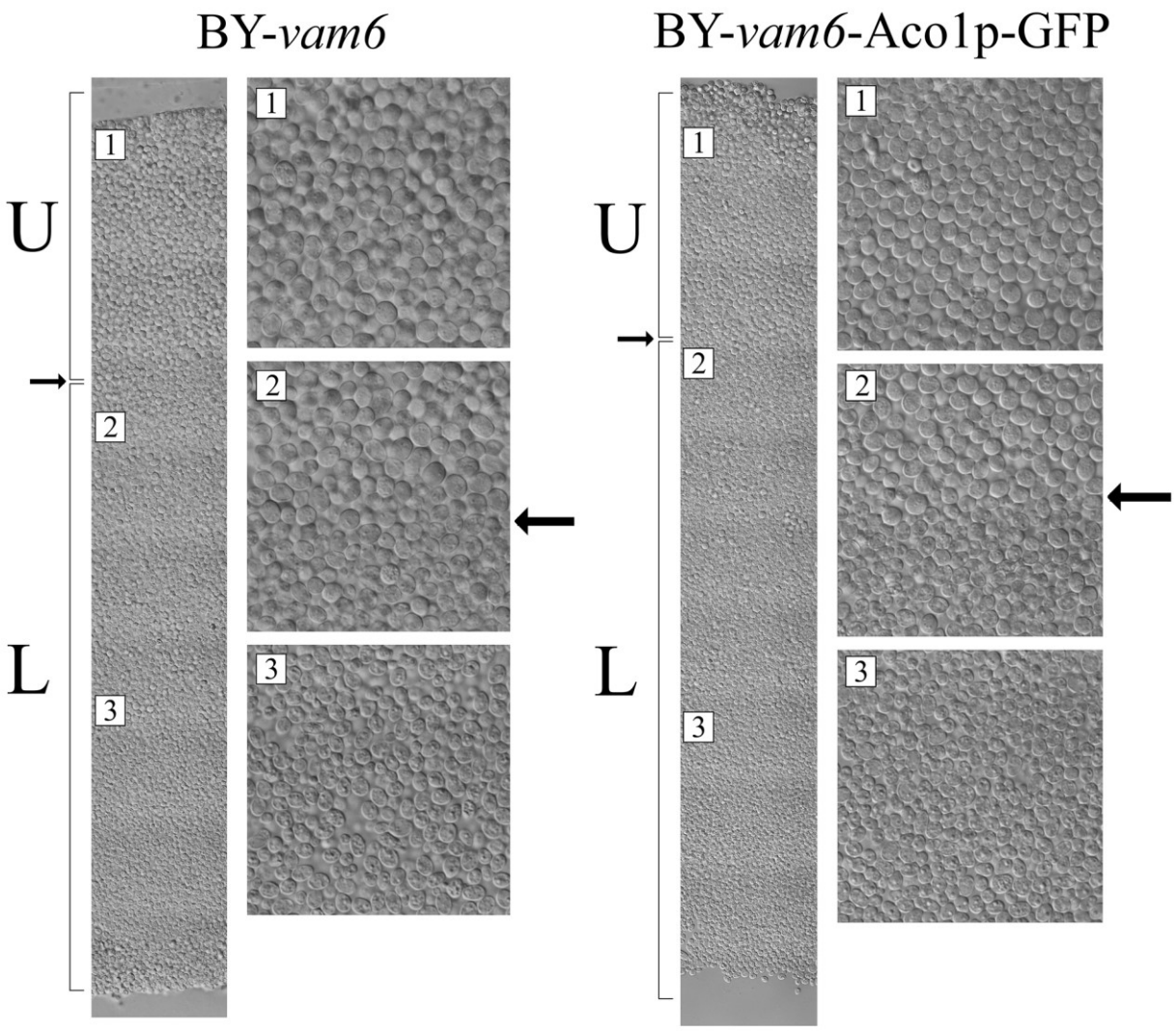

Figure 29. Vertical sections within giant colonies of BY and BY-*vam6*-Aco1p-GFP strains. Arrows show the boundary between U and L cells. Numbers on enlargement squares correspond with numbers on section, where the enlarged segment was taken from. Letters U and L represent Upper and Lower cells, respectively.

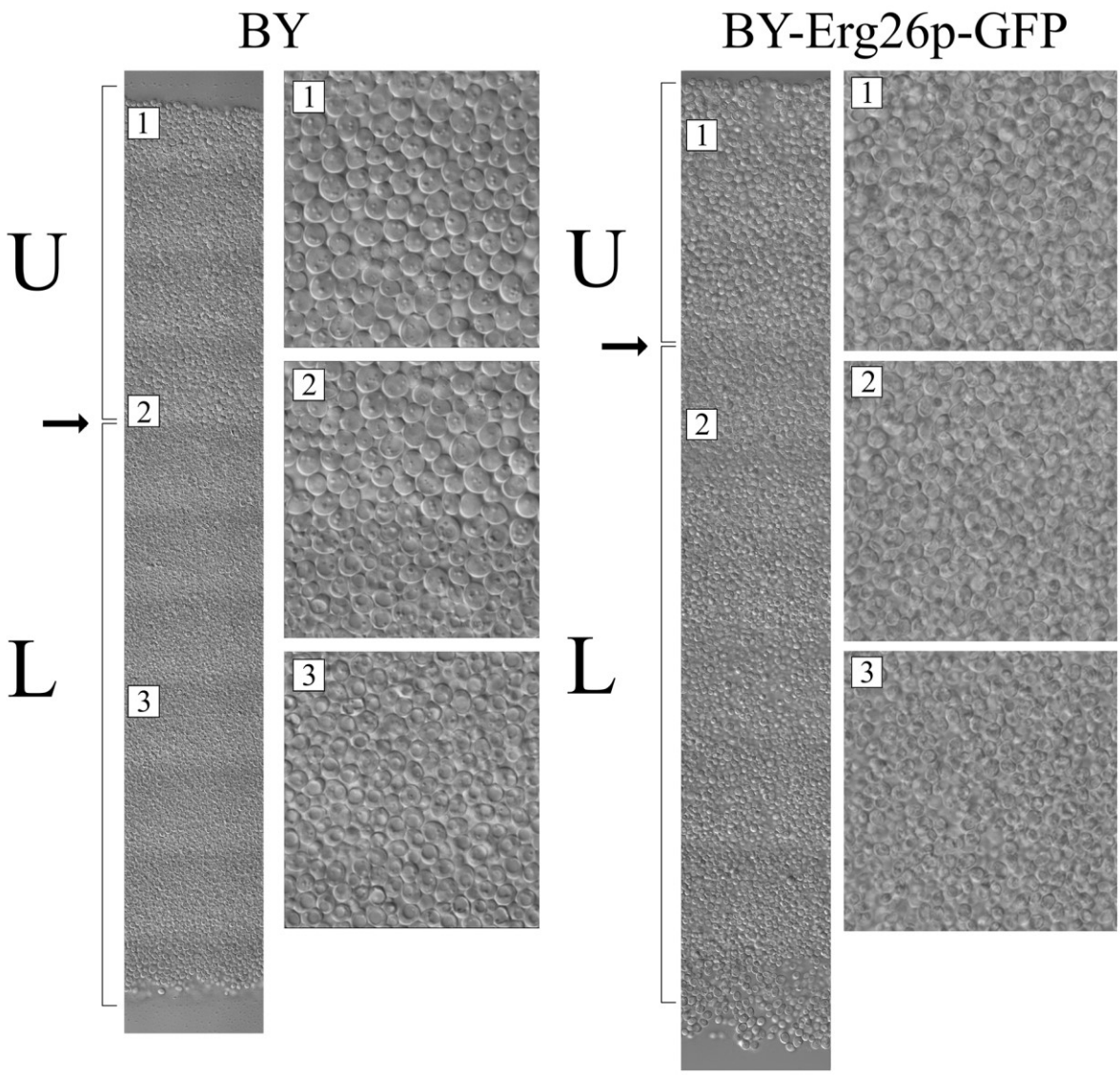

Figure 30. Vertical sections within giant colonies of BY and BY-Erg26p-GFP strains. Arrows show the boundary between U and L cells. Numbers on enlargement squares correspond with numbers on section, where the enlarged segment was taken from. Letters U and L represent Upper and Lower cells, respectively.

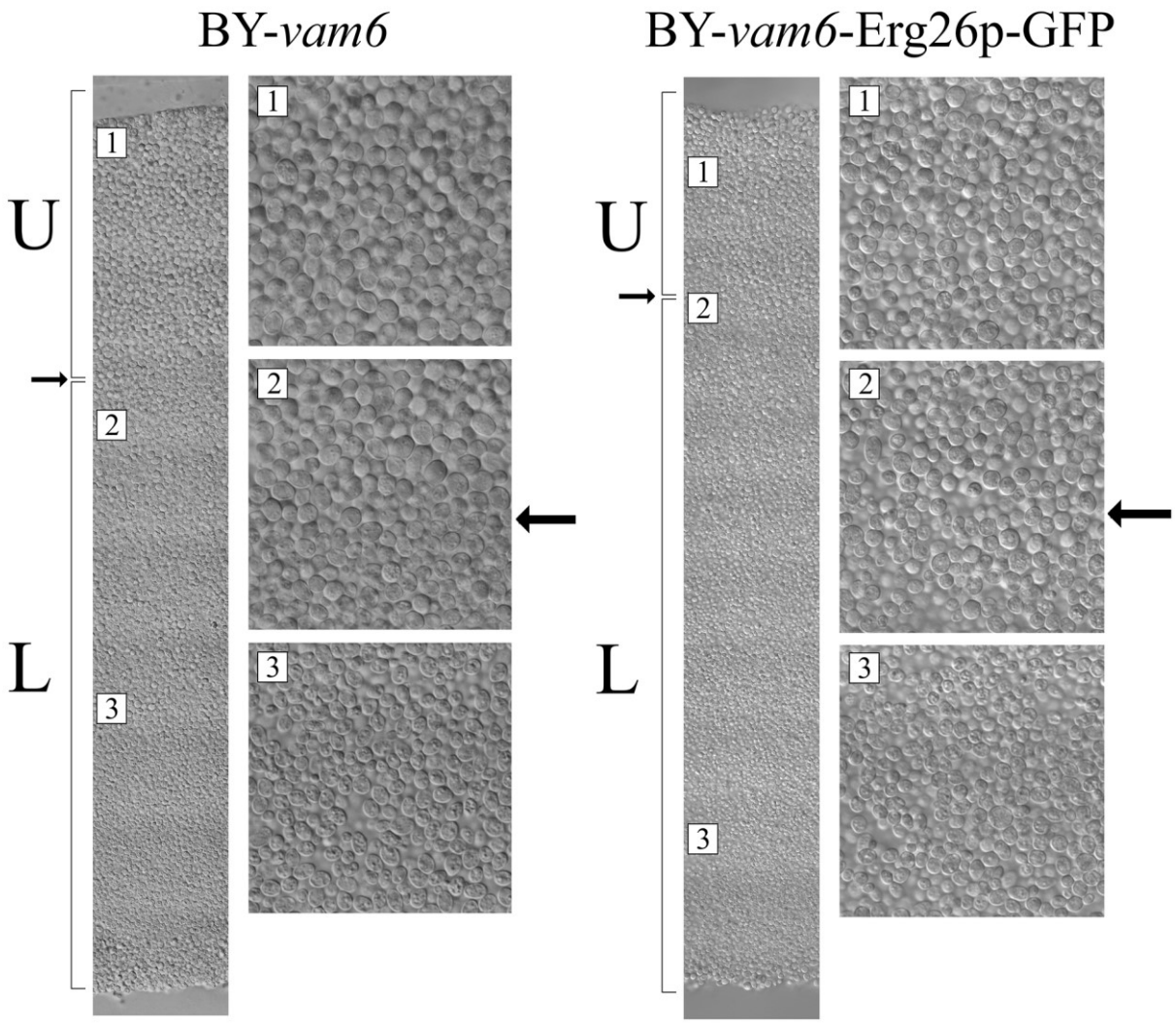

Figure 31. Vertical sections within giant colonies of BY and BY-*vam6*-Erg26p-GFP strains. Arrows show the boundary between U and L cells. Numbers on enlargement squares correspond with numbers on section, where the enlarged segment was taken from. Letters U and L represent Upper and Lower cells, respectively.

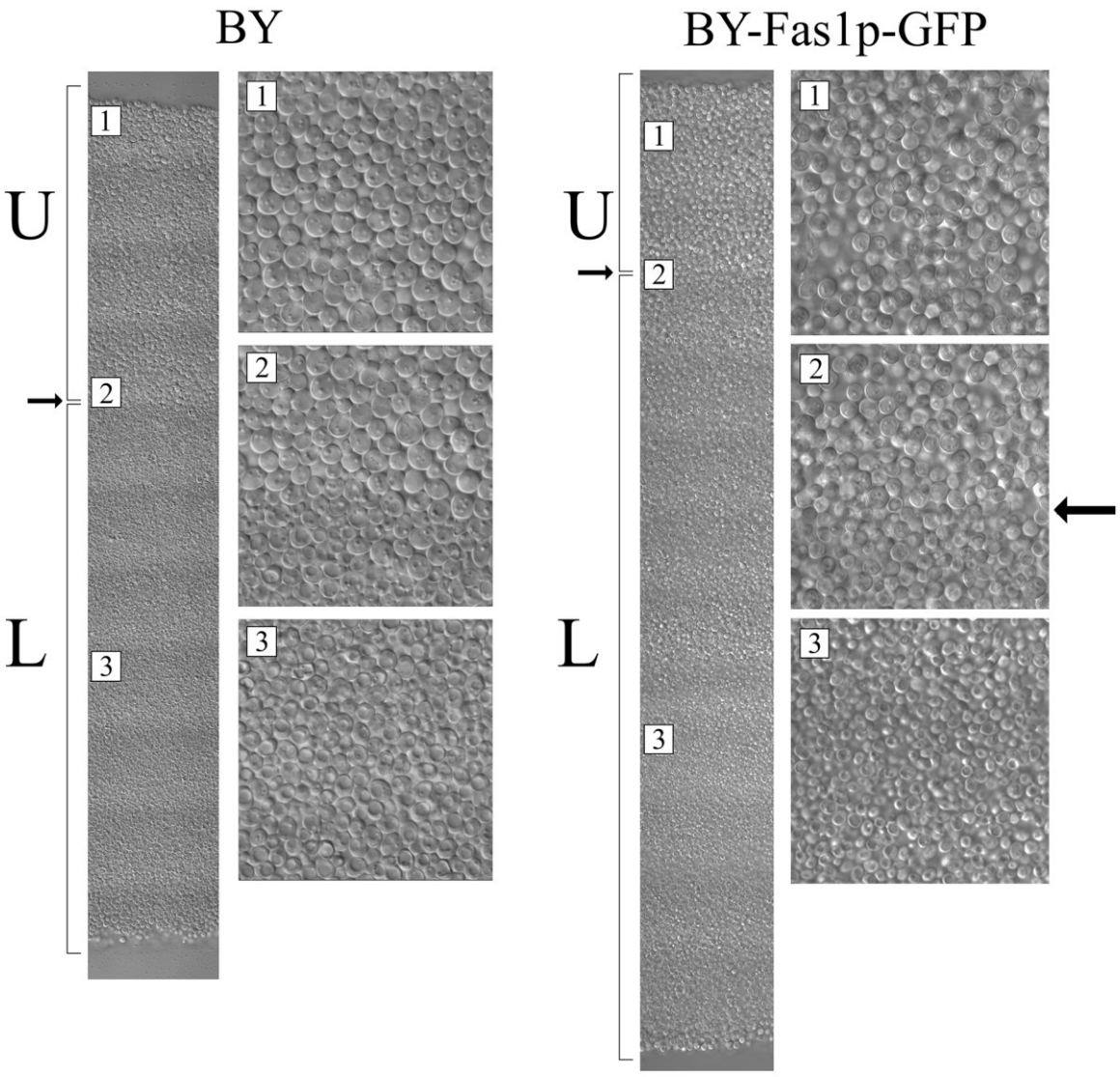

Figure 32. Vertical sections within giant colonies of BY and BY-Fas1p-GFP strains. Arrows show the boundary between U and L cells. Numbers on enlargement squares correspond with numbers on section, where the enlarged segment was taken from. Letters U and L represent Upper and Lower cells, respectively.

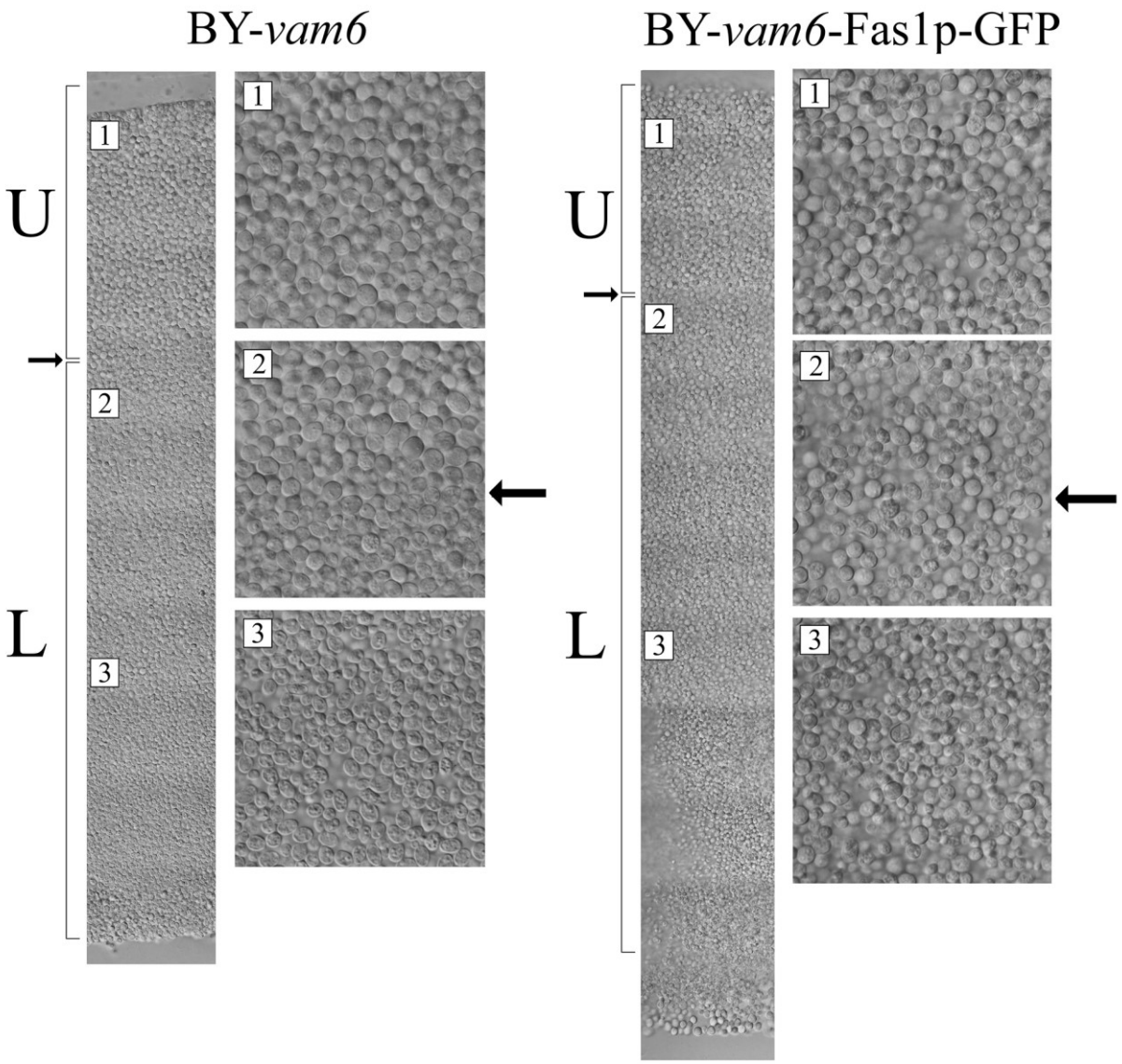

Figure 33. Vertical sections within giant colonies of BY and BY-*vam6*-Fas1p-GFP strains. Arrows show the boundary between U and L cells. Numbers on enlargement squares correspond with numbers on section, where the enlarged segment was taken from. Letters U and L represent Upper and Lower cells, respectively.

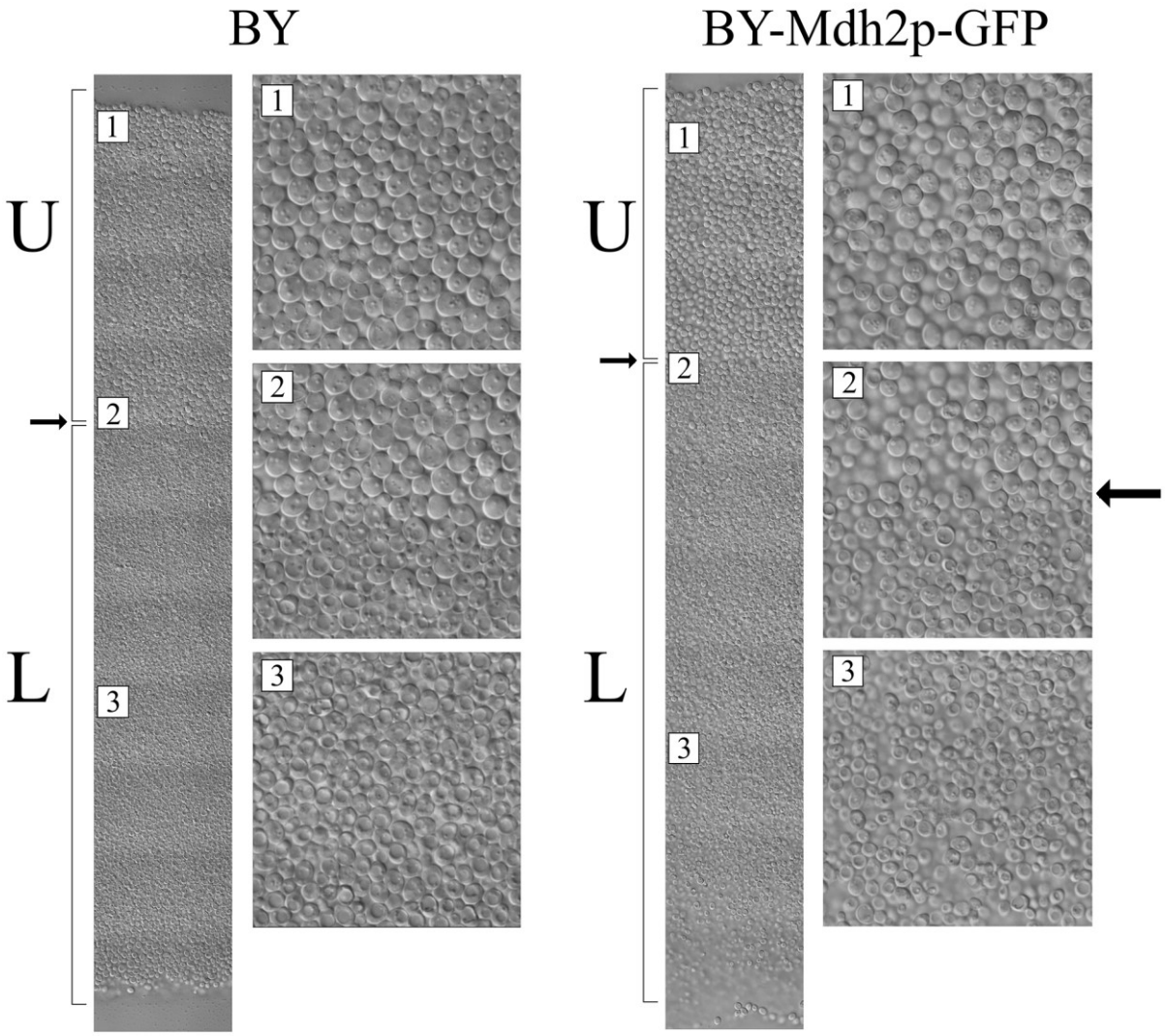

Figure 34. Vertical sections within giant colonies of BY and BY-Mdh2p-GFP strains. Arrows show the boundary between U and L cells. Numbers on enlargement squares correspond with numbers on section, where the enlarged segment was taken from. Letters U and L represent Upper and Lower cells, respectively.

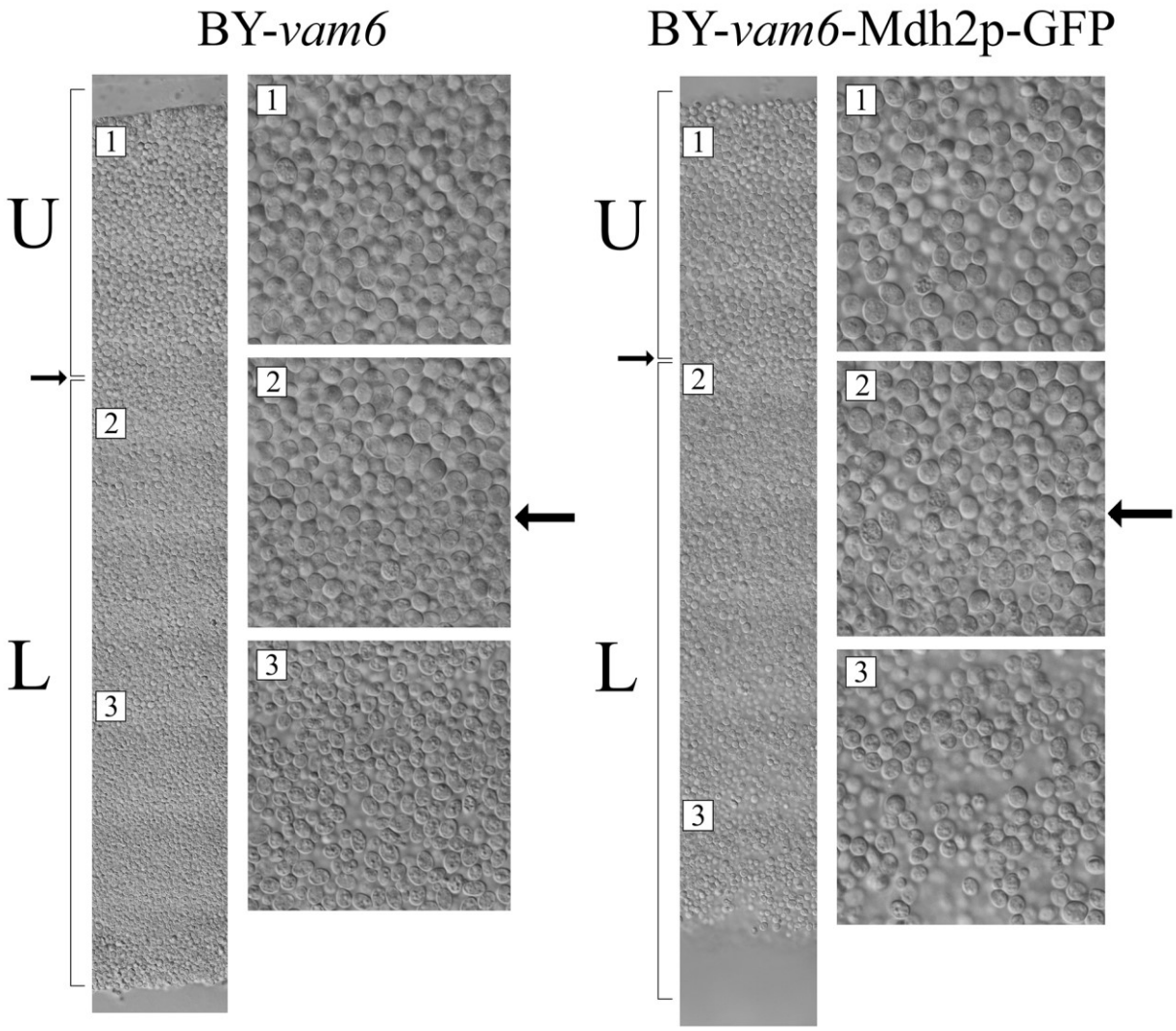

Figure 35. Vertical sections within giant colonies of BY and BY-*vam6*-Mdh2p-GFP strains. Arrows show the boundary between U and L cells. Numbers on enlargement squares correspond with numbers on section, where the enlarged segment was taken from. Letters U and L represent Upper and Lower cells, respectively.

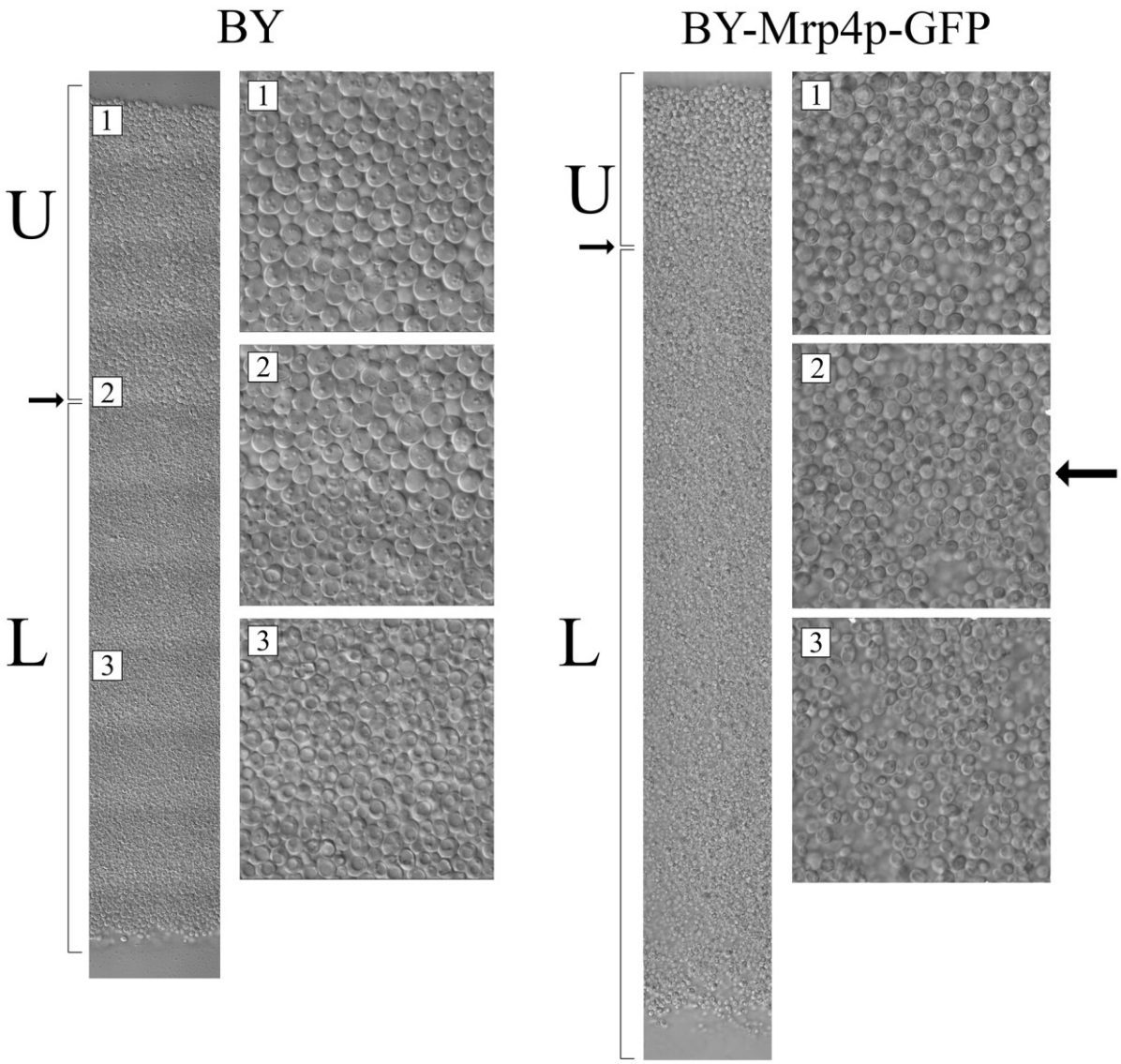

Figure 36. Vertical sections within giant colonies of BY and BY-Mrp4p-GFP strains. Arrows show the boundary between U and L cells. Numbers on enlargement squares correspond with numbers on section, where the enlarged segment was taken from. Letters U and L represent Upper and Lower cells, respectively.

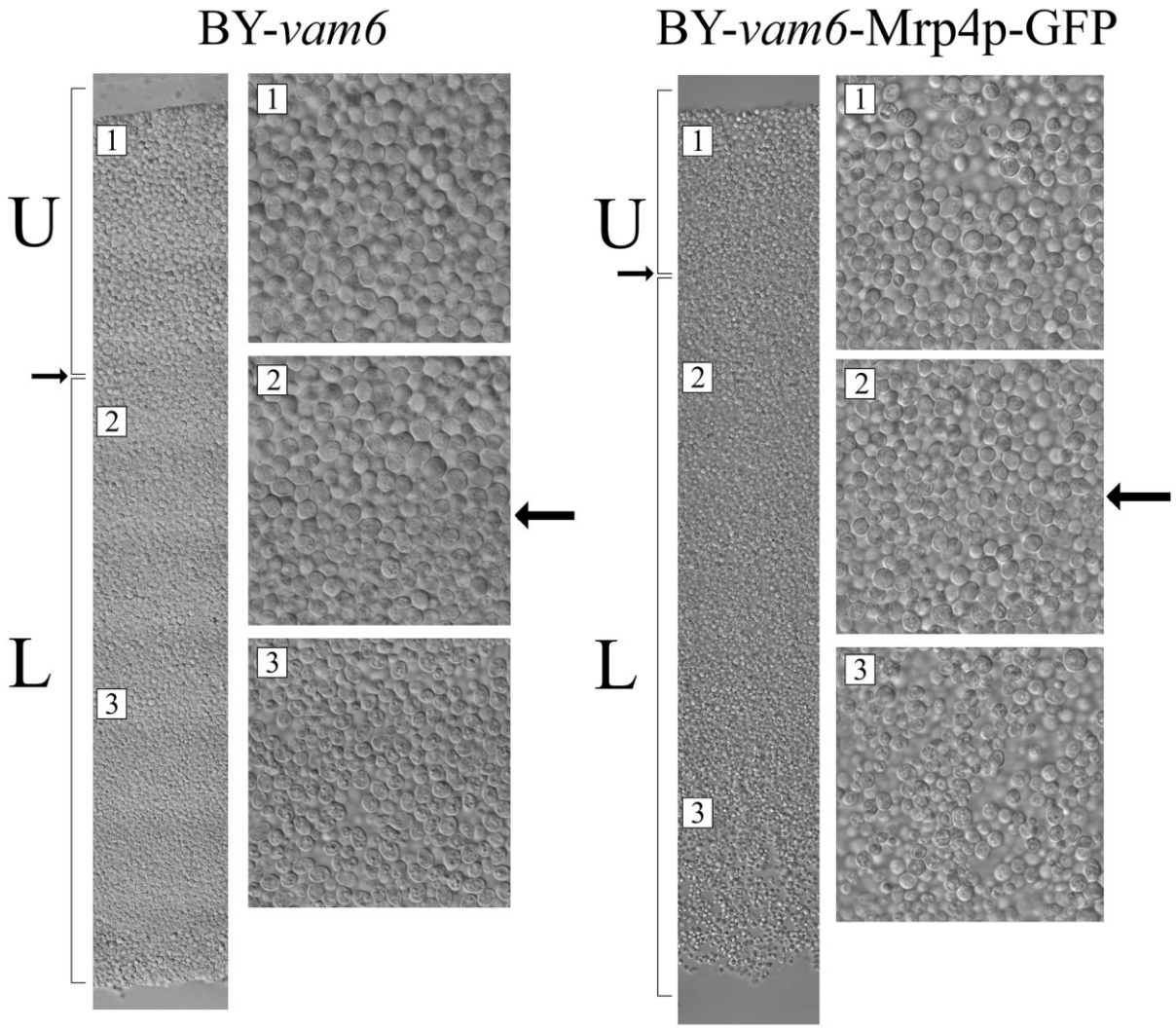

Figure 37 . Vertical sections within giant colonies of BY and BY-*vam6*-Mrp4p-GFP strains. Arrows show the boundary between U and L cells. Numbers on enlargement squares correspond with numbers on section, where the enlarged segment was taken from. Letters U and L represent Upper and Lower cells, respectively.

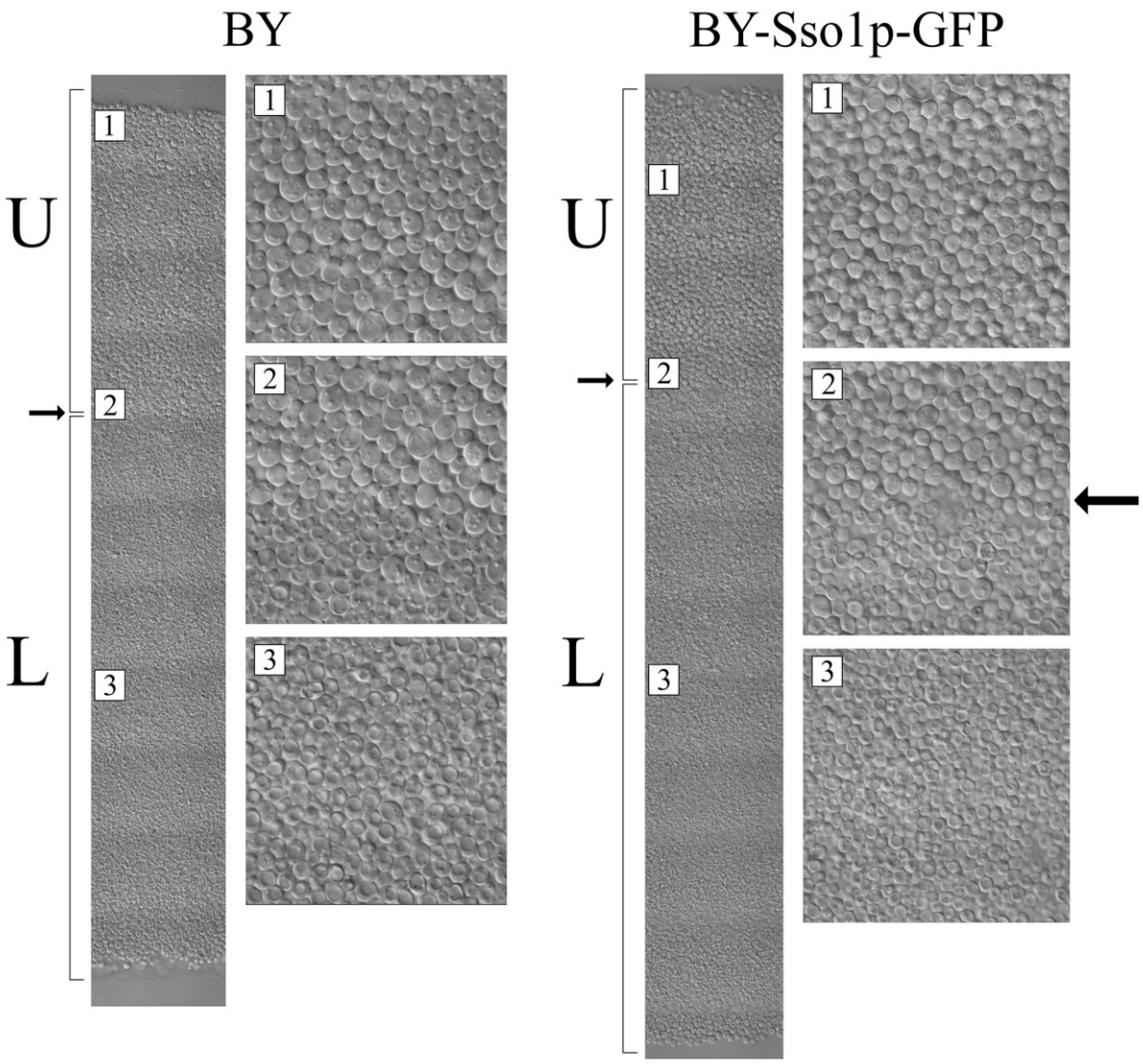

Figure 38. Vertical sections within giant colonies of BY and BY-Sso1p-GFP strains. Arrows show the boundary between U and L cells. Numbers on enlargement squares correspond with numbers on section, where the enlarged segment was taken from. Letters U and L represent Upper and Lower cells, respectively.

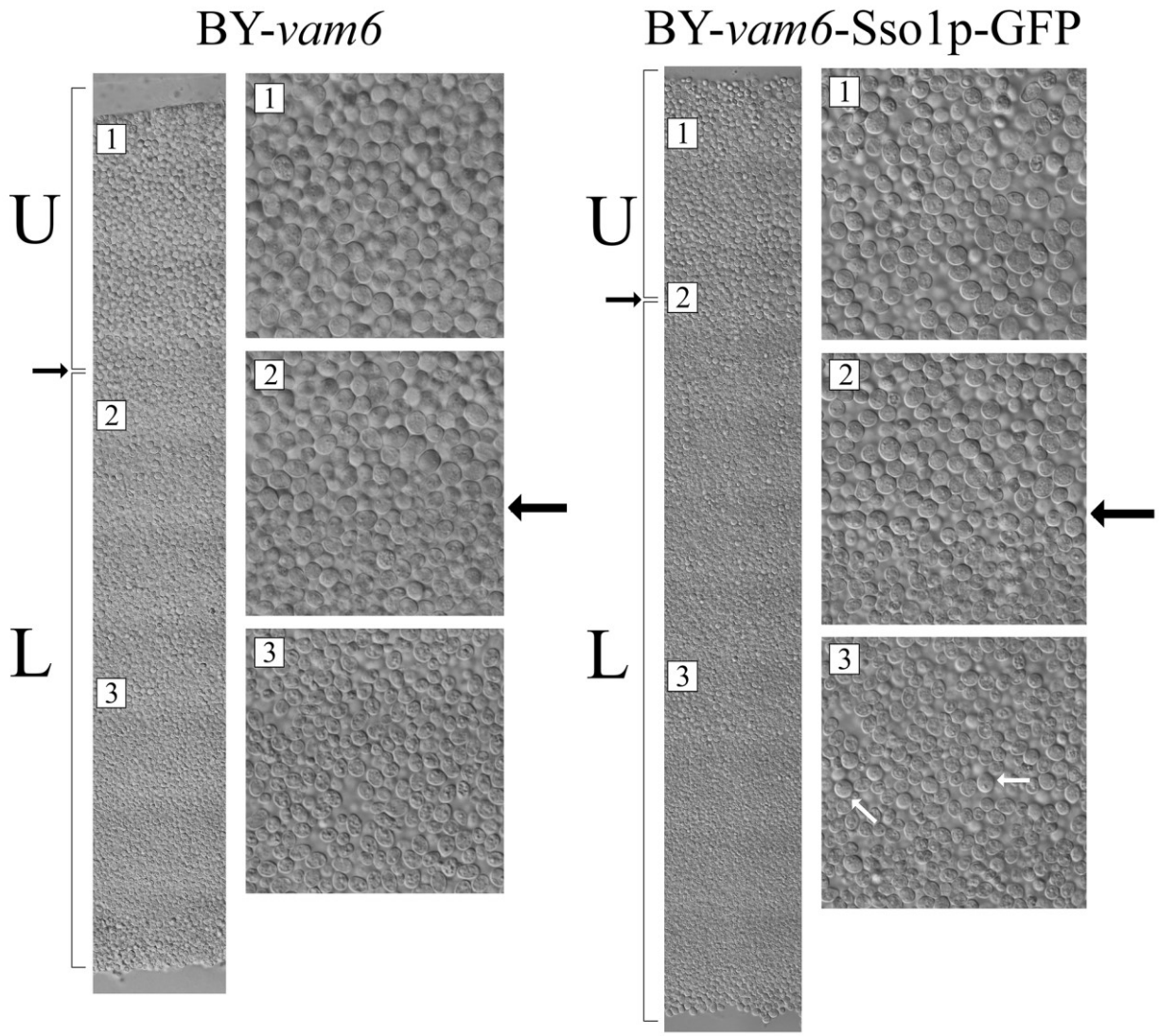

Figure 39. Vertical sections within giant colonies of BY and BY-*vam6*-Sso1p-GFP strains. Arrows show the boundary between U and L cells. Numbers on enlargement squares correspond with numbers on section, where the enlarged segment was taken from. Letters U and L represent Upper and Lower cells, respectively.

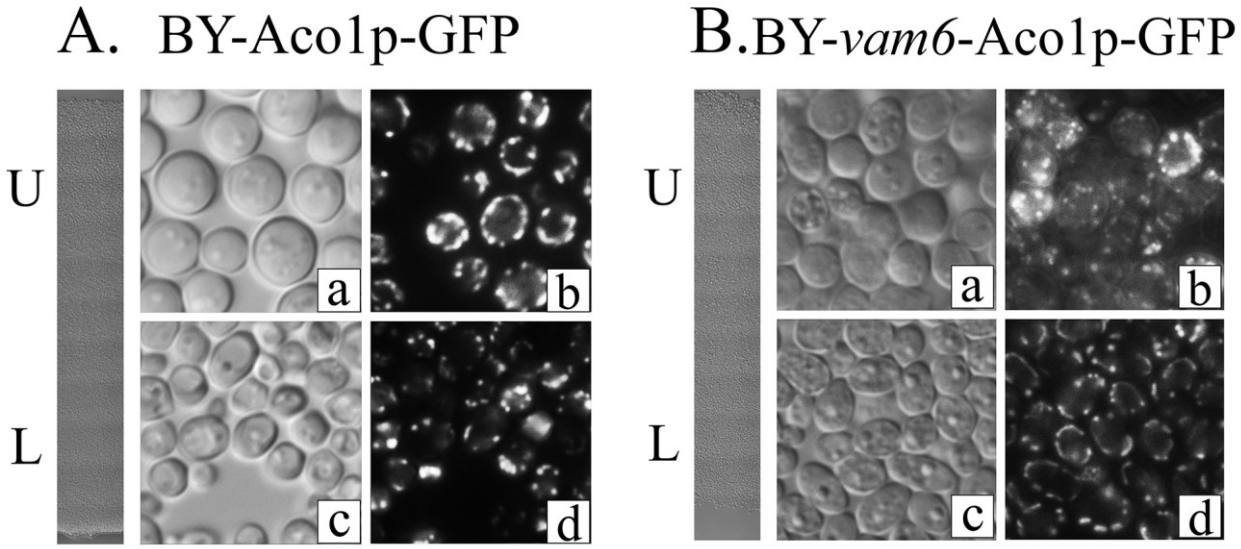

Figure 40. Summarized comparison of U and L cells: **A.** BY-Aco1p-GFP strain **a.** Morphology of U cells in Nomarski contrast. **b.** Morphology of U cells in Nomarski contrast. **c.** Localization of Aco1p-GFP in U cells. **d.** Localization of Aco1p-GFP in L cells. **B.** BY-*vam6*-Aco1p-GFP strain **a.** Morphology of U cells in Nomarski contrast. **b.** Morphology of U cells in Nomarski contrast. **c.** Localization of Aco1p-GFP in U cells. **d.** Localization of Aco1p-GFP in L cells. Exposition used: 100 ms.

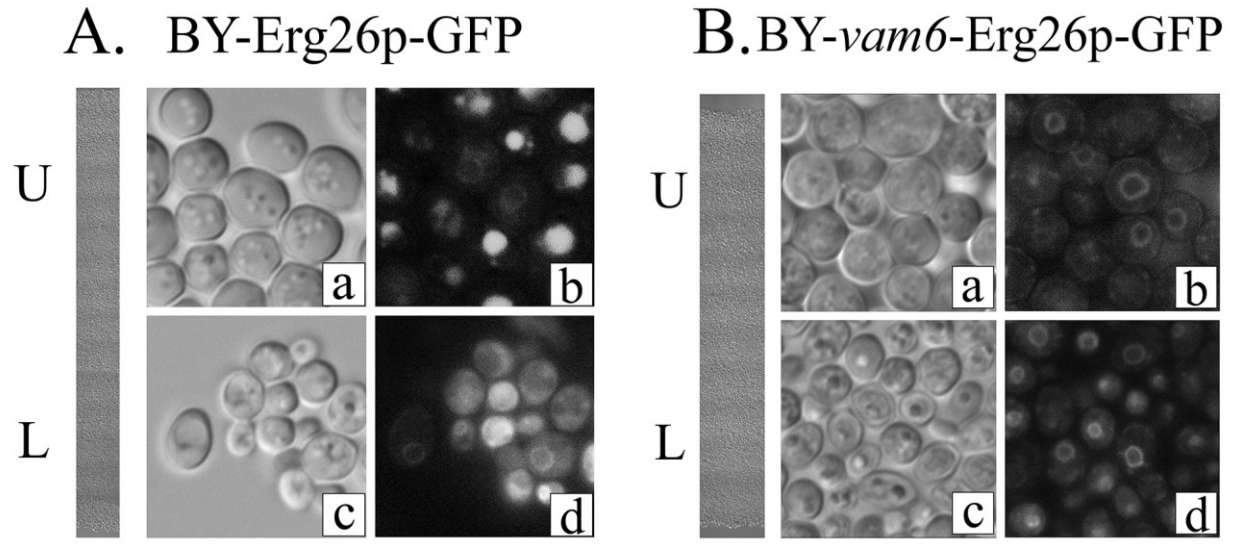

Figure 41. Summarized comparison of U and L cells: **A.** BY-Erg26p-GFP strain **a.** Morphology of U cells in Nomarski contrast. **b.** Morphology of U cells in Nomarski contrast. **c.** Localization of Erg26p-GFP in U cells. **d.** Localization of Erg26p-GFP in L cells. **B.** BY-*vam6*-Erg26p-GFP strain **a.** Morphology of U cells in Nomarski contrast. **b.** Morphology of U cells in Nomarski contrast. **c.** Localization of Erg26p-GFP in U cells. **d.** Localization of Erg26p-GFP in L cells. Exposition used: 700 ms.

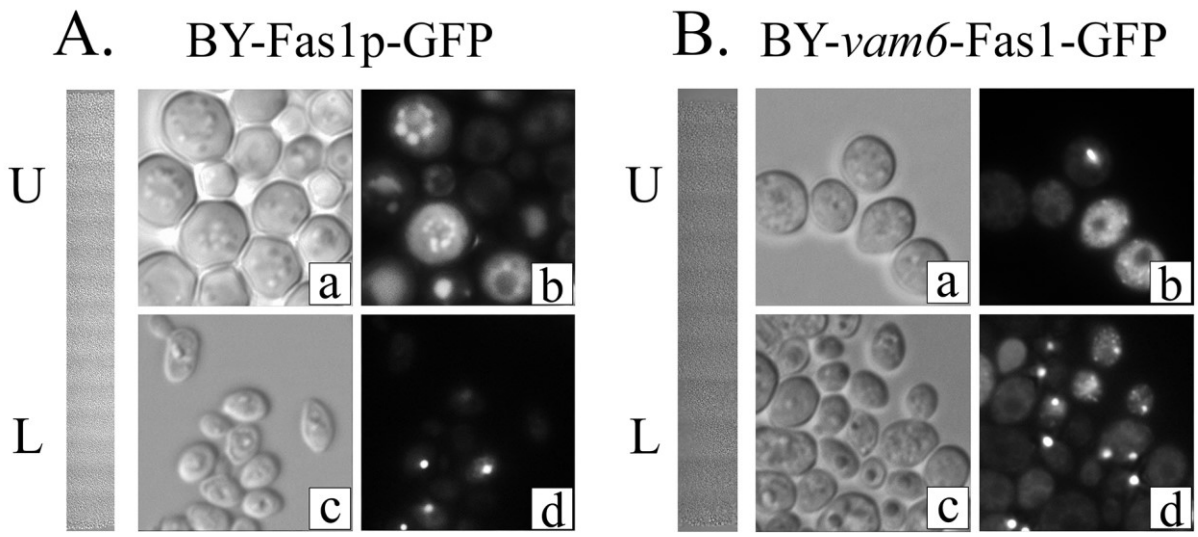

Figure 42. Summarized comparison of U and L cells: **A.** BY-Fas1p-GFP strain **a.** Morphology of U cells in Nomarski contrast. **b.** Morphology of U cells in Nomarski contrast. **c.** Localization of Fas1p-GFP in U cells. **d.** Localization of Fas1p-GFP in L cells. **B.** BY-*vam6*-Fas1p-GFP strain **a.** Morphology of U cells in Nomarski contrast. **b.** Morphology of U cells in Nomarski contrast. **c.** Localization of Fas1p-GFP in U cells. **d.** Localization of Fas1p-GFP in L cells. Exposition used: 700 ms.

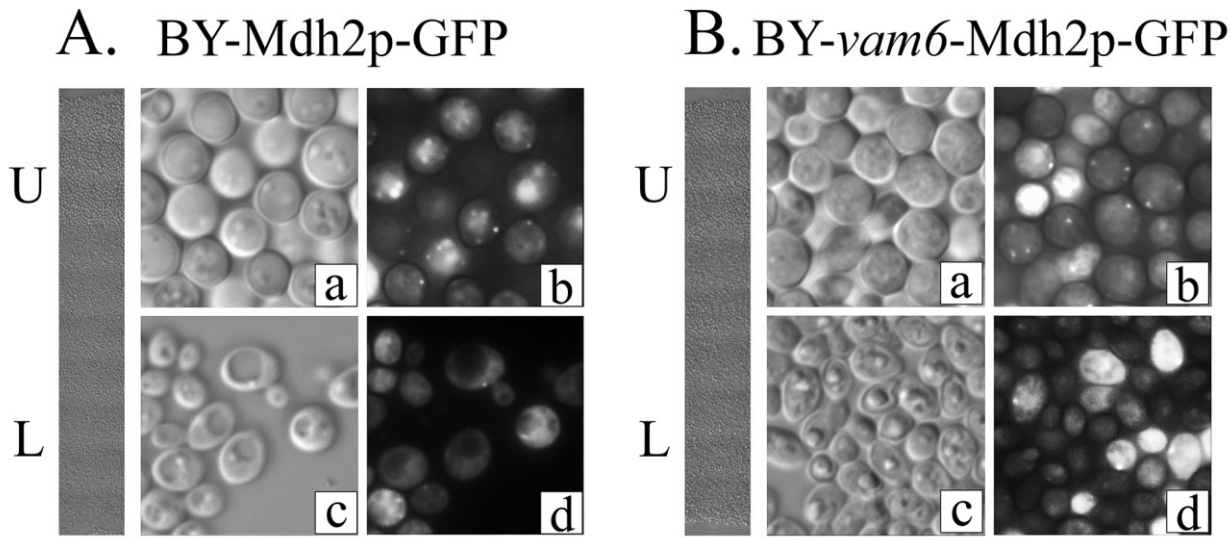

Figure 43. Summarized comparison of U and L cells: **A.** BY-Mdh2p-GFP strain **a.** Morphology of U cells in Nomarski contrast. **b.** Morphology of U cells in Nomarski contrast. **c.** Localization of Mdh2p-GFP in U cells. **d.** Localization of Mdh2p-GFP in L cells. **B.** BY-*vam6*-Mdh2p-GFP strain **a.** Morphology of U cells in Nomarski contrast. **b.** Morphology of U cells in Nomarski contrast. **c.** Localization of Mdh2p-GFP in U cells. **d.** Localization of Mdh2p-GFP in L cells. Exposition used: 700 ms

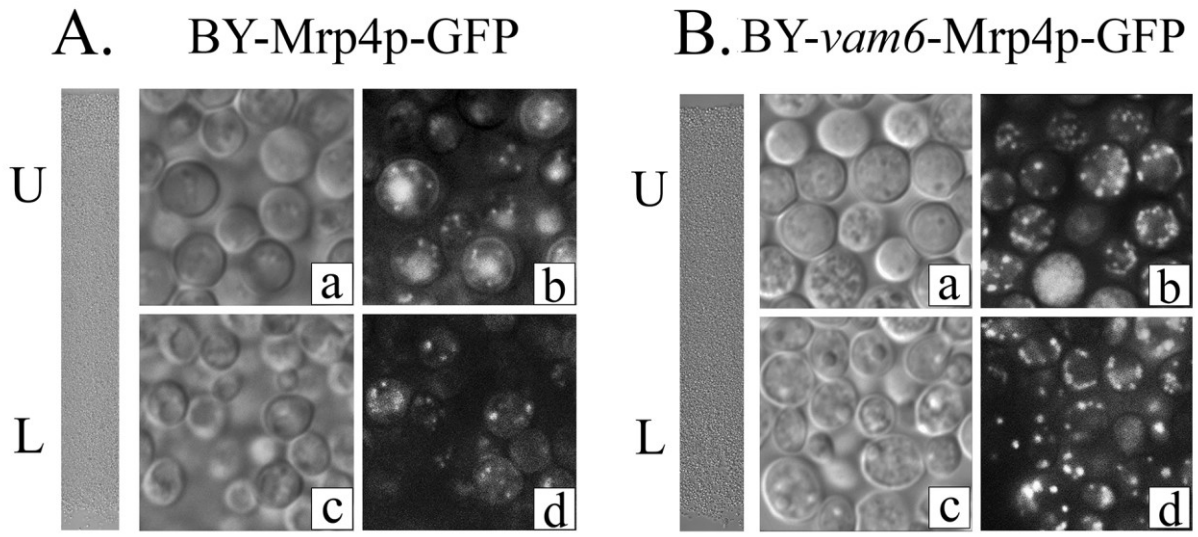

Figure 44. Summarized comparison of U and L cells: **A.** BY-Mrp4p-GFP strain **a.** Morphology of U cells in Nomarski contrast. **b.** Morphology of U cells in Nomarski contrast. **c.** Localization of Mrp4p-GFP in U cells. **d.** Localization of Mrp4p-GFP in L cells. **B.** BY-*vam6*-Mrp4p-GFP strain **a.** Morphology of U cells in Nomarski contrast. **b.** Morphology of U cells in Nomarski contrast. **c.** Localization of Mrp4p-GFP in U cells. **d.** Localization of Mrp4p-GFP in L cells. Exposition used: 700 ms.

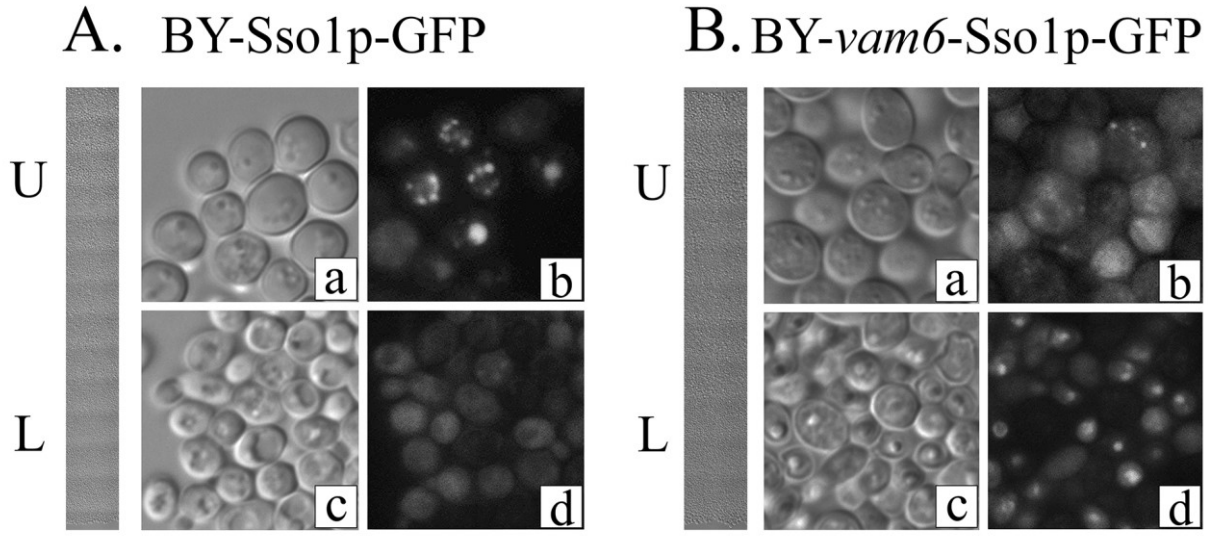

Figure 45. Summarized comparison of U and L cells: **A.** BY-Sso1p-GFP strain **a.** Morphology of U cells in Nomarski contrast. **b.** Morphology of U cells in Nomarski contrast. **c.** Localization of Sso1p-GFP in U cells. **d.** Localization of Sso1p-GFP in L cells. **B.** BY-*vam6*-Sso1p-GFP strain **a.** Morphology of U cells in Nomarski contrast. **b.** Morphology of U cells in Nomarski contrast. **c.** Localization of Sso1p-GFP in U cells. **d.** Localization of Sso1p-GFP in L cells. Exposition used: 700 ms.

In colonies created by BY-Erg26p-GFP, BY-*vam6*-Erg26p-GFP, BY-*vam6*-Mdh2p-GFP, BY-*vam6*-Fas1p-GFP, BY-Mrp4p-GFP, BY-*vam6*-Mrp4p-GFP strains, the boundary between U and L cells was less defined, although the differentiation process was induced. (**Figures 30-31, 33, 35-37, respectively**). In colonies created by BY-Aco1p-GFP, BY-*vam6*-Aco1-GFP, BY-Mdh2p-GFP, BY-Fas1p-GFP, BY-Sso1p-GFP and BY-*vam6*-Sso1p-GFP (**Figures 28-29, 32, 34 and 38-39**) a sharp boundary was present, and morphology of U and L cells was very similar to parental strain. Giant colonies created by BY-*vam6*-Sso1p-GFP demonstrated well defined boundary between U and L cells, however, in L cells subpopulation was also present cells with U-morphology. In Figure 39, those cells are pointed on with white arrows. One of partial aims of this chapter was to investigate, whether proteins of interest localization and intensity of GFP-signal differs in U and L cells of giant colonies formed by BY- and BY-*vam6* derived strains.

In Figure 40, a comparison of fluorescent signal intensity and localization in U and L cells of colonies created by strains BY-Aco1p-GFP and BY-*vam6*-Aco1p-GFP is shown. Aco1p-GFP exhibited the same localization in both U and L cells of both strains and very strong signal, which was captured in exhibition 100ms.

In Figure 41 demonstrated significant differences of Erg26p-GFP localization colonies created by BY-Erg26p-GFP and BY-*vam6*-Erg26p-GFP strains. The majority of Erg26p-GFP is localized on endoplasmic reticulum in both U and L cells of colony created by BY-*vam6*-Erg26p-GFP strain. In case of BY-Erg26p-GFP strain, where Erg26p-GFP is localized on ER, U cells additionally exhibit fluorescent signal in nucleus, and L cells in cytosol.

Mdh2p-GFP in giant colonies of both BY-Mdh2p-GFP and BY-*vam6*-Mdh2p-GFP strains is present in peroxisomes in U. Some L cells of BY-*vam6*-Mdh2p-GFP colony also exhibit fluorescent signal in cytosol (Figure 43).

Mrp4p-GFP in U and L cells of colonies created by BY-Mrp4p-GFP and BY-*vam6*-Mrp4p-GFP were present in mitochondria. On case of BY-Mrp4p-GFP strain, Mrp4p-GFP was also present in the nucleus (Figure 44).

In Figure 42, Fas1p-GFP fluorescent signal is detectable in U and L cells of colonies of both BY-Fas1p-GFP and BY-*vam6*-Fas1p-GFP strains; however, U cells show a less intensive signal in comparison with L cells. Localization of Fas1p-GFP does not differ between the two examined strains.

BY-Sso1p-GFP and BY-*vam6*-Sso1p-GFP strains showed very low intensity of fluorescent

signal (Figure 45). Sso1p is present in lipid particles of U cells of both examined strains. It is barely noticeable, that in L cells of colony created by BY-Sso1p-GFP strain, Sso1p-GFP is also present in lipid droplets. In L cells of the colony created by BY-*vam6*-Sso1p-GFP, fluorescent signal was observed in the nucleus.

Fluorescent microscopy of U and L cells of colonies created by above mentioned strains aimed to verify the presence of the fluorescent signal in both U and L cells. It further aimed to verify whether the protein of interest localization is affected by *VAM6* knock-out and whether the localization and signal intensity differs between U and L cells. In that experiment it was possible to observe the intensity of fluorescent signal from GFP-tagged proteins of interest, however, this observation does not allow to quantify the level of expressed proteins. To determine levels of protein expression in U and L cells of giant colonies, Western Blot analysis was performed as described in Section 4.2.11. The results **are demonstrated in Figure 46.**

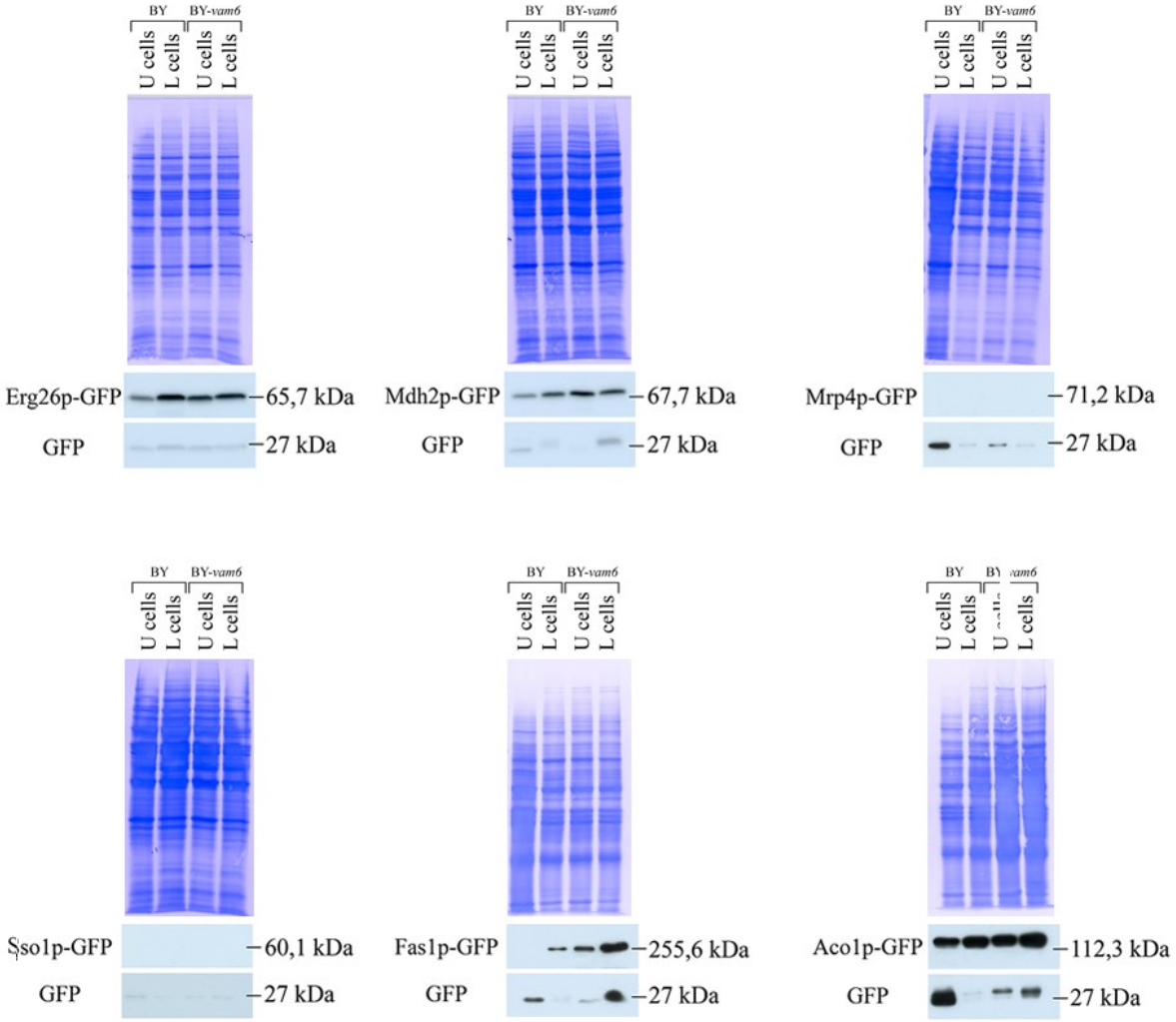

Figure 46. Western Blot results.

5.2 Characterization of selected vacuolar proteins role in development of colonies and in regulation of TORC1 activity.

The yeast vacuole is an organelle involved in many important processes such as: degradation of intracellular and extracellular substrates, metabolite storage, and nutrient recycling. TORC1 complex, the conserved serine/threonine kinase, is localized on the vacuolar membrane, together with one of its regulators, EGO complex.

Some other TORC1 regulators, such as Vam6p, are also involved in processes such as vacuole and other membranous organelles fusion and trafficking, being components of various complexes. The mentioned Vam6p is a subunit of HOPS complex. Vam6p is required for the assembly of HOPS complex and also modulate activity of TORC1. Hence, deletion of *VAM6* could affect not only TORC1 activity, but also other processes. The aim of this part of the study was to analyze whether defect in other components of the complexes (HOPS, CORVET and V-ATPase) affects colony development and differentiation. Furthermore, to evaluate the potential influence on TORC1 activity in U cells. Based on literature search, several proteins of the complexes were selected to investigate their role in the development of giant colonies.

Strains with deleted genes for selected proteins were created to investigate the impact of absence of selected proteins on development of colonies, on TORC1 activity, and on the viability of U and L cells.

5.2.1 Construction of new strains

Aim: To prepare strains with deleted genes for selected proteins.

The following proteins were selected to inspect the impact of their absence on giant colony development, differentiation, and TORC1 pathway activity: Vps3p and Vps8p, the subunits of CORVET complex, Vps33p and Vps41p, the subunits of HOPS complex, Vph2p, required for V-Atpase assembly, Vac7p, one of $PI(3,5)P_2$ regulators, and Vac14p, scaffold protein for $PI(3,5)P_2$regulatory complex. Both Vac7p and Vac14p are required for interconversion of PI3P and $PI(3,5)P_2$.

BY-Gat1p-GFP was used as the parental strain for gene deletions to be able to monitor TORC1 activity via Gat1p-GFP localization. Gat1p is TOR-responsive transcription factor and its localization is dependent on TORC1 activity. When TORC1 is active, Gat1p is cytosolic and when TORC1 is inactive, Gat1p changes localization to nuclear.

Deletion of the selected genes (*VPS3, VPS8, VPS33, VPS41* and *VPH2)* could be lethal under some conditions. Therefore, strain variants in which inducible promotor was placed in front of the respective gene were constructed, to achieve a low basal level of proteins of interest under conditions without galactose. Construction of new strains is described in Section 4.2.3. and also shown in Figure 47.

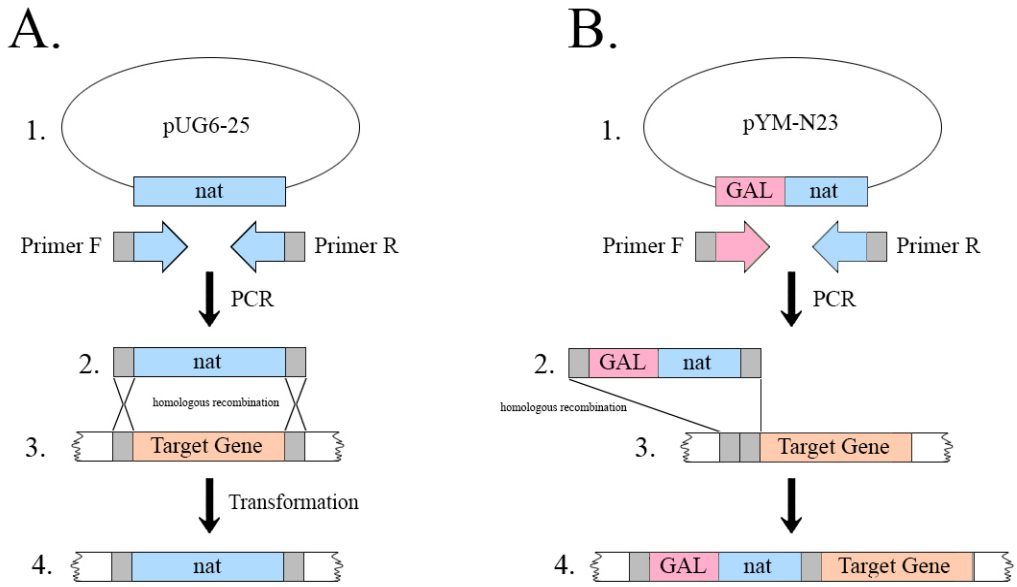

Figure 47. A. Scheme of construction of deletion strains derived from BY-Gat1p1-GFP strain. Fragment of plasmid pUG6-25 (1.) with nat gene (Nourseothricin resistance) was amplified by PCR. 2. – transformation cassette. 3. – target gene. 4. – target gene fragment was replaced by nat gene (Nourseothricin resistance), which was used for following positive selection of clones. B. Scheme of promoter change in BY-Gat1p1-GFP strain. (1.) Fragment of pYM-N23 plasmid coding GAL promoter sequence and nat gene (Nourseothricin resistance) was amplified by PCR. 2. – transformation cassette. 3 – target gene. 4. – GAL promotor and nat gene were placed upstream of the target gene. Nourseothricin resistance was used for following positive selection of clones.

For preparation of knock-out strains, plasmid pUG6-25 was used. This plasmid was derived from pUG6 plasmid by Ing. Otakar Hlaváček, Ph.D. KanMX (Kanamycin resistance) in pUG6 was replaced by NatMX (Nourseothricin resistance). For pGAL promoter insertion was used pYM-N23 promoter, which contains sequence coding GAL promoter and Nourseothricin resistance. Primers used for amplification of future transformation cassettes, are stated in Tables 4 and 5, Section 4.1.4.a. Transformation cassettes were prepared as per 4.2.4 and transformation was performed as described in 4.2.5. Strains prepared in this study are listed in Table 13.

Parental strain	Prepared Strain	Phenotype
BY-Gat1p-GFP	BY-Gat1p-GFP-*vps3*	MATα, *his3Δ, ura3Δ, leu2Δ, lys2Δ*, KanMX, nat1, *vps3Δ*
	BY-Gat1p-GFP-*vps8*	MATα, *his3Δ, ura3Δ, leu2Δ, lys2Δ*, KanMX, nat1, *vps8Δ*
	BY-Gat1p-GFP-*vps33*	MATα, *his3Δ, ura3Δ, leu2Δ, lys2Δ*, KanMX, nat1, *vps33Δ*
	BY-Gat1p-GFP-*vps41*	MATα, *his3Δ, ura3Δ, leu2Δ, lys2Δ*, KanMX, nat1, *vps41Δ*
	BY-Gat1p-GFP-*vph2*	MATα, *his3Δ, ura3Δ, leu2Δ, lys2Δ*, KanMX, nat1, *vph2Δ*
	BY-Gat1p-GFP-*vac7*	MATα, *his3Δ, ura3Δ, leu2Δ, lys2Δ*, KanMX, nat1, *vac7Δ*
	BY-Gat1p-GFP-*vac14*	MATα, *his3Δ, ura3Δ, leu2Δ, lys2Δ*, KanMX, nat1, *vac14Δ*
	BY-Gat1p-GFP-p*GAL*-*VPS3*	MATα, *his3Δ, ura3Δ, leu2Δ, lys2Δ*, KanMX, nat1, p*GAL*-*VPS3*
	BY-Gat1p-GFP-p*GAL*-*VPS8*	MATα, *his3Δ, ura3Δ, leu2Δ, lys2Δ*, KanMX, nat1, p*GAL*-*VPS8*
	BY-Gat1p-GFP-p*GAL*-*VPS33*	MATα, *his3Δ, ura3Δ, leu2Δ, lys2Δ*, KanMX, nat1, p*GAL*-*VPS33*
	BY-Gat1p-GFP-p*GAL*-*VPS41*	MATα, *his3Δ, ura3Δ, leu2Δ, lys2Δ*, KanMX, nat1, p*GAL*-*VPS41*
	BY-Gat1p-GFP-p*GAL*-*VPH2*	MATα, *his3Δ, ura3Δ, leu2Δ, lys2Δ*, KanMX, nat1, p*GAL*-*VPH2*

Table 14. List of strains prepared in this study.

5.2.2. Strain verification.

Aim: To verify correct cassette integration to the genome and gene deletion.

After transformation, cells were plated on YEPG medium with antibiotic nourseothricin, which was used as a positive selection marker. The transformation cassette contained gene *NAT1* encoding nourseothricin resistance, and therefore only successfully transformed cells were supposed to grow on medium with nourseothricin. Newly constructed strains were verified by PCR reactions as described in 4.2.4., primers, calculated product sizes and expected PCR reaction results Tables 7 and 8 (4.1.4.a.) In Figure 48 is shown a principle of primers design for verification of transformation cassette presence in the genome and in Figure 49 is demonstrated an example of veridication reaction.

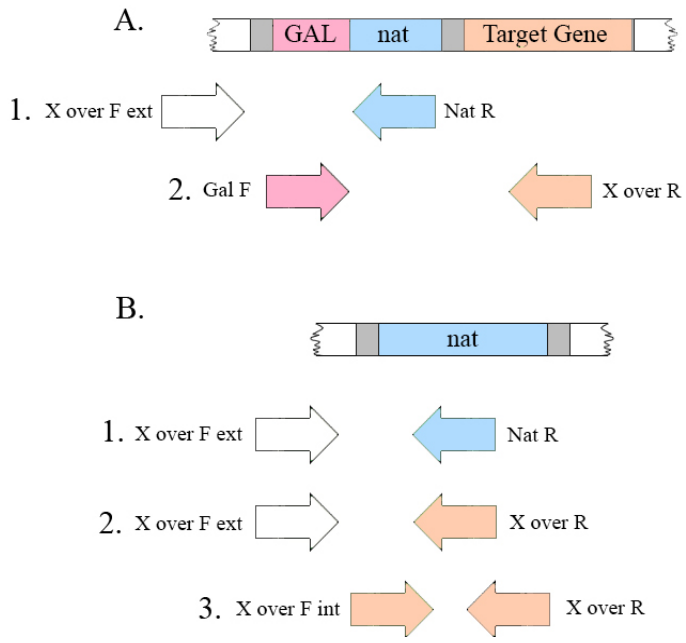

Figure 48. Scheme of the principle of primers design for verification after transformation. Arrows represent reverse and forward primers, colors of primers correspond with color of complementary sequence: pink – GAL promoter sequence, blue – nat1 gene sequence, orange – gene of interest sequence and white – sequence +/- 1000 bp upstream target gene sequence. **A.** Principle of primer design for verification of GAL promoter knock-in upstream of target gene. **1, 2** – Reactions verifying presence of cassette in a genome. X is a target gene name. **B**. Principle of primer design for verification of target gene knock-out. **1**. – reaction verifying presence of cassette in a genome. **2, 3** – reactions verifying successful knock-out and confirming, that gene of interest sequence is missing within the genome.

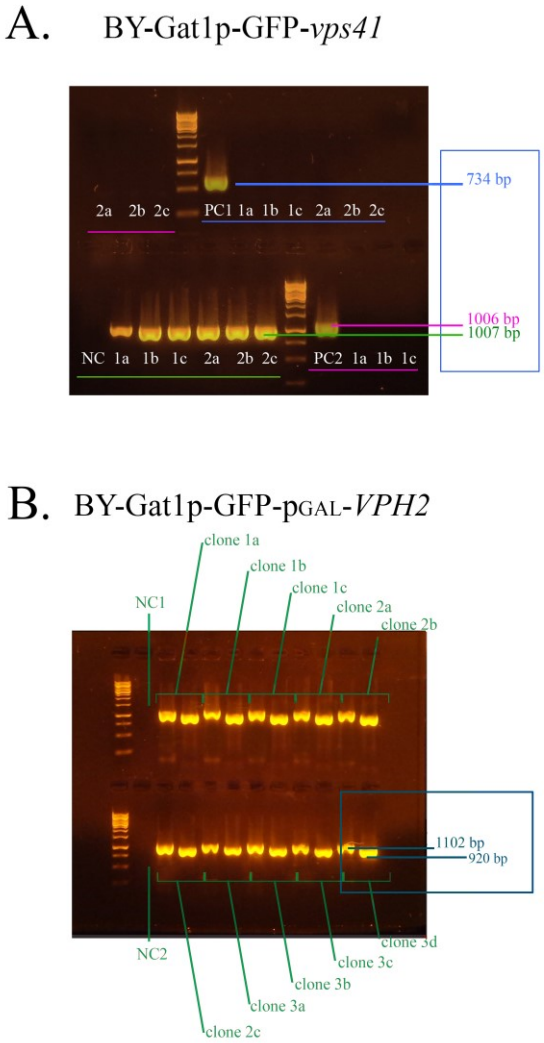

Figure 49. Images of electrophoresis gels – examples of verification after transformation. **A**. Image of electrophoresis gel – example of verification after transformation for strain BY-Gat1p-GFP-*vps41*. Bands underlined with green color represent reaction confirming successful cassette integration; bands underlined with blue and pink represent reaction confirming successful knockout. Abbreviations NC and PC represent negative and positive controls respectively, where DNA isolated from parental strain was used. **B.** Image of electrophoresis gel – example of verification after transformation for strain BY-Gat1p-GFP-pGAL-*VPH2*. Two verification reactions confirming successful integration of cassette were performed for each clone. Abbreviations NC1 and NC2 represent negative controls for both reactions. DNA isolated from parental strain was used in NC1 and NC2 reaction mixtures.

5.2.3. Monitoring of colony development.

As shown in Figures 50 and 51, the alkalization of medium surrounding colonies of BY-Gat1p-GFP strain, started at 14th day. Alkalization of medium surrounding colonies of BY-Gat1p-GFP-*vps8*, BY-Gat1p-GFP-*vps41* and BY-Gat1p-GFP-*vac7* strains began at the same time as the parental strain.

For all examined strains, only alkalization of colonies formed by BY-Gat1p-GFP-*vps3* strains started two days before the alkalization of the medium surrounding colonies of the parental strain. Other strains, including strains containing exchanged GAL promoter (Figure 51), started to alkalize the medium two days later as compared to the parental strains. The exception was BY-Gat1p-GFP-*vph2* strain, for which the colonies started to alkalize the surrounding medium after 16th day.

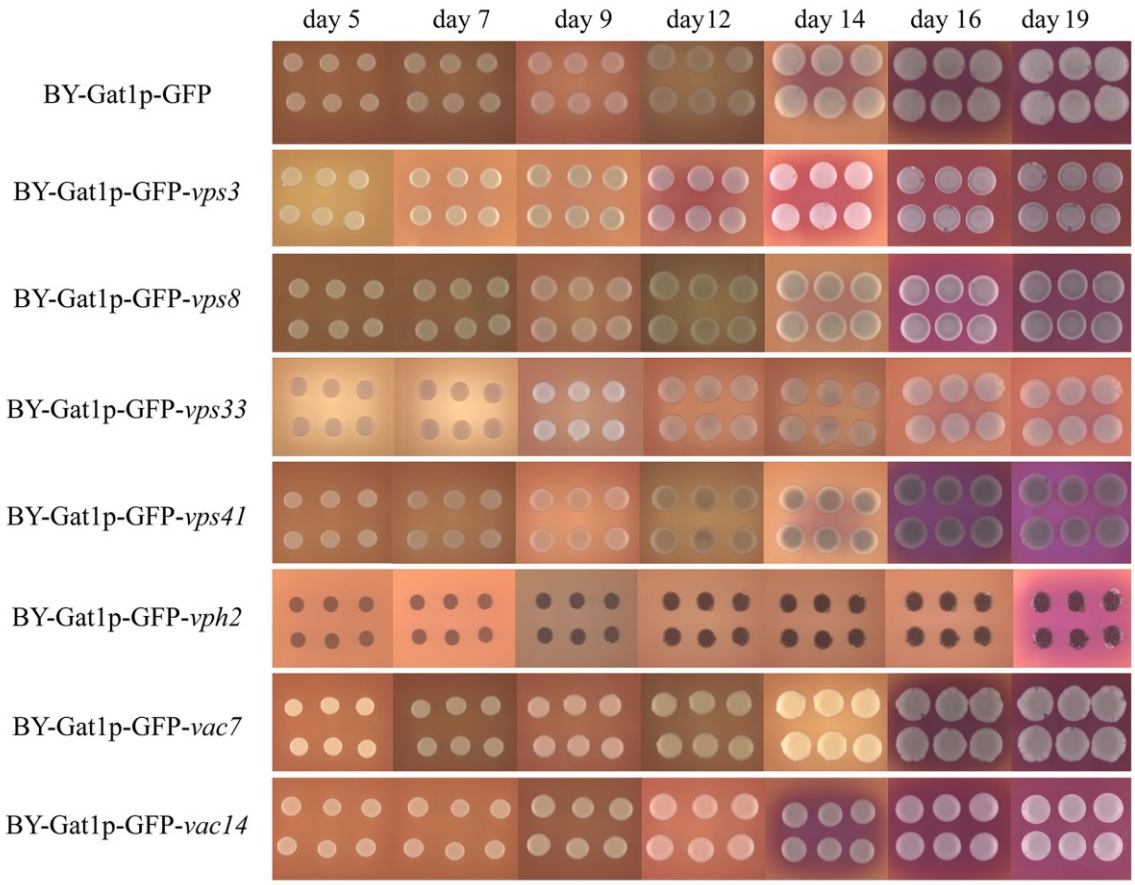

Figure 50. Comparison of BY-Gat1p-GFP derived strains with deletions of genes of interest. Representative data out of 9 experiments. Lines represent different clones' development and alkalization period (days 5 to 19), rows represent age of colonies in days.

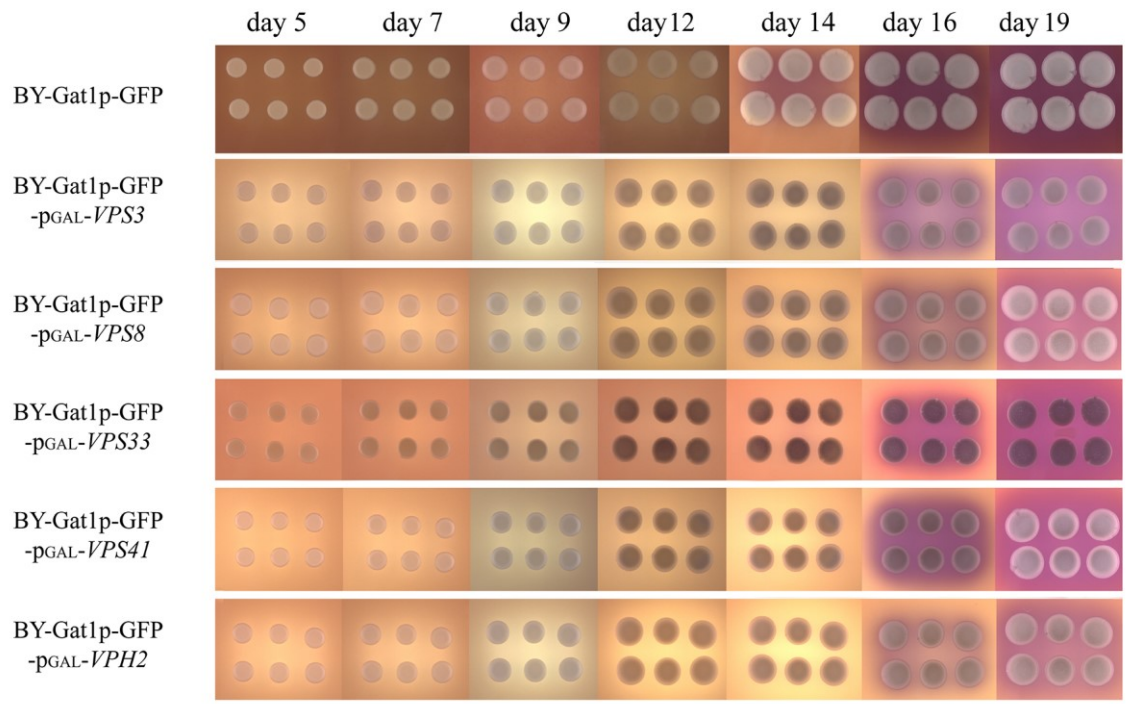

Figure 51. Comparison of BY-Gat1p-GFP derived strains with GAL promoter knock-in, targeting genes of interest. Representative data out of 9 experiments. The lines represent different clones' development and alkalization period (days 5 to 19), rows represent age of colonies in days.

For more detailed examination of morphology changes in strains derived from BY-Gat1p-GFP, the morphology of developing colonies was also observed with binocular magnifier loupe. The morphology was observed on both GM and GM+BKP plates. As mentioned above, nine clones from each strain were examined and they demonstrated similar behavior. Morphology of giant colonies was affected in case of *VAC7*, *VAC14* and *VPH2* genes knock-outs. Colonies formed by BY-Gat1p-GFP-*vac7* and BY-Gat1p-GFP-*vac14* strains were more sectored, and colonies formed by BY-Gat1p-GFP-*vph2* strain demonstrated significant growth defects. Colonies formed by BY-Gat1p-GFP-*vac7* and BY-Gat1p-GFP-*vac14* strains, were more sectored. BY-Gat1p-GFP-*vac14* colonies were also bigger than the parental strain (Figure 52). Colonies created by strains with GAL promoter exchange in most cases resembled colonies formed by parental strain. BY-Gat1p-GFP-pGAL-*VPS41* strain created larger colonies in comparison with the parental strain (Figure 53).

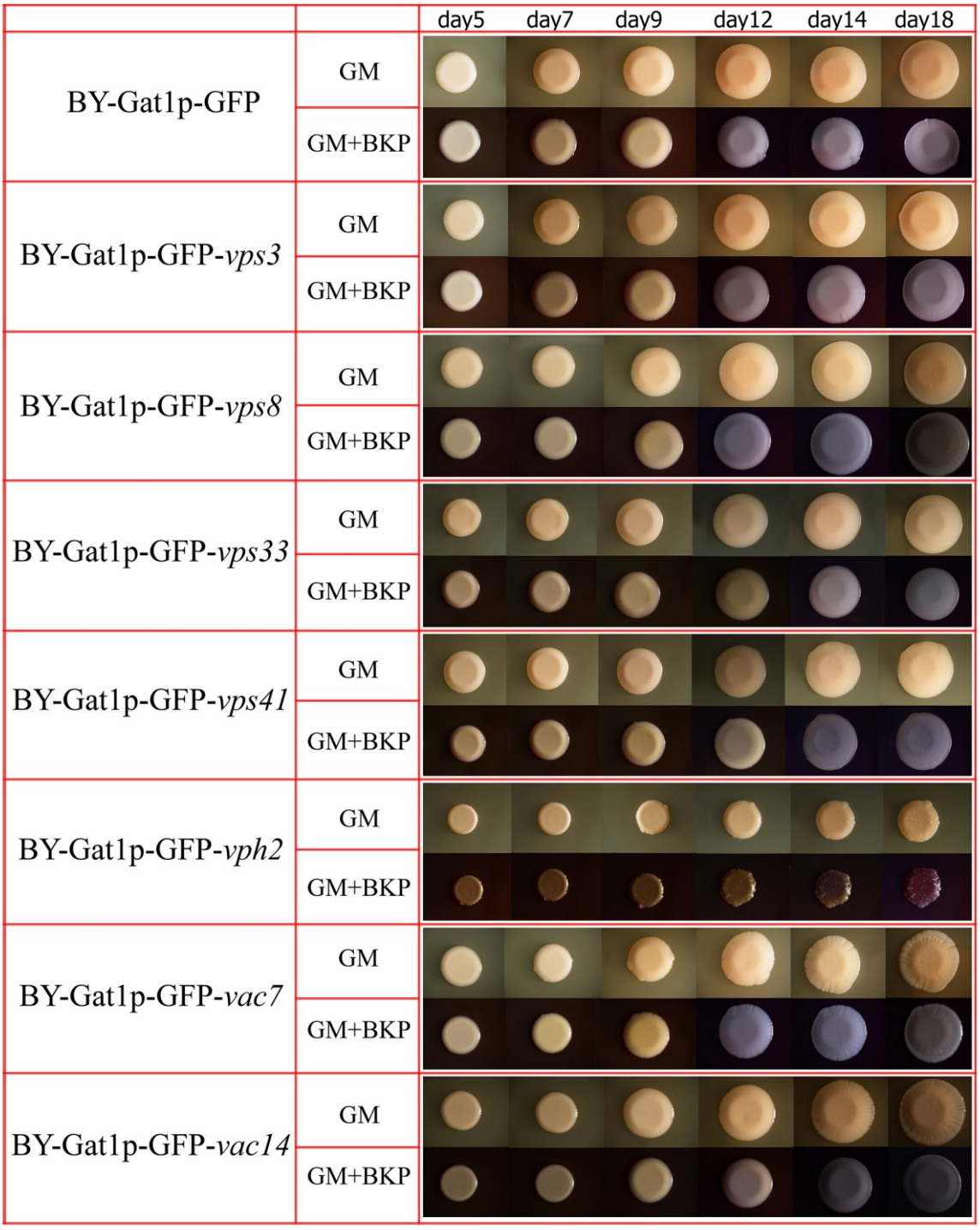

Figure 52. Representative data from nine experiments. Morphology changes monitoring during giant colonies development. All strains were derived from BY-Gat1p-GFP. Giant colonies development was observed on both GM and GM+BKP mediums. Photos were captured in two- or three-days intervals, starting from 5th day.

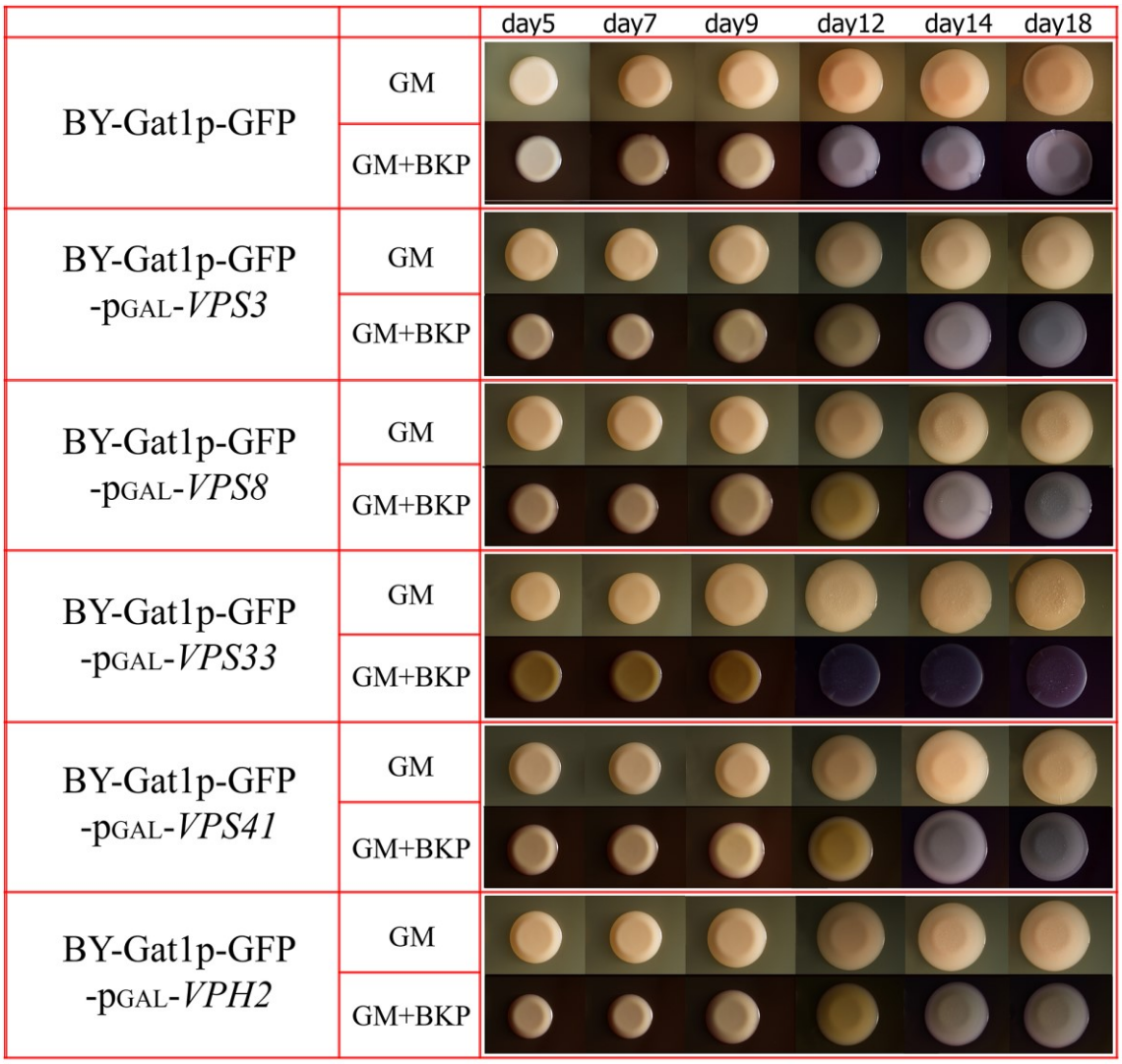

Figure 53. Representative data from nine experiments. Morphology changes monitoring during giant colonies development. All strains with GAL promoter knock-in were derived from BY-Gat1p-GFP. Giant colonies development was observed on both GM and GM+BKP mediums. Photos were captured in two- or three-days intervals, starting from 5th day.

5.2.4. Vertical sections within colonies

Aims:

1. To characterize differentiation to U and L cells of colonies formed by BY-Gat1p-GFP derived strains. To inspect whether genes of interest deletion and/or GAL promoter exchange affects differentiation of colonies

2. To characterize TOR pathway activity in U and L cells of colonies formed by BY-Gat1p-GFP derived strains.

3. To compare presence of dead cells in U and L layers of colonies formed by BY-Gat1p-GFP derived strains.

Vertical cross-sections of colonies formed by strains listed in Table 13 were examined to inspect how those colonies are able to differentiate, how is morphology of U and L cells affected by target gene knock-out, and to outline the vitality of cells in upper and lower layers (Figures 54-66). Colonies grown on GM were used for preparation of vertical cross-sections for observation of differentiation, morphology of U and L cells, and for tracking of TORC1 activity. pH-dependent indicator BKP is also known as a chemical that enters dead cells or cells with decreased ability to export toxic compounds (e.g., with lower membrane potential or non-functional MDR pumps). Colonies grown on GM+BKP plates were used for preparation of vertical cross-sections to observe the presence of dead cells in both in U and L cells (Figure 67).

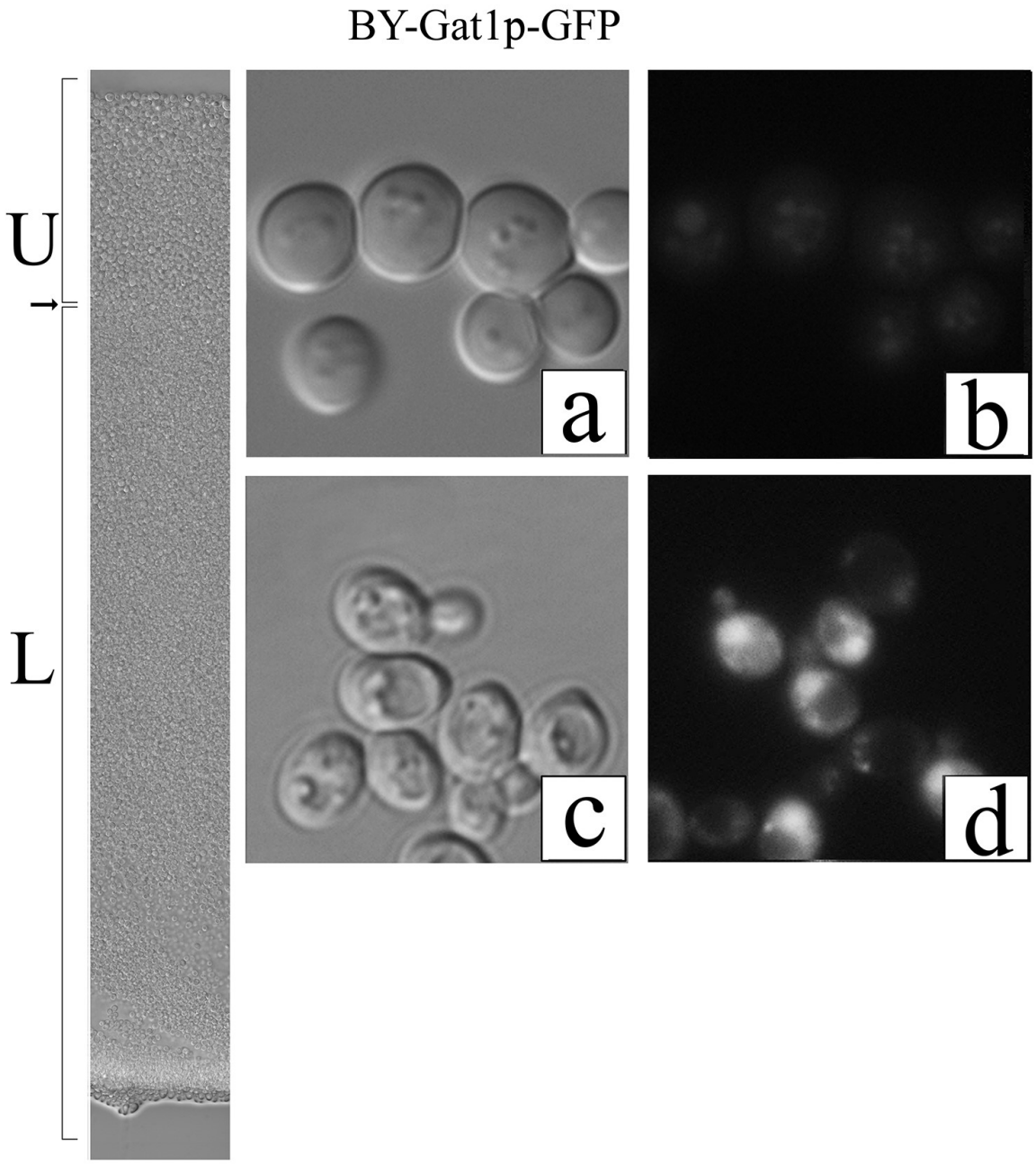

Figure 54. Vertical cross-section of the colony formed by parental strain BY-Gat1p-GFP**.** Letters U and L represent U and L cells, arrow is pointing on the boundary between two layers. **a** – morphology of U cells in Nomarski contrast, **b** – localization of Gat1p-GFP in U cells, **c** – morphology of L cells in Nomarski contrast, **d** – localization of Gat1p-GFP in L cells.

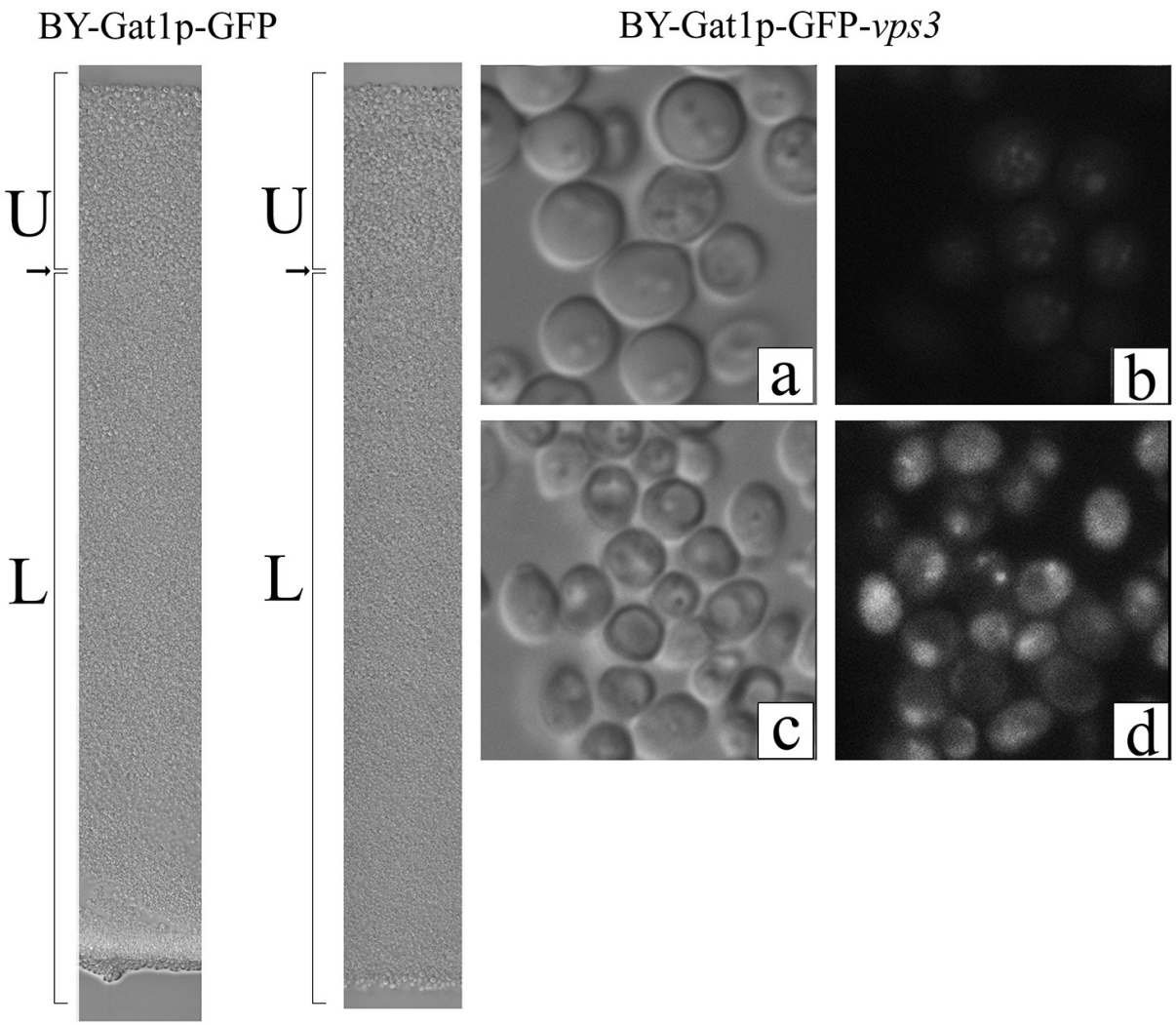

Figure 55. Vertical cross-section of the colony formed by BY-Gat1p-GFP and BY-Gat1p-GFP-*vps3* strains**.** Letters U and L represent U and L cells, arrow indicates the boundary between two layers. **a,b,c,d** refer to BY-Gat1p-GFP-*vps3* strain: **a** – morphology of U cells in Nomarski contrast, **b** – localization of Gat1p-GFP in U cells, **c** – morphology of L cells in Nomarski contrast, **d** – localization of Gat1p-GFP in L cells.

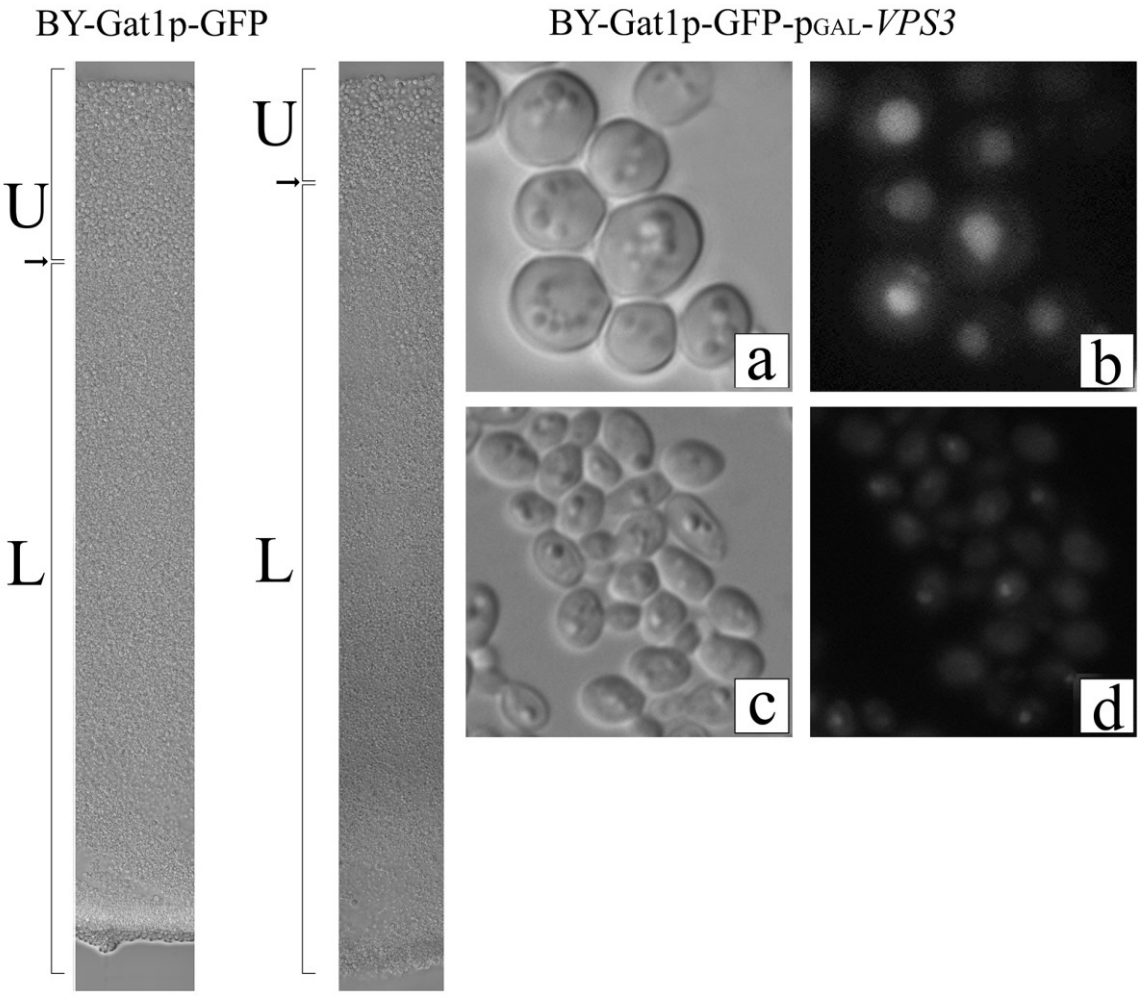

Figure 56. Vertical cross-section of the colony formed by BY-Gat1p-GFP and BY-Gat1p-GFP-pGAL-*VPS3***.** Letters U and L represent U and L cells, arrow is pointing on the boundary between two layers. **a,b,c,d** refer to BY-Gat1p-GFP-*vps3* strain **a** – morphology of U cells in Nomarski contrast, **b** – localization of Gat1p-GFP in U cells, **c** – morphology of L cells in Nomarski contrast, **d** – localization of Gat1p-GFP in L cells.

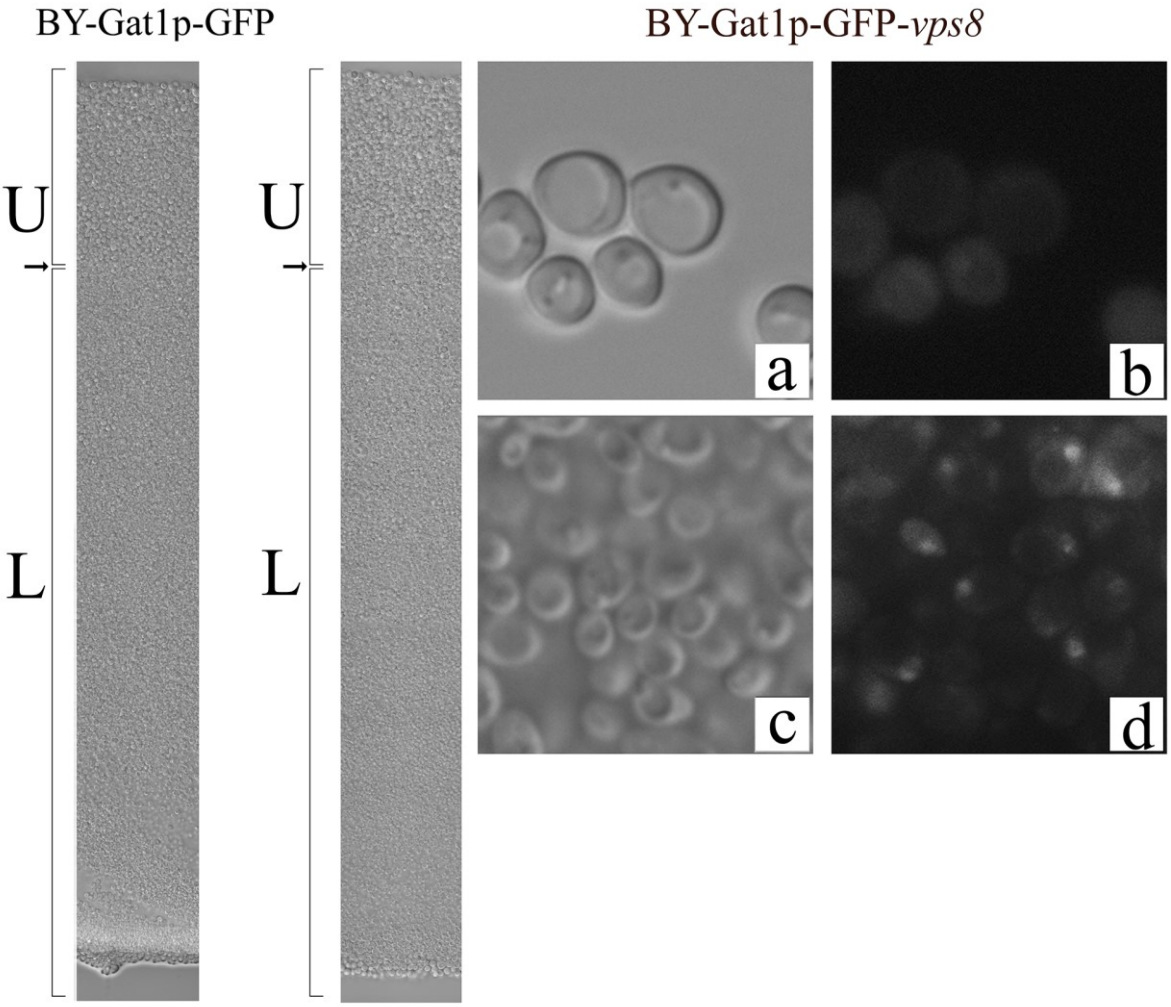

Figure 57. Vertical cross-section of the colony formed by BY-Gat1p-GFP and BY-Gat1p-GFP-*vps8* strains**.** Letters U and L represent U and L cells, arrow is pointing on the boundary between two layers. **a,b,c,d** refer to BY-Gat1p-GFP-*vps8* strain: **a** – morphology of U cells in Nomarski contrast, **b** – localization of Gat1p-GFP in U cells, **c** – morphology of L cells in Nomarski contrast, **d** – localization of Gat1p-GFP in L cells.

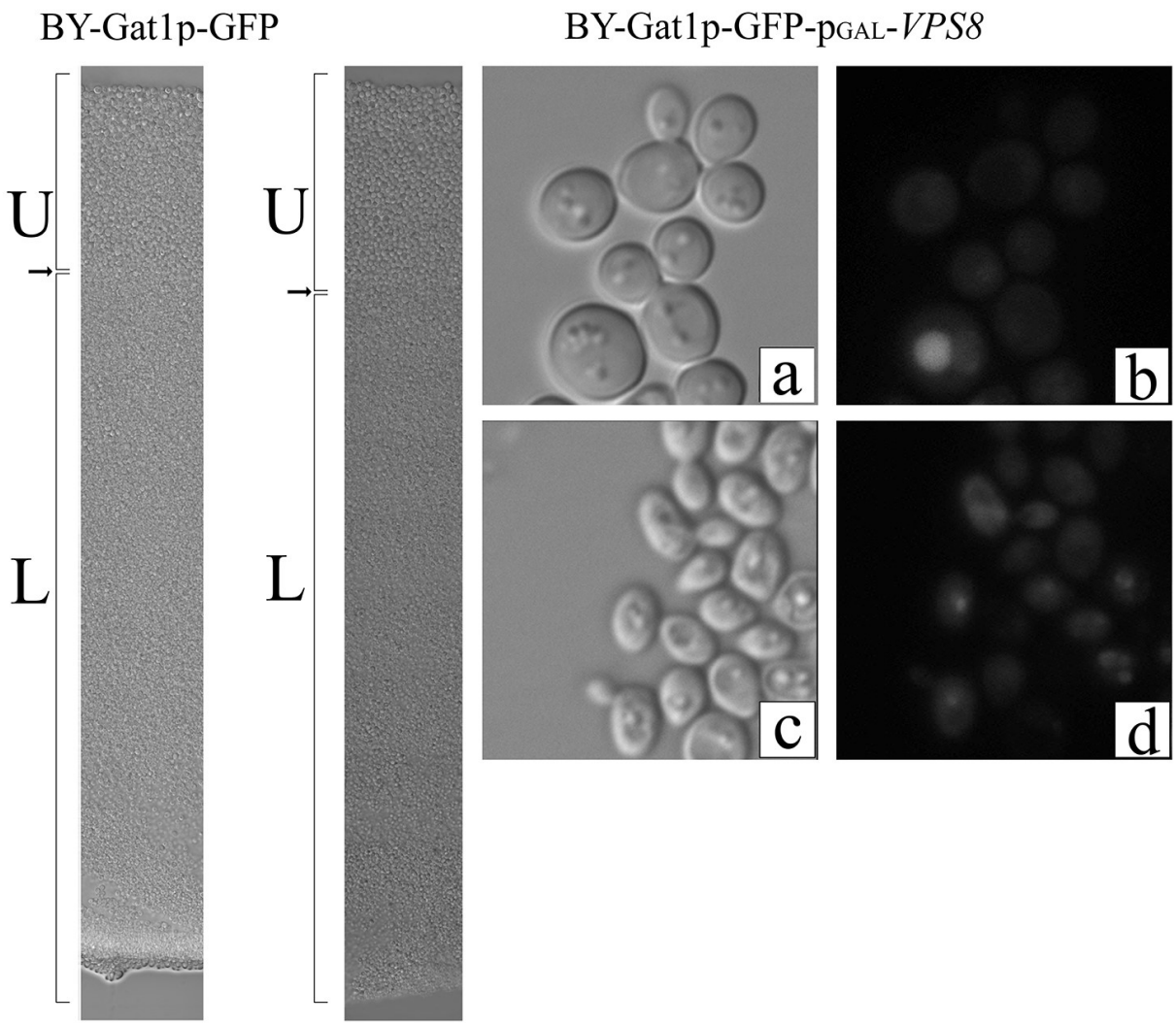

Figure 58. Vertical cross-section of the colony formed by BY-Gat1p-GFP and BY-Gat1p-GFP-pGAL-*VPS8***.** Letters U and L represent U and L cells, arrow is pointing on the boundary between two layers. **a,b,c,d** refer to BY-Gat1p-GFP-*vps8* strain **a** – morphology of U cells in Nomarski contrast, **b** – localization of Gat1p-GFP in U cells, **c** – morphology of L cells in Nomarski contrast, **d** – localization of Gat1p-GFP in L cells.

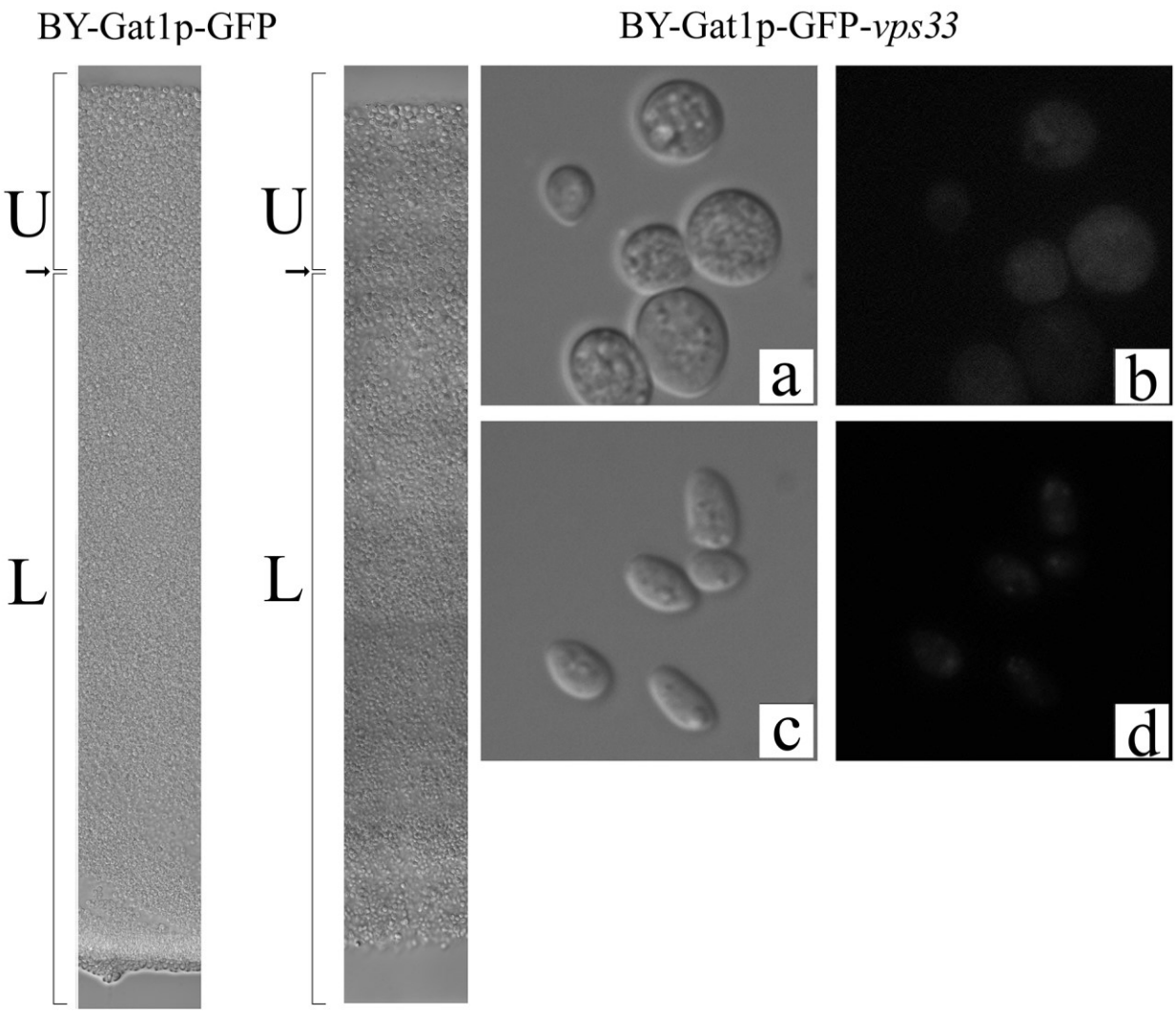

Figure 59. Vertical cross-section of the colony formed by BY-Gat1p-GFP and BY-Gat1p-GFP-*vps33* strains**.** Letters U and L represent U and L cells, arrow is pointing on the boundary between two layers. **a,b,c,d** refer to BY-Gat1p-GFP-*vps33* strain: **a** – morphology of U cells in Nomarski contrast, **b** – localization of Gat1p-GFP in U cells, **c** – morphology of L cells in Nomarski contrast, **d** – localization of Gat1p-GFP in L cells.

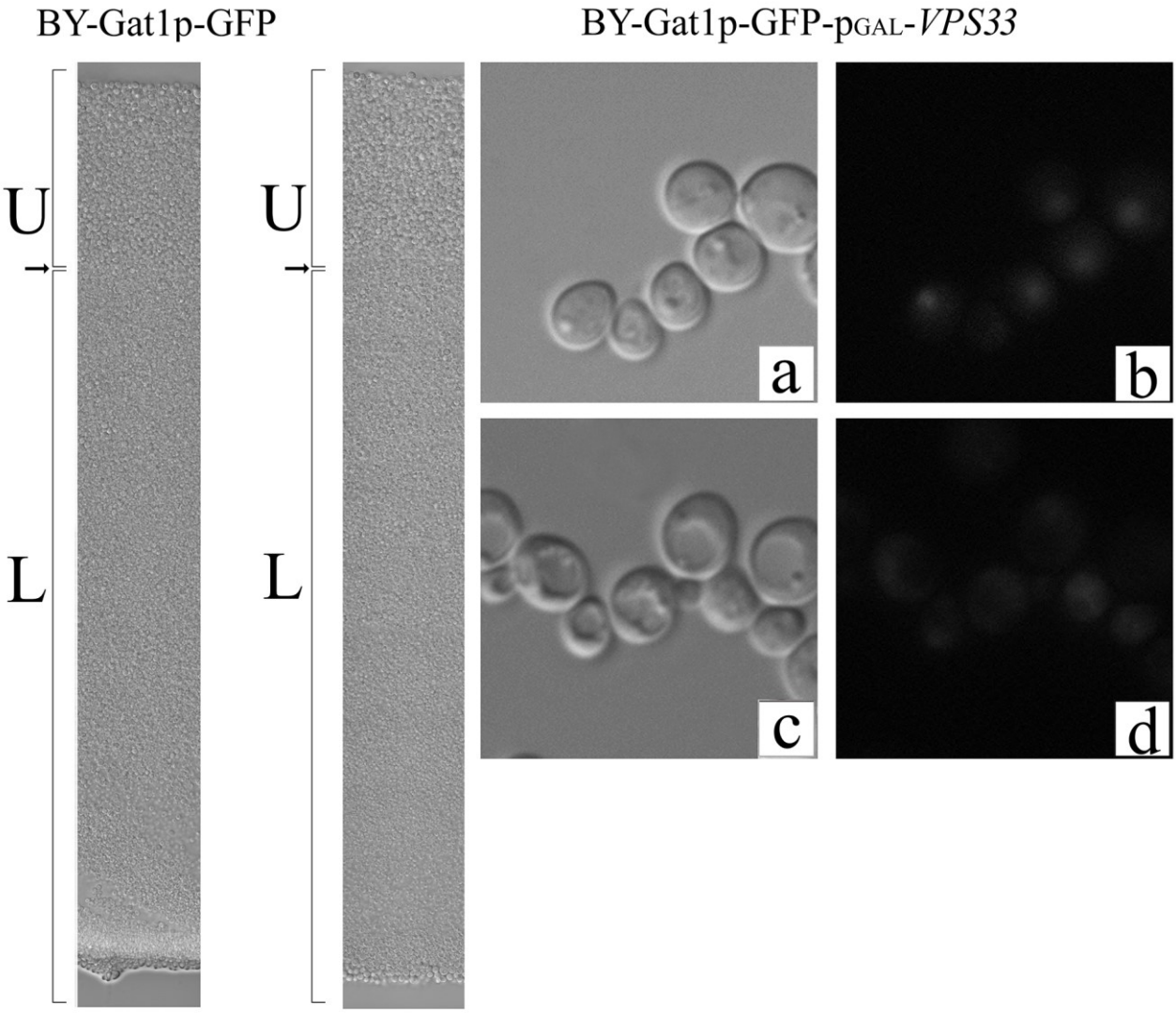

Figure 60. Vertical cross-section of the colony formed by BY-Gat1p-GFP and BY-Gat1p-GFP-pGAL-*VPS33*. Letters U and L represent U and L cells, arrow is pointing on the boundary between two layers. **a,b,c,d** refer to BY-Gat1p-GFP-pGAL-*VPS33* strain **a** – morphology of U cells in Nomarski contrast, **b** – localization of Gat1p-GFP in U cells, **c** – morphology of L cells in Nomarski contrast, **d** – localization of Gat1p-GFP in L cells.

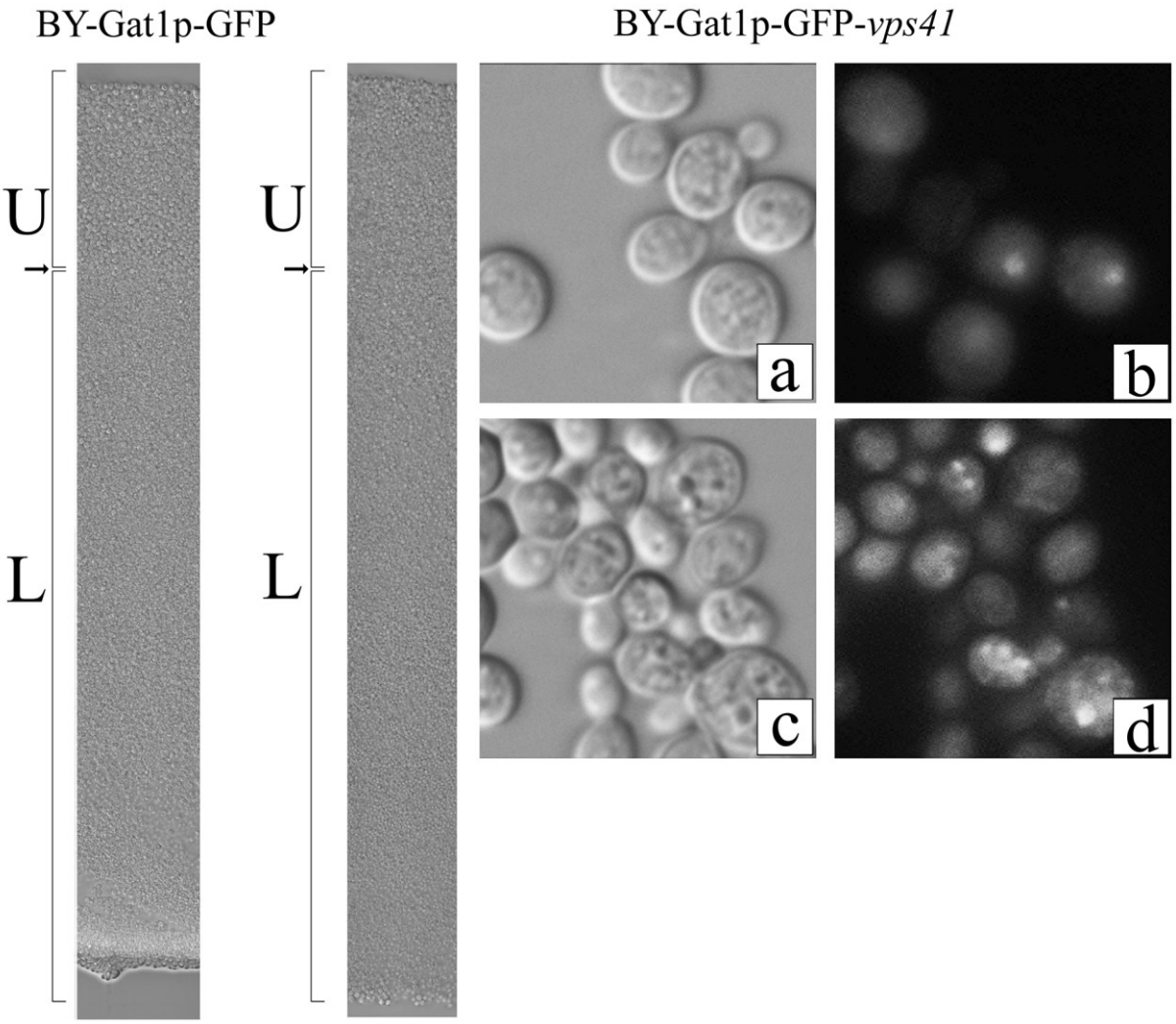

Figure 61. Vertical cross-section of the colony formed by BY-Gat1p-GFP and BY-Gat1p-GFP-*vps41* strains**.** Letters U and L represent U and L cells, arrow is pointing on the boundary between two layers. **a,b,c,d** refer to BY-Gat1p-GFP-*vps41* strain: **a** – morphology of U cells in Nomarski contrast, **b** – localization of Gat1p-GFP in U cells, **c** – morphology of L cells in Nomarski contrast, **d** – localization of Gat1p-GFP in L cells.

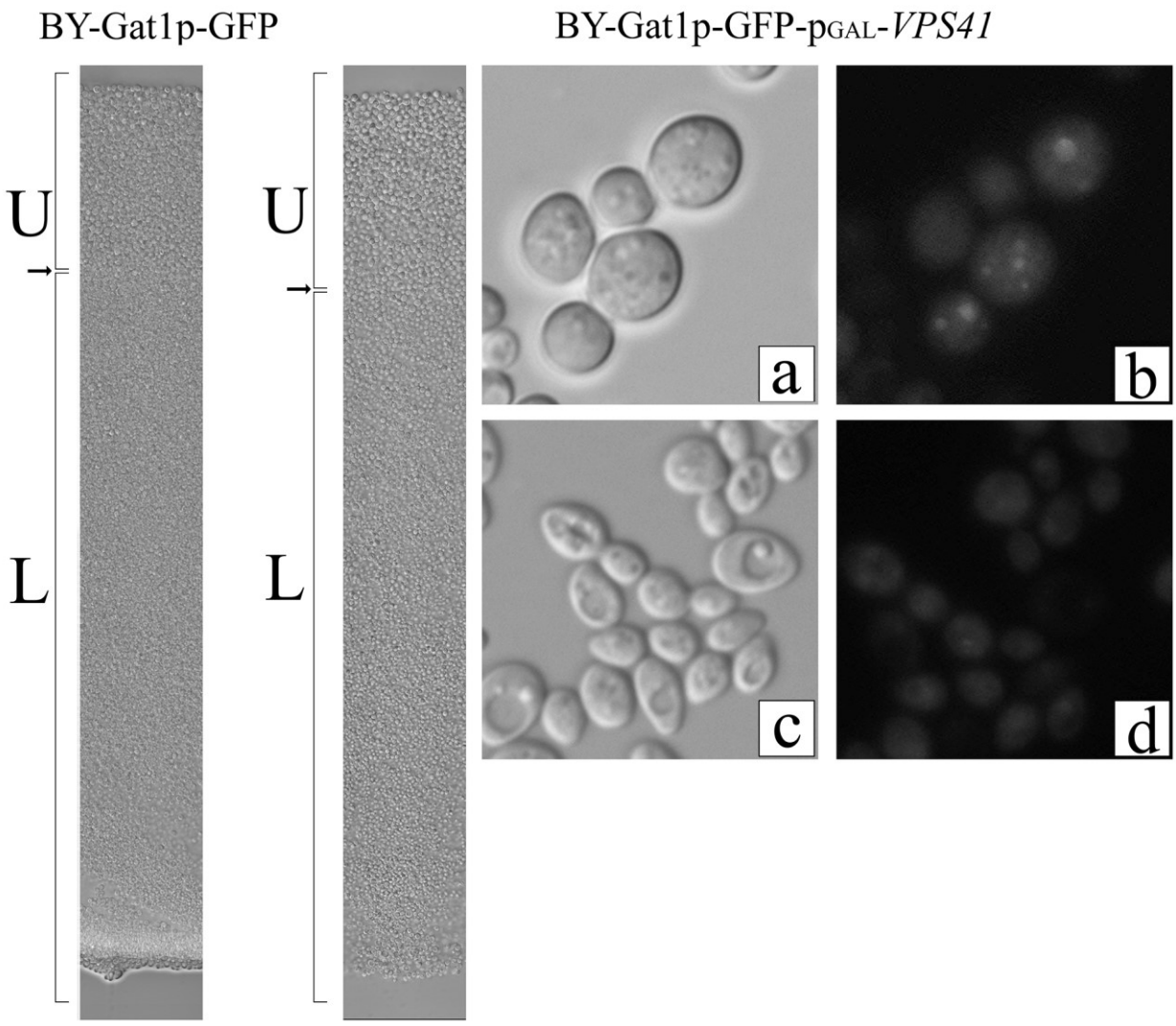

Figure 62. Vertical cross-section of the colony formed by BY-Gat1p-GFP and BY-Gat1p-GFP-pGAL-*VPS41*. Letters U and L represent U and L cells, arrow is pointing on the boundary between two layers. **a,b,c,d** refer to BY-Gat1p-GFP-pGAL-*VPS41* strain **a** – morphology of U cells in Nomarski contrast, **b** – localization of Gat1p-GFP in U cells, **c** – morphology of L cells in Nomarski contrast, **d** – localization of Gat1p-GFP in L cells.

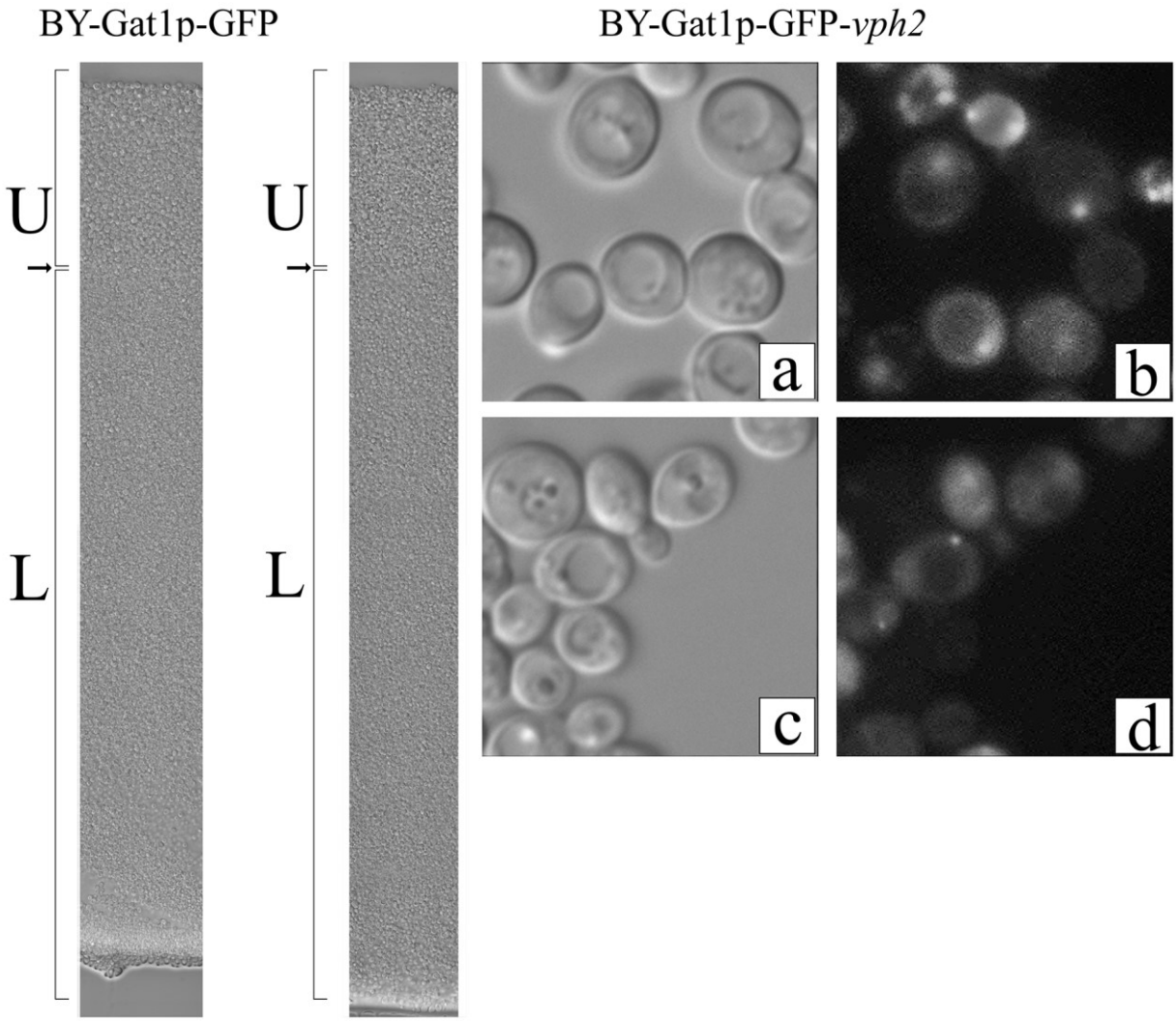

Figure 63. Vertical cross-section of the colony formed by BY-Gat1p-GFP and BY-Gat1p-GFP-*vph2* strains**.** Letters U and L represent U and L cells, arrow is pointing on the boundary between two layers. **a,b,c,d** refer to BY-Gat1p-GFP-*vph2* strain: **a** – morphology of U cells in Nomarski contrast, **b** – localization of Gat1p-GFP in U cells, **c** – morphology of L cells in Nomarski contrast, **d** – localization of Gat1p-GFP in L cells.

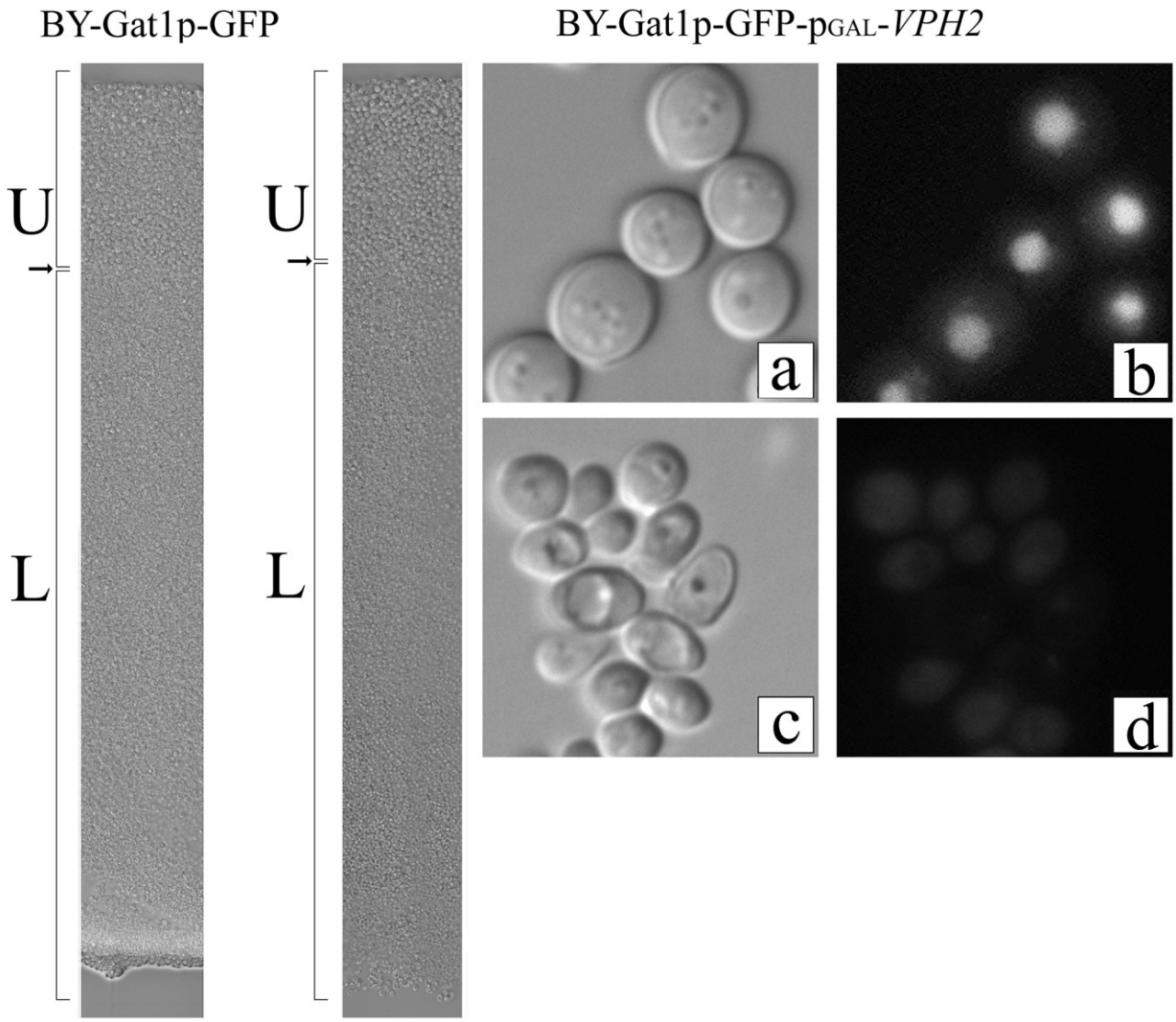

Figure 64. Vertical cross-section of the colony formed by BY-Gat1p-GFP and BY-Gat1p-GFP-pGAL-*VPH2*. Letters U and L represent U and L cells, arrow is pointing on the boundary between two layers. **a,b,c,d** refer to BY-Gat1p-GFP-pGAL-*VPH2* strain **a** – morphology of U cells in Nomarski contrast, **b** – localization of Gat1p-GFP in U cells, **c** – morphology of L cells in Nomarski contrast, **d** – localization of Gat1p-GFP in L cells.

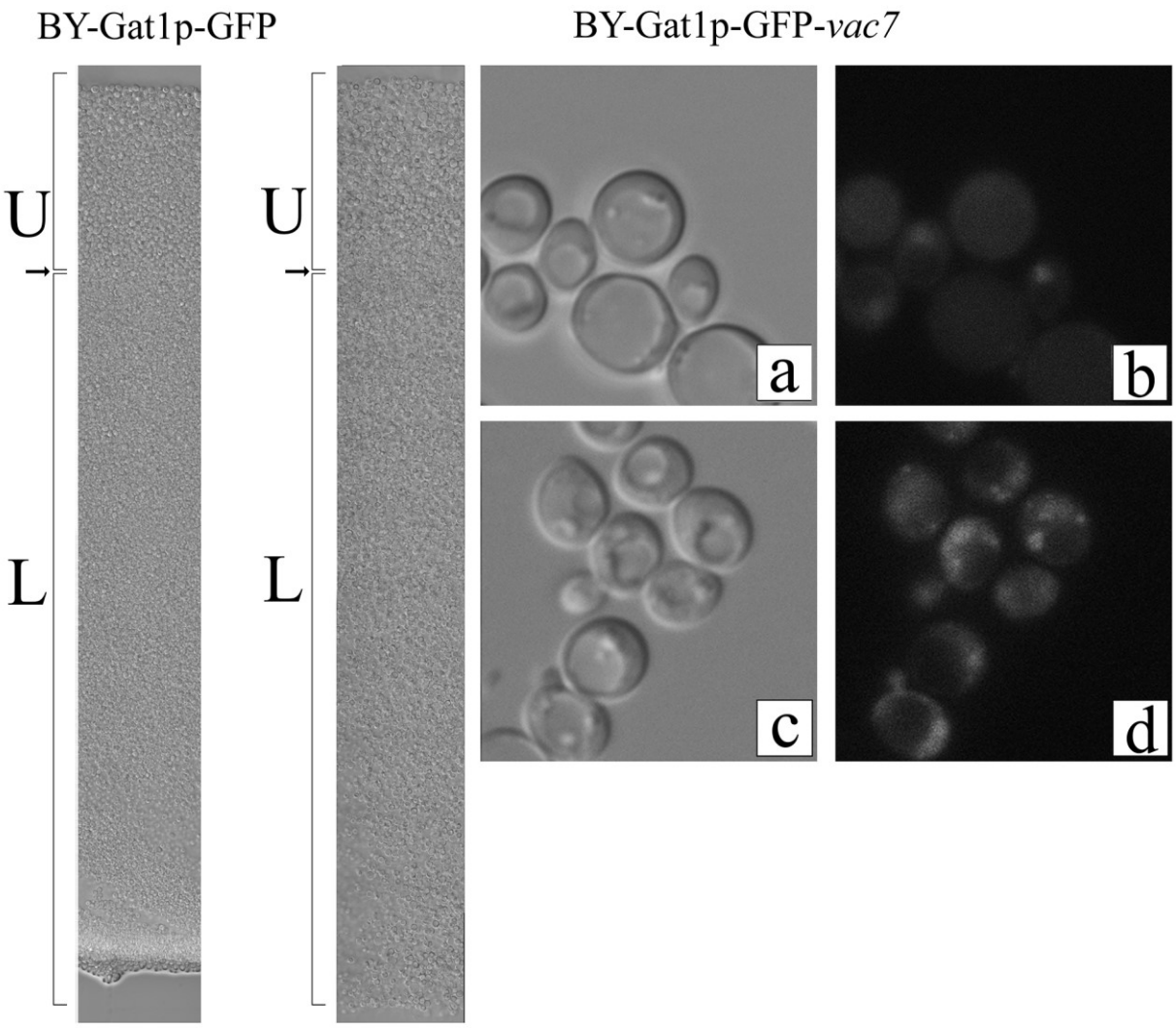

Figure 65. Vertical cross-section of the colony formed by BY-Gat1p-GFP and BY-Gat1p-GFP-*vac7* strains**.** Letters U and L represent U and L cells, arrow is pointing on the boundary between two layers. **a,b,c,d** refer to BY-Gat1p-GFP-*vac7* strain: **a** – morphology of U cells in Nomarski contrast, **b** – localization of Gat1p-GFP in U cells, **c** – morphology of L cells in Nomarski contrast, **d** – localization of Gat1p-GFP in L cells.

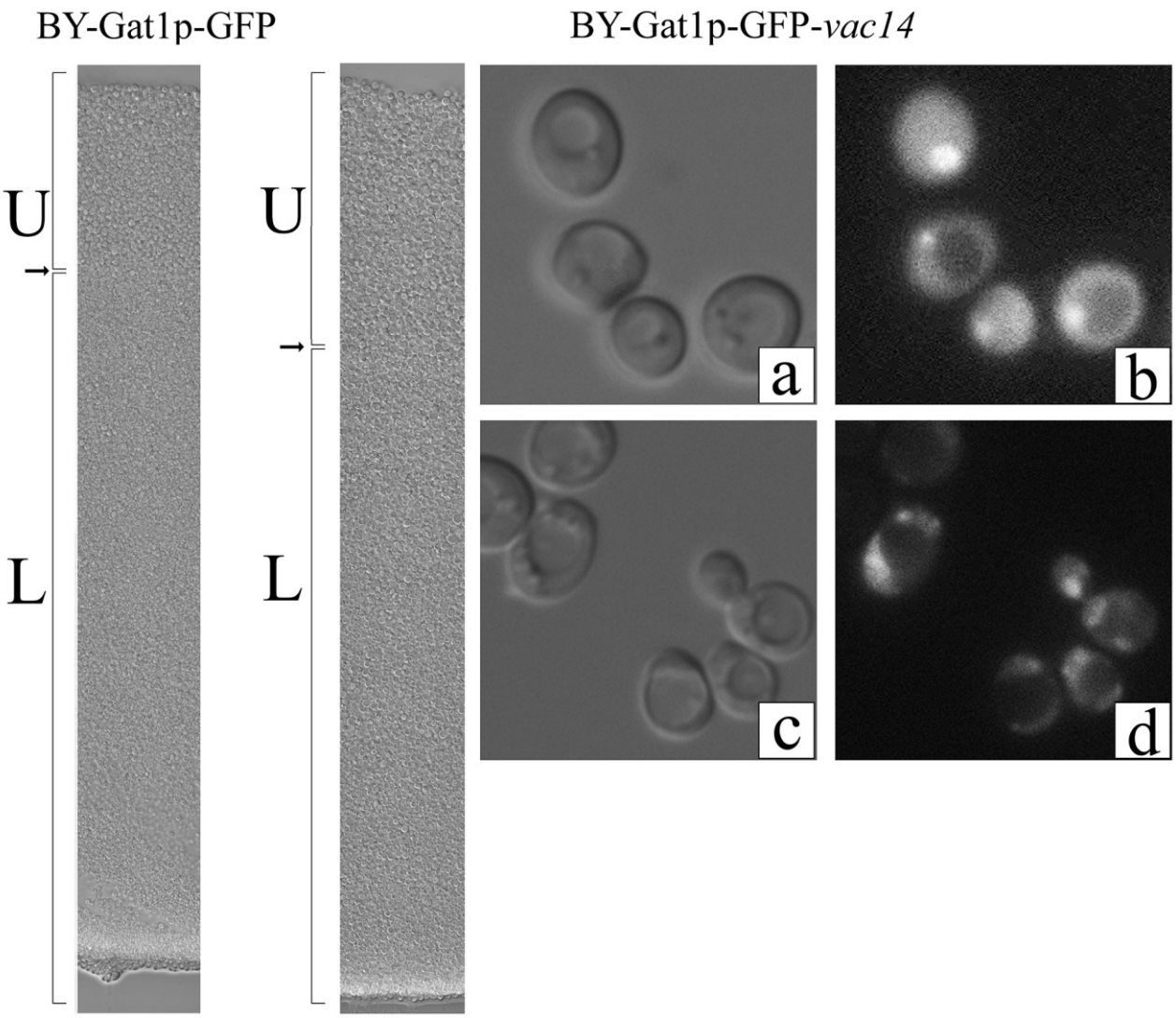

Figure 66. Vertical cross-section of the colony formed by BY-Gat1p-GFP and BY-Gat1p-GFP-*vac14* strains**.** Letters U and L represent U and L cells, arrow is pointing on the boundary between two layers. **a,b,c,d** refer to BY-Gat1p-GFP-*vac14* strain: **a** – morphology of U cells in Nomarski contrast, **b** – localization of Gat1p-GFP in U cells, **c** – morphology of L cells in Nomarski contrast, **d** – localization of Gat1p-GFP in L cells.

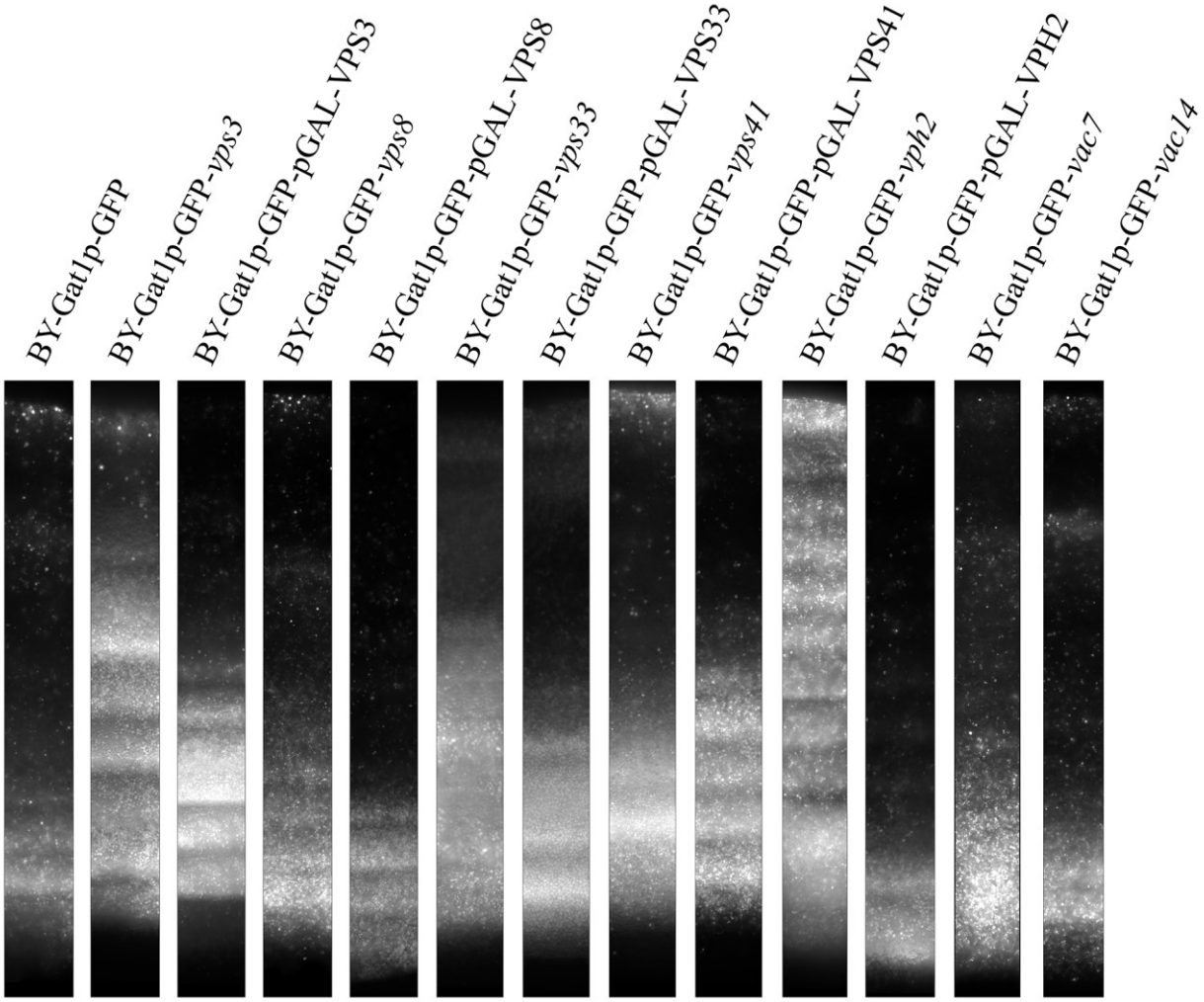

Figure 67. Presence of dead cells in U and L layers of colonies formed by BY-Gat1p-GFP derived strains.

In Figure 67 is shown the comparison of damaged cells presence in U and L cells of colonies formed by BY-Gat1p-GFP derived strains. Images were captured in exposition 700ms, with exception for the strain BY-Gat1p-GFP-*vps33*, where exposition 100ms was used.

6 Discussion

6.1. Comparison of BY and vam6 strains: Colony morphology and level of expression of selected proteins.

According to proteomic analysis performed in our laboratory, several proteins were differentially present in U and L cells, separated from differentiated colonies formed by BY and BY-*vam6* strains (non-published data). These results allowed to suggest that Vam6p can influence expression of these proteins.

Proteins of interest were tagged with GFP in both BY and BY-*vam6* strains. Newly prepared strains were verified by PCR analysis and by fluorescent microscopy. C-terminal GFP fusion aimed to visualize proteins of interest and to investigate whether localization and expression of proteins is different in U and L cells. To ensure that GFP is assembled correctly and did not result in protein mis-localization, data from fluorescent microscopy was compared to reference data from Yeast GFP Fusion Localization Database and literature.

For further investigation, the next criteria for selection of clones was the monitoring of developmental phases visualized by changes in pH of the surrounding medium. Three clones from each strain were compared to parental strains in their ability to alkalize the medium during the colony development. The clones chosen for preparation of vertical cross-sections were the most similar to parental strain`s behavior. The reason for this selection was to ensure that analyzed clones do not have additional physiology changes caused by mutations.

Finally, the results obtained from Western Blot analysis, fluorescent microscopy and proteomics analysis were compared to each other. The correlation of these results aimed to outline the difference in production of selected proteins in U and L cells of both wt strain and strain deleted in VAM6 gene.

6.1.1. Comparison of selected proteins localization and level of expression in differentiated and non-differentiated colonies.

Reference photos for some of GFP-tagged proteins of interest were accessible in very low quality, especially in the case of Sso1p-GFP. No reference photos were available for Aco1p-GFP. It is known that aconitase Aco1p is typically localized in mitochondria and cytosol [56]. In this study, Aco1p-GFP was present mostly in mitochondria. Data from fluorescent microscopy corresponded with data from literature and with Yeast GFP Fusion Localization Database (yeastgfp.yeastgenome.org). Western Blot analysis partially correspond to proteomics data. According to the proteomic analysis, level of Aco1p is 7.81 times higher in U cells when *VAM6* gene is deleted. Western Blot results confirmed the difference in Aco1p levels, however, this difference was not as significant as proteomic results demonstrated.

The membrane-associated Erg26p involved in ergosterol synthesis, is localized on endoplasmic reticulum membrane[57]. The data from fluorescent microscopy of non-differentiated colonies corresponded to the literature. However, during colony growth and development, the fluorescent signal was also present in vacuoles and cytosol in U and L cells of colonies formed by BY-Erg26p-GFP strain. It is known that GFP protein can be present in vacuoles even after the tagged protein was degraded [58]. Western Blot results correspond with proteomic results for Erg26p. Considering the fact that Erg26p-GFP was present only on endoplasmic reticulum membrane in U and L cells of colonies formed by BY-*vam6*-Erg26p-GFP strain, it could be suggested that the lack of Vam6p results increased stability of Erg26p.

Mdh2p is a cytosolic malate-dehydrogenase. According to prediction from Yeast GFP Fusion Localization Database (yeastgfp.yeastgenome.org), Mdh2p is localized in cytosol and peroxisomes. Data obtained from fluorescent microscopy corresponds to the reference data. While observing the fluorescent signal in cells isolated from one-day old colonies, the signal from nucleus was also present. This signal however, appeared to be an auto-fluorescence. The same finding was observed in U and L cells of colonies formed by both BY-Mdh2p-GFP and BY-*vam6*-Mdh2p-GFP strains. [52]

The localization of Mrp4p-GFP corresponded to the Yeast GFP Fusion Localization Database prediction in cells that were isolated from both differentiated and non-differentiated colonies. Mrp4p is a component of the small mitochondrial ribosome subunit, required for translation in mitochondria [53], [59]. U cells of colonies formed by

BY-*vam6*-Mrp4p-GFP strain exhibited stronger GFP signal from mitochondria compared to U cells of BY-Mrp4p-GFP strain. The data from the proteomic analysis demonstrated 3.82 times higher level of Mrp4p in U cells of colonies formed by strain deleted in *VAM6* in comparison with wt strain. Mrp4p was not detectable by Western Blot, possibly due to a very low level of Mrp4p expression in analyzed cells.

Another protein which was not detected on Western Blot is Sso1p-GFP. The proteomic analysis demonstrates 3.58 higher level of Sso1p in U cells of colonies formed by BY-*vam6* strains than in U cells of wt colonies. According to Yeast Genome Database prediction, Sso1p typical localization is cytosolic and peroxisomal. Data obtained from fluorescent microscopy of cells isolated from non-differentiated colonies corresponded with this prediction. In case of differentiated colonies formed by wt strain and strain deleted in *VAM6* gene, Sso1p-GFP signal was stronger in U cells. L cells of colonies formed by BY-*vam6* exhibited GFP signal from vacuoles only.

Fas1p-GFP, the beta-subunit of fatty acid synthetase [51], was present in lipid particles of cells isolated from non-differentiated colonies. The fluorescent microscopy data corresponds to Western Blot data. No Fas1p was detected in U cells of colonies formed by BY-Fas1-GFP strain. As demonstrated in Figure 42, the fluorescent signal was present in vacuoles. As discussed above, the GFP protein can be present in vacuoles even after the tagged protein was degraded [58]. The GFP from U cells was detected on Western Blot, while no Fas1p was detected. The Western Blot data appeared to be opposite to the proteomics data for BY-*vam6*-Fas1-GFP strain. Proteomics results stated a higher level of Fas1p in U cells, while Western Blot demonstrated a higher level of Fas1p in L cells.

Western Blot was performed for all analyzed samples at a time. For Sso1p-GFP and Mrp4p-GFP no bands occurred film, however, degraded GFP was detected. Other analyzed proteins (Aco1p, Erg26p, Fas1p and Mdh2p) were detectable. The possible reasons could be low level of Sso1p-GFP and Mrp4p-GFP or the prolonged washing [60]. Different exposure times were used to achieve a visible band for mentioned proteins. It is also necessary to clarify the fact, that Western Blot was performed only once and for more reliable result it needs to be repeated.

The vertical sections within colonies formed by examine strains did not demonstrate significant morphology changes in U and L cells, except for BY-vam6-Fas1p-GFP strain. The U layer of examined colonies appeared to be thinner in comparison with U layer of parental strain colonies.

6.2. Characterization of selected vacuolar proteins role in development of colonies and in regulation of TORC1 activity.

For investigation of the impact of selected genes deletion on colonies morphology, physiology and TORC1 activity in U and L cells 12 new strains were prepared. As parental strain was used BY-Gat1p-GFP strain, derived from BY4742(in this thesis - BY) strain. This strain contained GFP-tagged Gat1p, the effector of TORC1, the localization of which is dependent on TORC1 activity. This enabled to track TORC1 activity in U and L cells and define whether it is affected by lack of each of selected genes [2], [10].

6.2.1. Construction of new strains

Based on literature search following proteins were selected to investigate their role in development of yeast colonies: Vps3p, Vps8p, Vps33p, Vps41p, Vph2p, Vac7p, Vac14p and Fab1p. Vps3p and Vps8p are subunits of CORVET complex and Vps33p and Vps41p are subunits of HOPS complex. Vph2p is required for V-ATPase assembly. Vac7p, Vac14p and Fab1p are subunits of the complex required for PI3P and PI(3,5)P2 interconversion [7], [41]. Vam6p/Vps39p is required for HOPS complex assembly [30] and modulates activity of TORC1 complex [8]. It was indicated in our laboratory that Vam6p contributes to TORC1 activity in U cells of differentiated colonies (non-published data). The linkage between vacuolar fission and TORC1 was also proposed for Vph2p [45]. Therefore, it was suggested that other subunits of HOPS and CORVET complexes, and proteins required for V-ATPase assembly and stability can also contribute to the regulation of TORC1 activity in U cells.

In this part of study, it was investigated: i.) whether other selected subunits of above-mentioned complexes affect TORC1 activity in U cells of differentiated colonies, ii.) whether absence of candidate proteins influences colony development and U and L cell formation and viability.

Seven strains, deleted in *VPS3, VPS8, VPS33, VPS41, VPH2, VAC7* and *VAC14* genes were prepared. Also, five strains with promoter exchange were constructed using the GAL promoter for *VPS3, VPS8, VPS33, VPS41, VPH2* genes in order to achieve basal level of protein expression and compare it to parental and to deletion strains. The purpose of promoter exchange was to ensure basal level of protein expression in case if deletion for the same gene would be lethal. For example, strains deleted in *VPH2* gene showed a significant growth defects whereas BY-Gat1p-GFP-pGAL-*VPH2* phenotype remained the

phenotype of the parental strain. The promoter exchange was not performed for *VAC7* and *VAC14* genes, as strains with deletions in these genes were published and proved to be viable [61].

Vac14 complex consists of Vac7p, Vac14 p, Fab1p and Fig4p subunits, and is important for PI3P conversion to PI (3,5)P2 [42], [61]. As literature states, Fab1p is a lipid kinase, and it`s function is to convert PI3P into PI(3,5)P2 and therefore to ensure V-ATPase stabilization [38], [39]. Also it was indicated, that PI(3,5)P2 plays an important role in cell survival during the osmotic stress [62]. The aim was to delete *VAC7*, *VAC14* and *FAB1* genes in order to characterize absence of Vac7p, Vac14p and Fab1p on TORC1 activity in U cells. Unfortunately, it was not possible to isolate any of clones with *FAB1* gene deletion. *FAB1* is however not an essential gene, as there are reports that *fab1Δ* and even double mutants *fab1Δ, vac7Δ* were isolated and were viable [42], [62].

6.2.2. Characterization of development of giant colonies formed by BY-Gat1p-GFP derived strains.

Colonies grown on a solid medium pass through developmental phases, which can be visualized by changes in pH of surrounding medium using pH-sensitive indicator BKP. After first acidic phase the alkali phase occurs. Yeast colonies produce ammonia as a signaling molecule which is important for the population development. The ammonia production starts during the early alkali phase [55]. The decrease of ammonia production during the colony growth results in the second acidic phase. The transition to the alkali phase indicates the development phase of the colony. The ability of colonies to differentiate, to produce and to release ammonia also depends on the yeast strain [5], [15], [55].

The deletion of *VPS3* gene caused earlier transition to alkali phase. The deletion of *VPS8*, *VPS41* and *VAC7* genes did not affect the transition timing. The deletion of *VPS33*, *VAC14*, *VPH2* result in delayed transition with *VPH2* knock-out having a greater effect. Also, when the expression of proteins Vps3p, Vps8p, Vps33p, Vps41p and Vph2p was on a low basal level due to the promoter exchange, the transition to alkali phase was delayed in two days.

The detailed examination of colonies' morphology demonstrated that deletion of *VAC7* and *VAC14* genes caused loss of smooth structure. These findings indicate that Vac7p and Vac14p could be potentially involved in the maintenance of smooth structure of the colonies.

The yeast cells with mutations in V-ATPase genes (*VMA* genes) are viable in acidic media but fail to grow in alkaline medium with addition of CaCl2 [63]. The lack of Vph2p, which is required for V-ATPase assembly, caused significant growth defects in acidic medium.

The morphology of colonies did not seem to be affected by lack of Vps3p, Vps8p, Vps33 and Vps41p, when observed by magnifier loupe. The effects of these proteins absence however, were visible on vertical cross-sections within the colonies.

6.2.3. Vertical sections within colonies.

The cross-sections for colonies formed by all examined strains were prepared on 14th day. Considering the different timing of transition to alkali phase, which indicates the transition to next development and differentiation phase[64], it would be also interesting to investigate cross-sections for these colonies in different days of development. For example, to examine BY-Gat1p-GFP-vps3 strain for which the surrounding medium began to be alkaline on 11-12th day.

In order to characterize differentiation to U and L cells of colonies formed by BY-Gat1p-GFP derived strains, colony sections were observed in Nomarski contrast [65], [66]. On 14th day all examined colonies were differentiated. However, the boundary between U and L cells of colonies formed by BY-Gat1p-GFP-*vps33* was not as well-defined as compared to the parental strain. Together with the later transition of colonies formed by the strain deleted in *VPS33* gene to alkali phase, these results correspond to the statement that the alkalization of the medium surrounding the colonies and differentiation to U and L cells are closely related [5], [55], [64].

The morphology of vacuoles in U cells was affected dramatically in colonies formed by strains lacking Vac7p, Vac14p, Vph2p and Vps8p. The enlarged vacuoles were also detected in L cells of colonies formed by strains deleted in *VAC7* and *VAC14* genes. The size and morphology of yeast vacuole is affected by stress conditions [45], [67]. It was reported by Duex and colleagues, that the vacuole volume decreases with increased increasing levels of PI(3,5)P2. The vacuole level is restored when PI(3,5)P2 returns to a basal level. The lack of Vac7p and Vac14p, which is required for functionality of PI(3,5)P2 interconversion complex, causes decrease of PI(3,5)P2 level and the enlargement of vacuoles. Also, enlarged vacuoles were detected in cells lacking Fab1p [41]. These data are consistent with results obtained in this study. Apparently, lack of any component of Vac14 complex results in vacuole enlargement.

The Vps8p is the membrane-anchoring subunit of CORVET complex which is required for endosomal vesicular trafficking to vacuole [68], [69]. The role of Vps8p in the fusion process was also reported by Peplowska and colleagues [31]. As authors demonstrate, Vps8p acts independently in vacuolar fusion even when other components of CORVET complex are missing. The phenotype of U and L cells of colonies formed by strain deleted in *VPS8* gene partially correspond to published data. Peplowska and colleagues report only a small number of cells with enlarged vacuole in the cell population.

In this study almost all the cells isolated from upper layer of differentiated colonies formed by BY-Gat1p-GFP-*vps8* evinced enlarged vacuoles. The yeast cells lacking Vps8p, Vac7p, Vac14p and Vph2p were observed in already differentiated colonies in this study and were not compared to cells isolated from non-differentiated strains. It would be also reasonable to investigate in which stage of development the vacuole enlargement occurs.

The absence of Vps33p and Vps41p caused the vacuolar fragmentation in U cells. The morphology od L cells was also affected. The low basal level of Vps33p and Vps41p affected only U cells; however, the effect was not as dramatic as compared to lack of mentioned proteins.

6.2.4. The characterization of TOR pathway activity in U and L cells of colonies formed by BY-Gat1p-GFP derived strains.

The U and L cells were isolated from differentiated colonies formed by BY-Gat1p-GFP derived strains on 14^{th} day in order to track the activity of TORC1 in strains deleted in genes of interest. The TORC1 activity was tracked by TORC1-responsive transcription factor Gat1p labelled with GFP. As it was mentioned above, the Gat1p localization depends on TORC1 activity. The cytosolic localization occurs when TORC1 is active and inactivation of TORC1 results in nuclear localization of Gat1p [10], [70]. Due to a strong background while capturing the Gat1p-GFP signal from colonies' cross-sections, the U and L cells were isolated from the colonies and observed separately. The signal from vacuoles was considered to demonstrate the cytosolic localization of Gat1p-GFP or GFP degraded in vacuoles [58].

It was reported that HOPS and CORVET complexes and the vacuolar ATPase can contribute to TORC1 activity. The results obtained in this study demonstrate that the lack of some components of these complexes results in TORC1 deactivation in U cells.

The nuclear localization of Gat1p and therefore inactive TORC1 was detected in U cells of colonies formed by strains deleted in *VPS41*, *VPH2*, *VAC7* and *VAC14*. The deletion of *VPS3*, *VPS8* and *VPS33* did not affect Gat1p localization in comparison to the parental strain. Interestingly, absence and a low basal level of Vps3p resulted in TORC1 activation in L cells.

Kingsbury and colleagues propose the model of Vps-C complex in TORC1 signaling promoting where the disruption of HOPS and CORVET complexes result in vacuolar fragmentation, which causes the reduced activation of EGO complex and decreased TORC1 activity [7]. The deletion of *VPS8* gene did not cause the vacuolar fragmentation. Oppositely, the cells lacking Vps8p demonstrated enlarged vacuoles and also TORC1 was active in U cells. However, the exact level of TORC1 activity was not measured in this study.

6.2.5. Comparison of dead or damaged cells presence in U and L layers of colonies formed by BY-Gat1p-GFP derived strains.

pH-dependent indicator BKP is also known as a chemical that enters dead cells or cells with decreased ability to export toxic compounds (e.g., with lower membrane potential or non-functional MDR pumps) or cells with damaged plasma membrane [71]. The drug resistance mechanism in *S.Cerevisiae* is ensured by existence of conserved ABC transporters localized in the plasma membrane. ABC transporters efflux the chemicals, metabolites and drugs from the cells on ATP-dependent manner. Several superfamilies of ABC transporters are known, for example, MDR, PDR, MRP superfamilies (rev. [72], [73]).

Colonies grown on GM+BKP plates were used for preparation of vertical cross-sections in order to determine whether lack of proteins of interest affects U and L cells viability. It was detected, that the deletion of *VPS3, VPS33, VPS41* and *VPH2* genes caused a significant decrease of both U and L cells' ability to efflux the BKP. These data correspond to dramatical growth defect caused by VPH2 deletion. The colonies formed by strain deleted in *VPS3, VPS33* and *VPS41* did not demonstrate the morphology change, however, almost all lower layer of the colony was exhibiting the strong signal from the damaged cells.

7 Conclusions

- In this study, Aco1p, Erg26p, Fas1p, Mdh2p, Mrp4p and Sso1p were labelled with GFP in BY(BY4742) and BY-*vam6* strains.
- Absence of Vam6p affects production of Aco1p, Erg26p, Fas1p and Mdh2p in U and L cells. These results correlate to proteomics analysis results.
- The effect of *VAM6* gene deletion on production Mrp4p and Sso1p was not confirmed in this study. These proteins were not detected with Western Blot method possibly due to a low expression level.
- The strains deleted in *VPS3, VPS8, VPS33, VPS41, VPH2, VAC7* and *VAC14* genes constructed. Also, the GAL promoter was placed before *VPS3, VPS8, VPS33, VPS41, VPH2* genes in order to achieve basal level of protein expression.
- The most dramatic effect on U and L cells viability had the absence of Vps3p, Vps33p, and Vps41p. This effect was not compensated by the low basal level of these proteins contrarily to Vph2p. Interestingly, deletion of *VPS3, VPS33* and *VPS41*genes did not seem to affect the morphology of giant colonies while the colonies were observed using the magnifier loupe.
- The deletion of *VPH2* gene causes significant growth defect, enlarged vacuoles in both U and L cells and a massive cell damage. The low basal level of Vph2p is sufficient for U and L cells survival.
- The deletion of *VAC7* and *VAC14* genes resulted in loss of smooth structure of giant colonies and enlargement of vacuoles in U and L cells. U cells exhibited stronger signal from damaged cells as compared to the parental strain.
- The absence Vps8p also resulted in enlarged vacuoles; however, only U cells were affected.
- In further investigation it is possible to try to determine the development stage, in which the vacuole enlargement occurs.
- The inactivation of TORC1 in U cells was resulted by the deletion of *VPS41*, *VPH2*, *VAC7* and *VAC14* genes.
- The results obtained in this study must be confirmed by additional experiments.

8 References

[1] R. Diaz-Ruiz, S. Uribe-Carvajal, A. Devin, and M. Rigoulet, "Tumor cell energy metabolism and its common features with yeast metabolism," *Biochim. Biophys. Acta - Rev. Cancer*, vol. 1796, no. 2, pp. 252–265, 2009.

[2] M. Cap, L. Stepanek, K. Harant, L. Vachova, and Z. Palkova, "Cell Differentiation within a Yeast Colony: Metabolic and Regulatory Parallels with a Tumor-Affected Organism," *Mol. Cell*, vol. 46, no. 4, pp. 436–448, 2012.

[3] J. Heitman, N. R. Movva, and M. N. Hall, "Targets for cell cycle arrest by the immunosuppressant rapamycin in yeast.," *Science (80-.).*, vol. 253, no. 5022, pp. 905–909, 1991.

[4] M. Laplante and D. M. Sabatini, "mTOR signaling in growth control and disease," *Cell*, vol. 149, no. 2, pp. 274–293, 2013.

[5] L. Váchová, L. Hatáková, M. Čáp, M. Pokorná, and Z. Palková, "Rapidly developing yeast microcolonies differentiate in a similar way to aging giant colonies," *Oxid. Med. Cell. Longev.*, vol. 2013, pp. 18–20, 2013.

[6] S. Dokudovskaya and M. P. Rout, "SEA you later alli-GATOR - a dynamic regulator of the TORC1 stress response pathway.," *J. Cell Sci.*, vol. 128, pp. 2219–2228, 2015.

[7] J. M. Kingsbury, N. D. Sen, T. Maeda, J. Heitman, and M. E. Cardenas, "Endolysosomal membrane trafficking complexes drive nutrient-dependent TORC1 signaling to control cell growth in Saccharomyces cerevisiae," *Genetics*, vol. 196, no. 4, pp. 1077–1089, 2014.

[8] M. Binda *et al.*, "The Vam6 GEF Controls TORC1 by Activating the EGO Complex," *Mol. Cell*, vol. 35, no. 5, pp. 563–573, 2009.

[9] J. H. Jeong, K. H. Lee, Y. M. Kim, D. H. Kim, B. H. Oh, and Y. G. Kim, "Crystal structure of the Gtr1pGTP-Gtr2pGDP protein complex reveals large structural rearrangements triggered by GTP-to-GDP conversion," *J. Biol. Chem.*, vol. 287, no. 35, pp. 29648–29653, 2012.

[10] J. J. Tate, I. Georis, E. Dubois, and T. G. Cooper, "Distinct phosphatase requirements and GATA factor responses to nitrogen catabolite repression and

rapamycin treatment in Saccharomyces cerevisiae," *J. Biol. Chem.*, vol. 285, no. 23, pp. 17880–17895, 2010.

[11] L. Váchová, H. Kučerová, F. Devaux, M. Úlehlová, and Z. Palková, "Metabolic diversification of cells during the development of yeast colonies," *Environ. Microbiol.*, vol. 11, no. 2, pp. 494–504, 2009.

[12] B. Zikánová, M. Kuthan, M. Řičicová, J. Forstová, and Z. Palková, "Amino acids control ammonia pulses in yeast colonies," *Biochem. Biophys. Res. Commun.*, vol. 294, no. 5, pp. 962–967, 2002.

[13] T. Noda, Y. Ohsumi, and Tor, "a Phosphatidylinositol Kinase Homologue, Controls Autophagy," *yeast, J. Biol. Chem.*, vol. 273, no. 7, pp. 3963–3966, 1998.

[14] T. Yorimitsu, S. Zaman, and D. J. Klionsky, "Protein Kinase A and Sch9 Cooperatively Regulate Induction of Autophagy in Saccharomyces cerevisiae," *Mol. Biol. Cell*, vol. 18, no. August, pp. 4180–4189, 2007.

[15] Z. Palková and L. Váchová, "Life within a community: Benefit to yeast long-term survival," *FEMS Microbiol. Rev.*, vol. 30, no. 5, pp. 806–824, 2006.

[16] J. R. Broach, "search of a pathway IRASIGTP [/' IOutPu," vol. 7, no. 1, pp. 28–33, 1991.

[17] B. Smets *et al.*, *Life in the midst of scarcity: Adaptations to nutrient availability in Saccharomyces cerevisiae*, vol. 56, no. 1. 2010.

[18] J. M. Thevelein and J. H. De Winde, "Novel sensing mechanisms and targets for the cAMP-protein kinase A pathway in the yeast Saccharomyces cerevisiae," *Mol. Microbiol.*, vol. 33, no. 5, pp. 904–918, 1999.

[19] S. Zaman, S. I. Lippman, L. Schneper, N. Slonim, and J. R. Broach, "Glucose regulates transcription in yeast through a network of signaling pathways," *Mol. Syst. Biol.*, vol. 5, no. 245, 2009.

[20] R. Loewith and M. N. Hall, "Target of rapamycin (TOR) in nutrient signaling and growth control," *Genetics*, vol. 189, no. 4, pp. 1177–1201, 2011.

[21] J. Urban *et al.*, "Sch9 Is a Major Target of TORC1 in Saccharomyces cerevisiae," *Mol. Cell*, vol. 26, no. 5, pp. 663–674, 2007.

[22] N. Panchaud, M.-P. Péli-Gulli, and C. De Virgilio, "Amino acid deprivation inhibits

TORC1 through a GTPase-activating protein complex for the Rag family GTPase Gtr1.," *Sci. Signal.*, vol. 6, no. 277, pp. 1–7, 2013.

[23] D. Stracka, S. Jozefczuk, F. Rudroff, U. Sauer, and M. N. Hall, "Nitrogen source activates TOR (Target of Rapamycin) complex 1 via glutamine and independently of Gtr/Rag proteins," *J. Biol. Chem.*, vol. 289, no. 36, pp. 25010–25020, 2014.

[24] B. Magasanik and C. A. Kaiser, "Nitrogen regulation in Saccharomyces cerevisiae," *Gene*, vol. 290, no. 1–2, pp. 1–18, 2002.

[25] F. Dubouloz, O. Deloche, V. Wanke, E. Cameroni, and C. De Virgilio, "The TOR and EGO protein complexes orchestrate microautophagy in yeast," *Molecular Cell*, vol. 19, no. 1. pp. 15–26, 2005.

[26] S. Dokudovskaya *et al.*, "A conserved coatomer-related complex containing Sec13 and Seh1 dynamically associates with the vacuole in Saccharomyces cerevisiae.," *Mol. Cell. Proteomics*, vol. 10, no. 6, pp. 1–17, 2011.

[27] G. Bonfils, M. Jaquenoud, S. Bontron, C. Ostrowicz, C. Ungermann, and C. De Virgilio, "Leucyl-tRNA Synthetase Controls TORC1 via the EGO Complex," *Mol. Cell*, vol. 46, no. 1, pp. 105–110, 2012.

[28] K. Powis, T. Zhang, N. Panchaud, R. Wang, C. De Virgilio, and J. Ding, "Crystal structure of the Ego1-Ego2-Ego3 complex and its role in promoting Rag GTPase-dependent TORC1 signaling.," *Cell Res.*, vol. 25, no. 9, pp. 1043–59, 2015.

[29] C. K. Raymond, I. Howald-stevenson, C. A. Vater, and T. H. Stevens, "Mbc00070-0087," vol. 3, no. December, pp. 1–14, 2012.

[30] N. Nakamura, A. Hirata, Y. Ohsumi, and Y. Wada, "Vam2 / Vps41p and Vam6 / Vps39p Are Components of a Protein Complex on the Vacuolar Membranes and Involved in the Vacuolar Assembly in the Yeast Saccharomyces cerevisiae *," vol. 272, no. 17, pp. 11344–11349, 1997.

[31] K. Peplowska, D. F. Markgraf, C. W. Ostrowicz, G. Bange, and C. Ungermann, "The CORVET Tethering Complex Interacts with the Yeast Rab5 Homolog Vps21 and Is Involved in Endo-Lysosomal Biogenesis," *Dev. Cell*, vol. 12, no. 5, pp. 739–750, 2007.

[32] R. Puria, S. A. Zurita-Martinez, and M. E. Cardenas, "Nuclear translocation of Gln3 in response to nutrient signals requires Golgi-to-endosome trafficking in

Saccharomyces cerevisiae," *Proc. Natl. Acad. Sci.*, vol. 105, no. 20, pp. 7194–7199, 2008.

[33] J. Onodera and Y. Ohsumi, "Autophagy is required for maintenance of amino acid levels and protein synthesis under nitrogen starvation," *J. Biol. Chem.*, vol. 280, no. 36, pp. 31582–31586, 2005.

[34] A. E. Wurmser, T. K. Sato, S. D. Emr, and V. Vam, "New Component of the Vacuolar Class C-Vps Complex Couples Nucleotide Exchange on the Ypt7 GTPase to SNARE-dependent Docking and Fusion," vol. 151, no. 3, pp. 551–562, 2000.

[35] K. M. Collins, N. L. Thorngren, R. A. Fratti, and W. T. Wickner, "Sec17p and HOPS, in distinct SNARE complexes, mediate SNARE complex disruption or assembly for fusion," *EMBO J.*, vol. 24, no. 10, pp. 1775–1786, 2005.

[36] L. Li and K. L. Guan, "Amino Acid Signaling to TOR Activation: Vam6 Functioning as a Gtr1 GEF," *Mol. Cell*, vol. 35, no. 5, pp. 543–545, 2009.

[37] T. L. Baars, S. Petri, C. Peters, and A. Mayer, "Role of the V-ATPase in Regulation of the Vacuolar Fission–Fusion Equilibrium," *Mol. Biol. Cell*, vol. 18, pp. 3873–3882, 2007.

[38] R. M. Deranieh *et al.*, "Perturbation of the Vacuolar ATPase," *J. Biol. Chem.*, vol. 290, no. 46, pp. 27460–27472, 2015.

[39] S. A. Rudge, D. M. Anderson, and S. D. Emr, "Vacuole Size Control: Regulation of PtdIns(3,5)P2 Levels by the Vacuole-associated Vac14-Fig4 Complex, a PtdIns(3,5)P2-specific Phosphatase," *Mol. Biol. Cell*, vol. 15, no. January, pp. 24–36, 2004.

[40] S. K. Dove, F. T. Cooke, M. R. Douglas, L. G. Sayers, P. J. Parker, and R. H. Michell, "Osmotic stress activates phosphatidylinositol-3,5-bisphosphate synthesis," *Nature*, vol. 390, no. 6656, pp. 187–192, 1997.

[41] N. Jin *et al.*, "VAC14 nucleates a protein complex essential for the acute interconversion of PI3P and PI(3,5)P 2 in yeast and mouse," *EMBO J.*, vol. 27, no. 24, pp. 3221–3234, 2008.

[42] J. D. Gary, T. K. Sato, C. J. Stefan, C. J. Bonangelino, L. S. Weisman, and S. D. Emr, "Regulation of Fab1 Phosphatidylinositol 3-Phosphate 5-Kinase Pathway by Vac7 Protein and Fig4, a Polyphosphoinositide Phosphatase Family Member," *Mol.*

Biol. Cell, vol. 13, no. April, pp. 1238–1251, 2001.

[43] D. D. Jackson and T. H. Stevens, "VMA12 encodes a yeast endoplasmic reticulum protein required for vacuolar H+-ATPase assembly," *J. Biol. Chem.*, vol. 272, no. 41, pp. 25928–25934, 1997.

[44] A. K. Bachhawat, M. F. Manolson, D. G. Murdock, J. D. Garman, and E. W. Jones, "The VPH2 gene encodes a 25 kDa protein required for activity of the yeast vacuolar H+-ATPase," *Yeast*, vol. 9, no. 2, pp. 175–184, 1993.

[45] B. Stauffer and T. Powers, " Target of rapamycin signaling mediates vacuolar fission caused by endoplasmic reticulum stress in Saccharomyces cerevisiae ," *Mol. Biol. Cell*, vol. 26, no. 25, pp. 4618–4630, 2015.

[46] C. Jia *et al.*, "Roles of VPH2 and VMA6 in localization of V-ATPase subunits, cell wall functions and filamentous development in Candida albicans," *Fungal Genet. Biol.*, vol. 114, no. February, pp. 1–11, 2018.

[47] R. D. Gietz and R. A. Woods, "Transformation of yeast by lithium acetate/single-stranded carrier DNA/polyethylene glycol method," *Methods Enzymol.*, vol. 350, no. 2001, pp. 87–96, 2002.

[48] N. A. Stewart and T. Veenstra, *2D PAGE: Sample Preparation and Fractionation*, vol. 425, no. February. 2008.

[49] S. P. Gangloff, D. Marguet, and G. J. Lauquin, "Molecular cloning of the yeast mitochondrial aconitase gene (ACO1) and evidence of a synergistic regulation of expression by glucose plus glutamate.," *Mol. Cell. Biol.*, vol. 10, no. 7, pp. 3551–3561, 2015.

[50] D. Gachotte, R. Barbuch, J. Gaylor, E. Nickel, and M. Bard, "Characterization of the Saccharomyces cerevisiae ERG26 gene encoding the C-3 sterol dehydrogenase (C-4 decarboxylase) involved in sterol biosynthesis," *Proc. Natl. Acad. Sci.*, vol. 95, no. 23, pp. 13794–13799, 2002.

[51] M. Schweizer *et al.*, "The pentafunctional FAS1 gene of yeast: its nucleotide sequence and order of the catalytic domains," *MGG Mol. Gen. Genet.*, vol. 203, no. 3, pp. 479–486, 1986.

[52] K. I. Minard and L. McAlister-Henn, "Isolation, nucleotide sequence analysis, and disruption of the MDH2 gene from Saccharomyces cerevisiae: evidence for three

isozymes of yeast malate dehydrogenase.," *Mol. Cell. Biol.*, vol. 11, no. 1, pp. 370–380, 1991.

[53] X. Gan, M. Kitakawa, K. I. Yoshino, N. Oshiro, K. Yonezawa, and K. Isono, "Tag-mediated isolation of yeast mitochondrial ribosome and mass spectrometric identification of its new components," *Eur. J. Biochem.*, vol. 269, no. 21, pp. 5203–5214, 2002.

[54] M. K. Aalto, H. Ronne, and S. Keränen, "Yeast syntaxins Sso1p and Sso2p belong to a family of related membrane proteins that function in vesicular transport.," *EMBO J.*, vol. 12, no. 11, pp. 4095–4104, 1993.

[55] Z. Palkova, B. Janderova, J. Gabriel, B. Zikanova, M. Pospisek, and J. Forstova, "Ammonia mediates communication between yeast colonies," *Nature*, vol. 390, no. 6659, pp. 532–536, 1997.

[56] N. Regev-Rudzki, S. Karniely, N. N. Ben-Haim, and O. Pines, "Yeast Aconitase in Two Locations and Two Metabolic Pathways: Seeing Small Amounts Is Believing," *Mol. Biol. Cell*, vol. 16, no. Septemer, pp. 4163–4171, 2005.

[57] C. Mo, M. Valachovic, S. K. Randall, J. T. Nickels, and M. Bard, "Protein–protein interactions among C-4 demethylation enzymes involved in yeast sterol biosynthesis," *Gaz. Medicale*, vol. 99, no. 15, pp. 9739–9744 BIOCHEMISTRY, 2002.

[58] K. Arai, S. Ohkuma, T. Matsukawa, and S. Kato, "A simple estimation of peroxisomal degradation with green fluorescent protein - An application for cell cycle analysis," *FEBS Lett.*, vol. 507, no. 2, pp. 181–186, 2001.

[59] S. C. Davis, Alexander Tzagoloff, and Steven R. Ellis, "Characterization of a yeast mitochondrial ribosomal protein structurally related to the mammalian 68-kDa high affinity laminin receptor," *J. Biol. Chem.*, vol. 267, no. 8, pp. 5508–5514, 1992.

[60] T. Mahmood and P. C. Yang, "Western blot: Technique, theory, and trouble shooting," *N. Am. J. Med. Sci.*, vol. 4, no. 9, pp. 429–434, 2012.

[61] J. E. Duex, F. Tang, and L. S. Weisman, "The Vac14p-Fig4p complex acts independently of Vac7p and couples PI3,5P 2 synthesis and turnover," *J. Cell Biol.*, vol. 172, no. 5, pp. 693–704, 2006.

[62] N. Jin, Y. Jin, and L. S. Weisman, "Early protection to stress mediated by CDK-

dependent PI3,5P 2 signaling from the vacuole/lysosome," *J. Cell Biol.*, vol. 216, no. 7, pp. 2075–2090, 2017.

[63] M. Sambade, M. Alba, A. M. Smardon, R. W. West, and P. M. Kane, "A genomic screen for yeast vacuolar membrane ATPase mutants," *Genetics*, vol. 170, no. 4, pp. 1539–1551, 2005.

[64] Z. Palkova, F. Devaux, M. Ricicova, L. Minarikova, S. Le Crom, and C. Jacq, "Ammonia Pulses and Metabolic Oscillations Guide Yeast Colony Development," *Mol. Biol. Cell*, vol. 13, no. November, pp. 3901–3914, 2002.

[65] W. Lang, "Nomarski differential interference-contrast microscopy I. Fundamentals and experimental designs," vol. 70, pp. 16–114, 1968.

[66] D. B. Murphy and M. W. Davidson, "Contrast Microscopy and Modulation Contrast Microscopy," *Fundam. Light Microsc. Electron. Imaging*, pp. 173–197, 2012.

[67] J. E. Duex, J. J. Nau, E. J. Kauffman, and L. S. Weisman, "Phosphoinositide 5-phosphatase Fig4p is required for both acute rise and subsequent fall in stress-induced phosphatidylinositol 3,5-bisphosphate levels," *Eukaryot. Cell*, vol. 5, no. 4, pp. 723–731, 2006.

[68] B. F. Horazdovsky, C. R. Cowles, P. Mustol, M. Holmes, and S. D. Emr, "A novel RING finger protein, Vps8p, functionally interacts with the small GTPase, Vps21p, to facilitate soluble vacuolar protein localization," *J. Biol. Chem.*, vol. 271, no. 52, pp. 33607–33615, 1996.

[69] W. J. Luo and A. Chang, "Novel genes involved in endosomal traffic in yeast revealed by suppression of a targeting-defective plasma membrane ATPase mutant," *J. Cell Biol.*, vol. 138, no. 4, pp. 731–746, 1997.

[70] T. Beck and M. N. Hall, "The TOR signalling pathway controls nuclear localization of nutrient- regulated transcription factors," *Nature*, vol. 402, pp. 689–692, 1999.

[71] H. Kurzweilová and K. Sigler, "Fluorescent staining with bromocresol purple: A rapid method for determining yeast cell dead count developed as an assay of killer toxin activity," *Yeast*, vol. 9, no. 11, pp. 1207–1211, 1993.

[72] C. M. Paumi, M. Chuk, J. Snider, I. Stagljar, and S. Michaelis, "ABC Transporters in Saccharomyces cerevisiae and Their Interactors: New Technology Advances the Biology of the ABCC (MRP) Subfamily," *Microbiol. Mol. Biol. Rev.*, vol. 73, no. 4,

pp. 577–593, 2009.

[73] B. E. Bauer, H. Wolfger, and K. Kuchler, “Inventory and function of yeast ABC proteins: About sex, stress, pleiotropic drug and heavy metal resistance,” *Biochim. Biophys. Acta - Biomembr.*, vol. 1461, no. 2, pp. 217–236, 1999.